Scalar Fields in Cosmology and Astrophysics

Andrew R Liddle

Ph.D Thesis

Department of Physics and Astronomy

Glasgow University

Glasgow G12 8QQ

September 1989

ProQuest LLC.
789 East Eisenhower Parkway
P.O. Box 1346
Ann Arbor, MI 48106 – 1346

" 'What is the use of a book', thought Alice, 'without pictures or conversations? ' "

Alice's Adventures in Wonderland

Lewis Carroll

"I've never heard of him."

"*In what context* have you never heard of him? "

The Singing Detective

Dennis Potter

Dedicated to my parents, on their twenty-fifth wedding anniversary.

(Whether they understand it or not!)

Declaration

The work described in this thesis is original to the author, except where indicated otherwise by references and with the exception of chapter one which describes the background to the rest of this thesis. The work in chapters two, three, five and six was carried out in collaboration with my supervisor, Professor R G Moorhouse, here at Glasgow and with Professor A B Henriques from CFMC in Lisbon, Portugal. The work in chapter four was carried out entirely by myself. Some of the work in chapter two, particularly sections two and three, is based on an earlier paper by Professors Henriques and Moorhouse, though the treatment of the iteration therein is for the most part my own.

The work of chapters two and three can be found, in a more concise version, in the paper

"Early Cosmology and the Dilaton and H Field from Superstring Theory"
Andrew R Liddle, R G Moorhouse and A B Henriques,
Nucl Phys B311 (1989) 711

That of chapter four has appeared as

"Power Law Inflation with Exponential Potentials"
Andrew R Liddle
Phys Lett B220 (1989) 502

The work in chapters five and six will also appear as University of Glasgow preprints and will be submitted for publication in late 1989.

Acknowledgements

First and foremost, I would like to thank my supervisor, Gordon Moorhouse, for all his help and guidance over the last three years, and our collaborator, Alfredo Henriques, for his part in the work described in this thesis. Both have been extremely helpful throughout the last three years. In particular, I would like to thank Gordon for all the well-timed criticism that has kept me from wandering too far from the straight and narrow, and Alfredo for constant long distance prodding via electronic mail.

Along the way, I have received much helpful assistance from many of the inhabitants of the department of Physics and Astronomy. I am happy to acknowledge a series of useful conversations on physics and other things with, at varying times, David Alexander, David M^{c}Mullan, Jim Paterson, Chris Stephens and David Sutherland. My sometimes temporary control over the computing facilities at Glasgow has been much aided by Declan Diver and Alan M^{c}Lachlan; I have also benefited from discussions with Declan (again) and Norman M^{ac}Donald on the behaviour and solution of systems of differential equations. Thanks also to David Henty and Alan Bell for help with the IBM 3090, used to obtain the last results for chapter six in a panic rush a scant two days before the completed thesis went to the binders. I am also grateful for the helpfulness of the computer operators who aided a quick compilation of results over the last month.

I would also like to take this opportunity to thank all my friends both within the department and elsewhere. Within the department, thanks especially to the Astronomy Old Guard (whoever they may be ?!), the dreaded Solid State, and, of course, the ubiquitous Friday Nighters. Thanks also to Martin for making my drinking appear moderate, and Bill, Roddy and John for varying measures of insanity. I am also grateful to my family for concealing at least some of their

incredulity at my choice of profession. Finally, I would like to thank Mandy for, amongst other things, a deservedly critical proofreading of this thesis, and Christine for not having to type the page numbers.

The financial support for this work came primarily from a University of Glasgow Postgraduate Scholarship. Funds for travel to various conferences both home and abroad came from the Department of Physics at Glasgow and from the Institute of Physics, with some additional assistance from NATO. Finally, thanks to the University of Sussex for providing an opportunity to continue this work and finally escape seven years of studentship.

Andrew R Liddle

University of Glasgow

August 29th, 1989

Contents

Abstract

This thesis examines various applications of particle physics to topics in cosmology and astrophysics, with particular attention paid to the possible roles of scalar fields. The work can be broken down into four distinct, though related, pieces. The first of these pieces comprises both chapters two and three while the remainder, each one chapter long, are chapters four, five and six. The first two topics are cosmology based, examining the dynamics of cosmological solutions to various particle theories with consideration of compactification and inflation respectively. The remaining two are astrophysical in nature, with particular attention paid to compact stellar objects such as neutron stars and boson stars.

Chapter one provides an overview of the relevant parts of particle physics, cosmology and astrophysics in a non-technical manner, to introduce the ideas present throughout the rest of the thesis, and contains notes on the conventions used within it.

In chapters two and three, we investigate various cosmological solutions in ten dimensional supergravity, viewed as a low energy limit of the heterotic string theory. We use the three form field **H** to split up the nine spatial dimensions into three 3-spaces, and examine the influence of the scalar dilaton field. Both analytic and numerical means are used to examine two specific models, and the nature of approach to an initial cosmological singularity is examined. In one case, the future behaviour is governed by the existence of an unusual type of attractor, which precludes the possibility of compactification, while in the other, where the **H** field arises solely on one 3-space, sensible compactification scenarios can be obtained. The model is then enhanced by considering a simple mechanism for particle production using scalar field couplings to other (fermion) fields to provide viscous forces. The effect of this particle production on both the previous scenarios is examined.

In chapter four, models exhibiting power law inflation are considered and an exact solution specified. Once more, viscous forces from the inflaton's couplings are included and are found, primarily by numerical techniques, to improve the efficiency of the inflation. The basic ideas are then implemented in a specific particle theory in which the scalar field has a potential of the desired type, and it is illustrated how an inflationary model may be constructed from these ideas which is consistent with constraints from observations.

Chapter five considers the effect which higher dimensional theories may have on the structure of neutron stars. In particular, we examine the simplest Kaluza-Klein theory in which the size of the extra dimension behaves as a scalar field. The equations of stellar structure are derived and then solved numerically, with particular attention given to the function of total mass against the central density and to the description of matter in a five dimensional theory. Only some descriptions of matter are allowed, and they can lead to exterior solutions differing from the conventional Schwarzchild one. Finally, a sample model for dynamical gravitational collapse in these theories is examined, and surprisingly it is found that it can be solved analytically. Unfortunately, difficulties in attaching an exterior solution outside the collapsing matter conceal the full nature of this solution.

Chapter six examines the possibility of stellar objects comprised of both bosons and fermions, thus generalising the separate notions of neutron stars and boson stars. Again, the basic equations are derived, and numerical simulation is once more necessary to obtain solutions to them. Attention is given to the units used and the mass function is again of primary interest. A rudimentary stability analysis based on the binding energy of the stars is carried out, and an examination made of the results of varying the mass of the bosonic constituents. Briefly, the effect of an explicit interaction term between the bosons and fermions in the Lagrangian is considered.

Chapter seven provides some conclusions and details areas in which future work may be fruitful.

Chapter 1

Introduction

"Nothing ever begins.

There is no first moment; no single word or place from which this or any other story springs. The threads can always be traced back to some earlier tale, and to tales that preceded that; though as the narrator's voice recedes the connections will seem to grow more tenuous, for each age will want the tale told as if it were of its own making."

Weaveworld

Clive Barker

(i) Cosmology in the Eighties

One of the most impressive achievements of theoretical physics during the last century is in its description of the behaviour of the universe as a whole, a subject which has come to be known as cosmology. This came about with the recognition by Einstein that his theory of general relativity, basing gravitational interactions upon the concept of curvature of space and time, could be applied to the universe as a whole. In fact, as has been much documented, he only missed a marvellous opportunity to predict that the universe was expanding because at the time the philosophy that the universe must be unchanging was so rock solid that instead he resorted to a modification of his basic equations. Since then, these original ideas have been developed into what is commonly known as the 'hot big bang' model, and the extensive predictions of this model are so much in agreement with observations that the theory has no serious competitors.

The foundations of general relativity are set in the idea that it is the curvature of spacetime itself which causes the phenomenon we recognise as the gravitational

force, and that it is the presence of matter which creates this curvature. This relation is concisely expressed by what are known as the Einstein equations, which equate a purely geometrical term governing the curvature of space-time to a quantity, the energy-momentum tensor, describing the distribution of matter. This is sometimes summed up by saying "Space tells matter how to move; matter tells space how to curve".

The big bang model is founded on two important observations of the universe as we see it today, its homogeneity and isotropy. Homogeneity means that the matter in the universe is smoothly distributed; while it is certainly true that on a galactic scale we see clumps of galaxies in some places and large voids in others, if we look on a bigger scale the amount of matter in a given large volume varies very little from place to place. Hence homogeneity is a very good approximation on a large scale. Isotropy can be summed up by saying that the universe appears the same whichever way we look, again true on large scales. In combination, these imply that there are no preferred locations in the universe; at a given time it does not matter where you are, the universe will look essentially the same. This is the basic assumption of the big bang model.

Given these constraints, it can be shown that the universe must be described by what is known as a Friedmann-Robertson-Walker cosmology. The important quantity is the scale factor, which describes the distance between points in space-time. If, as time passes, the scale factor increases, then the universe can be said to be expanding. The actual form of the scale factor is determined from Einstein's equations, given some assumptions about the properties of matter present in the universe, and the solutions found indeed indicate that the universe must be expanding or contracting. This agrees with the interpretation of red shift observations first made by Hubble indicating that stars are moving away from us at a speed proportional to their distance, suggesting that we live in an expanding universe.

While this result in itself is a success, much more can be said when we include some detailed information about the types of matter in the universe. It can be shown that if we look back in the history of the universe, there must have been a time when it was very small, and that at this time it was much hotter. At such high temperatures, atoms and nuclei could not exist as there would be enough thermal energy to separate the protons, neutrons and electrons. At this time radiation will dominate the universe, governing its expansion. As the universe cools down, nuclei will begin to form, primarily those of low atomic number such as hydrogen and helium. Later still, the radiation will have cooled down sufficiently that it no longer interacts with the matter, allowing atoms to form, and will continue to disperse on its own (the temperature at which this occurs is known as the decoupling temperature). From then on, as today, matter will dominate the universe and determine its evolution.

These processes, which depend only on very well known physics, lead to startlingly accurate verifications of the big bang theory. From a knowledge of what proportion of protons and neutrons exist when nuclei form, it is possible to predict the relative abundances of hydrogen and helium, the lightest stable atoms and the most predominant products of the early universe. Essentially all the neutrons combine with protons to form helium; the remaining protons are left to form hydrogen. The hot big bang model predicts a relative abundance of about 73% to 27% in favour of hydrogen. This agrees almost exactly with observations, and indeed the discrepancy is well explained by the hydrogen to helium fusion processes which have occurred in stars during the lifetime of the universe. More detailed calculations can also tell us about the small quantities of more complicated atoms such as lithium formed.

The second important observation was of the decoupled radiation. As the universe expands, the energy of this radiation is diluted and consequently its temperature drops from the decoupling temperature. This radiation was accidentally

observed by Penzias and Wilson, who detected unexpected microwave radiation at a temperature of about three Kelvin while conducting antenna experiments. It turned out that this 'microwave background' was exactly as the big bang model predicted, and this fact alone was enough to win acceptance of the big bang model over rivals such as the steady state universe.

It was shown by Hawking and Penrose in the late sixties and early seventies that at the beginning of the universe it is inevitable that all the matter was concentrated at one point, known as a singularity, and that near the singularity one could expect temperatures to rise arbitrarily high. To study processes going on nearer to the big bang than those discussed above, we have to look at higher energies than those of the events considered above, which corresponds to looking at more fundamental interactions. This is where the role of particle physics in cosmology becomes evident, to try and investigate what might have gone on in the very early eras of the universe and perhaps to see whether the initial singularity might be avoided.

(ii) Particle Physics in the Eighties

At the basis of particle physics in recent times have been the attempts to formulate a consistent theory of the fundamental forces in the universe. There are four such forces, namely electromagnetism, the weak nuclear force, the strong nuclear force and the gravitational interaction. For the most part, particle theory has concentrated on the first three of these; it is only in very recent years that there have been any grounds, other than aesthetic ones, for supposing that gravity can be drawn into a common framework with the rest. (This ignores current speculation concerning the existence of a 'fifth force' related to gravity. Experiments have as yet failed to provide any clear confirmation of the existence of such a force.)

The first major breakthrough came in nineteen thirty when the theory of quantum electrodynamics was formulated. This introduced the idea that the

fundamental description of particles was to be made through fields, and this theory successfully incorporates quantum mechanics in an intrinsically relativistic manner. The agreement of this theory with experiment is startling; for example the magnetic moment of the electron can be correctly predicted to some eight significant figures. An important element of this theory is what has come to be known as a gauge invariance, a mechanism whereby the interaction can be viewed as being caused by the action of a particular symmetry group, in this case called U(1), and this theory sets the pattern for the description of the two nuclear forces. The notion of symmetry is now the most important tool in the description of fundamental interactions.

By the seventies, the gauge description of matter was well known and was used to provide a theory of the strong, weak and electromagnetic interactions; each interaction caused by a particular local symmetry group, here SU(3), SU(2) and U(1) respectively. A theory which combined these interactions could be formed simply by considering products of these gauge groups; first Weinberg and Salam developed the electroweak theory, vindicated by the recent discovery of the W and Z particles at CERN, around SU(2)xU(1), then the full 'standard model' was constructed using SU(3)xSU(2)xU(1). The standard model describes all current experimental data satisfactorily, and the reasons to go beyond it are based mostly on aesthetics rather than any experimental motivation.

One of the major drawbacks of the standard model is the huge number of free parameters present, which can only be determined by experiment (these include masses of the fundamental particles, mixing angles etc.). Also the idea of just sticking the groups together does not seem to be completely satisfactory. The natural idea is to look for a bigger symmetry group, around which to form what became known as a Grand Unified Theory, or GUT. If this group is chosen so as to include the standard model group as a subgroup, then the theory will contain the standard model, perhaps as a low energy limit if appropriate symmetry breakings are included, and will usually have fewer free parameters as there will be extra relations

between the standard model parameters. The simplest such group is SU(5), which like all GUTs includes extra interactions beyond the standard model, including the prediction of proton decay with a lifetime greater than 10^{30} years. Experimental tests of this may rule out the SU(5) model, but larger gauge groups generally predict longer lifetimes and are not ruled out by these measurements.

The unfortunate feature about GUTs is that almost any sufficiently large gauge group contains the standard model group, and we have no guidelines concerning which to choose. Also these theories suffer from what is known as the hierarchy problem; the theories must have two mass scales, one at about 10^{15} GeV where the symmetry of the GUT group breaks (perhaps in several stages) to that of the standard model group, and one at about 10^{2} GeV where the electroweak interaction separates into the weak force and electromagnetism. The problem is that having two such widely separated scales is unnatural, for one would expect quantum effects at high energies to destroy the low energy effects. Fine tuning of parameters must be introduced to avoid this.

A method for avoiding the hierarchy problem was proposed in the form of supersymmetric theories; in these theories bosons (particles of integer spin) and fermions (particles of half integer spin) appear on an equal footing. While at the energies we see today supersymmetry does not hold (e.g. there is no observed bosonic partner of the electron), the symmetry can be restored at fairly low energies. Then any interactions at higher energies will exactly cancel out, the fermion part being the negative of the bosonic contribution. Hence the electroweak scale will be protected from any high energy corrections and the hierarchy problem overcome.

All of the above theories were constructed without any regard for how the gravitational interaction might be included; gravity is very different from the other three forces and resists being drawn into the gauge framework. In the seventies there was renewed interest in an old idea of Kaluza and Klein, which was to add on extra

dimensions to the four dimensions of space and time we are familiar with from everyday experience. It turns out that gauge symmetries can be obtained from symmetries of the extra dimensions rather than being put in by hand using an arbitrary choice of gauge group. For example, by adding a circular extra dimension the equations of general relativity coupled to electromagnetism can be obtained; the symmetry of the circle is exactly that of the U(1) gauge group. Larger and more complicated extra dimensions can give the entire standard model. The fact that we do not see these dimensions can be explained by them being of a very small size, like a hosepipe which appears to be a one dimensional string from large distances but close up can be seen to be a two dimensional object. Thus these higher dimensional theories can incorporate gravity into a gauge theory (or rather, vice versa). This is illustrated in figure 1.1.

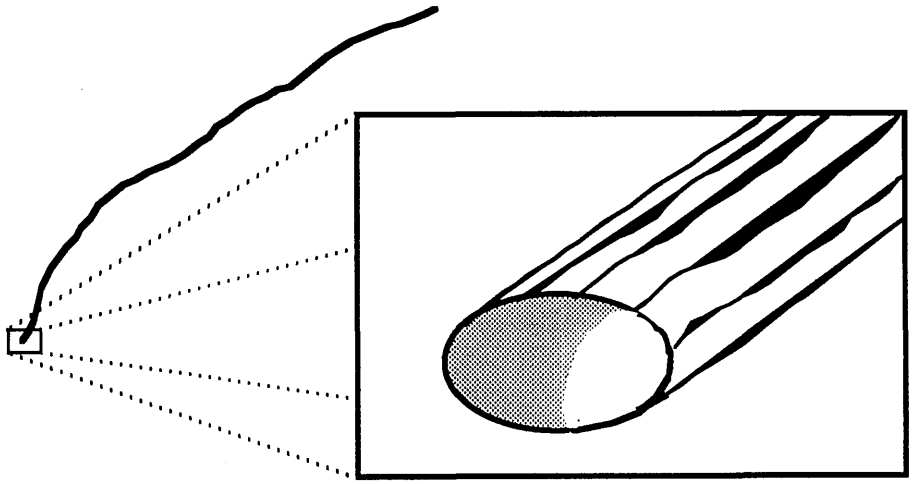

Figure 1.1 The hosepipe on the left, as viewed from large distances, looks like a line, but when magnified it can be seen to be two-dimensional. Modern theories suggest that if there are extra dimensions, they will be of a very small size (10^{-33} cm) and will be unobservable in experiments that can be carried out just now.

When people tried to make supersymmetry into a local symmetry, it was found that to make the theory consistent there was no option but to include gravity, and these theories were known as supergravity theories. It turns out that supergravity theories can be formulated particularly neatly if there are extra hidden dimensions, providing a link with Kaluza-Klein theories, but no way existed of picking out a preferred number of dimensions. Supergravity theories exist in all dimensions up to eleven, which is the highest number of dimensions in which supersymmetry can be consistently realised.

The next stage of development was the invention of superstring theories. Here the major conceptual step is to view the fundamental constituents of matter not to be particles at all, but to be extended one-dimensional objects. The particles we see, such as quarks, photons, electrons and so on, correspond to different excitations of the string, in the form of waves propagating round them. Strings can be open, with free ends, or closed into a loop by joining both ends together. Some versions of the theory have both types, but versions which only have closed strings are generally favoured. Interactions are provided by strings intersecting with each other, breaking up and reforming in new configurations.

The advantage of string theories is twofold; they are only consistent provided they have one of only two possible gauge groups, and they must be formulated in ten dimensions (that is, with six extra hidden dimensions). Hence the string theory allows us to pin down these two aspects which were unspecified in GUTs and in supergravity theories, a fact which inspired confidence that a consistent theory unifying all fundamental interactions might be attainable. More will be said about superstrings in chapter two. It should be pointed out that since the work in chapter two was carried out superstring theory has seen several developments which free it from some of the dimensionality and gauge group constraints, though these recent constructions seem somewhat arbitrary. There also exist theories based on higher dimensional objects, dubbed supermembranes, of which various versions exist, but

all of these lack the simple structure of the superstring theories.

Figure 1.2 provides a diagrammatic summary of the relationships between these theories, reading from the bottom up. Several comments are in order. The Theory of Everything is the current terminology for an ultimate description of matter, and the nature of such a theory is unknown. The route to it may be through superstrings, which are most promising current candidate for such an accolade but are a long way from being accepted as such by the physics community, or the route may be via some entirely different and as yet unknown theory which may be completely different from any theory we current have. The status of quantum gravity in the

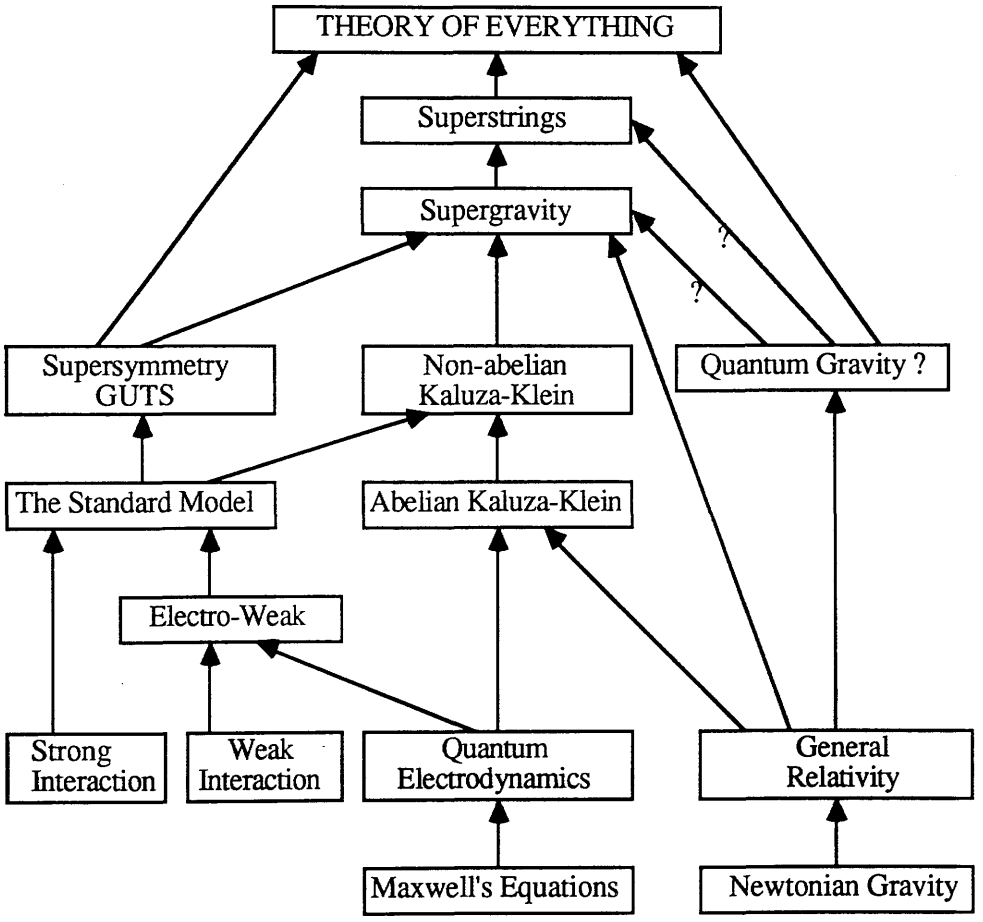

Figure 1.2 Relations between some of the popular particle theories of the eighties.

diagram is unclear; currently there is no theory which combines gravity with quantum effects and it is not known what such a theory may be like. It is possible that supergravity or superstrings may contain a quantum theory of gravity (certainly if superstrings are the theory of everything), but this is not known as present. Abelian Kaluza-Klein refers to the simple model of Kaluza which combines gravity with electromagnetism. Non-abelian Kaluza-Klein is the generalisation of this to contain more complicated symmetries such as the standard model. The highest levels of this diagram that can be said to be well understood are the standard model on one hand and general relativity on the other.

(iii) Cosmology and Particle Physics : Why?

Over the last ten years or so there has been a very fruitful interaction between particle theory and cosmology. It is worth examining here why these two topics have found so much common ground, and considering the motivations on either side of the cosmology and particle theory divide. This thesis is for the most part concerned with how particle theory can be absorbed into cosmology; in that sense it can be said to be a thesis on cosmology rather than on particle theory, though as we shall see the two subjects are becoming more and more indistinguishable. Hence we shall concentrate in this section on the cosmologist's side of things, and merely conclude with a few paragraphs on what particle theorists can expect to get out of cosmology.

Imagine tracing the history of the universe back towards the inevitable singularity of the big bang. The size of the universe reduces; the energy density within it increases and hence the corresponding temperature rises without limit. As the energy increases, we are forced to take into account interactions at shorter and shorter distances. The thermal energy will become enough to dissociate atoms into nuclei and electrons, then enough to separate the nuclear constituents themselves. A little higher and the hadrons themselves will be split into their constituent quarks. We

are now one millionth of a second from the big bang. Then, as the energy goes higher still, ...

All of the above is based on very well known physics, at energies well within the reach of current particle accelerators. But as the energies get higher, we enter a realm where we need a more complete knowledge of the fundamental particle theories than can as yet be obtained from these experiments. Various symmetries will be restored at high energies; electromagnetism and the weak force will combine into the unbroken electroweak interaction, then perhaps supersymmetry and GUT symmetries will be restored. As we reach 10^{19} GeV, we approach a region where quantum effects associated with gravity can be expected to become important. Here we know almost nothing of what might go on; extra dimensions may become visible, superstring effects may dominate, some form of quantum gravity may prevent us actually reaching the singularity itself. It is only with a better understanding of the underlying fundamental interactions that we can gain knowledge about these fantastically early eras of the universe.

Of course, when we study these eras, we have more in mind than gaining an overview of these early processes. While the standard cosmology can explain a huge number of features of the universe as a whole, there remain several problems which cannot be resolved without going into the details of yet earlier behaviour. Below we outline a few of these and some proposed solutions. These problems form the background for much of the work in this thesis.

Unexplained by the standard cosmology is why, when we look at the universe today, it consists almost entirely of matter rather than an even mix of matter and anti-matter, since low energy interactions conserve total baryon number. We need some mechanism which will create matter preferentially to anti-matter, a process known as baryogenesis. Here particle physics can provide prospective answers. The most favoured scheme is to use one of the GUT symmetry breakings mentioned above at high energies. These can violate baryon number; it is proposed that at this

point a small excess of baryons over antibaryons is created, perhaps only one part in a thousand million. As the universe cools, the baryons and antibaryons will efficiently annihilate giving photons, and so this small original excess will be amplified up to the baryon domination we see today.

Recently, an alternative scheme for baryogenesis has been proposed, using just the electroweak theory. While at a classical level this conserves baryon number, when we quantise the theory we find there is an anomaly which leads to a baryon non-conserving current. Over the electroweak phase transition this can lead to the generation of a baryon asymmetry, though the details of such a model have yet to be fully worked out to see if it is viable. In some cosmological scenarios this method can be favourable because it occurs at much lower energies than the GUT scenarios.

Another unsolved problem is that of how galaxies, galaxy clusters and other large scale structures came to form. What is needed, at an early stage in the universe, is that the energy density be slightly greater (around one part in ten thousand) in some places than in others. The greater gravitational attraction of these regions will draw matter in to form clumps that will evolve into galaxies. We wish to consider possible sources of these original density perturbations.

One candidate for such a role is the theory based on the esoterically named cosmic strings. When gauge symmetries are broken, the phase transition does not necessarily occur completely smoothly, because different regions are not in direct contact and so there is no information about how the symmetries are broken. It is possible for flaws to occur in the gauge fields when the symmetry breaking occurs; this is exactly analogous to cracks forming in ice crystals as they solidify because the lattices in different regions are not aligned, or domain formation in a ferromagnet as it is cooled down sufficiently for the spins to align. These flaws show up as three types, monopoles, cosmic strings and domain walls, and the particular type we would expect to find can be predicted from the nature of the phase transition. The masses of these objects are extremely high, related to the energy at which the

symmetry breaking occurs. Monopoles are pointlike, cosmic strings one-dimensional and domain walls two dimensional, and of the three cosmic strings are the most favoured. Indeed, there are strong constraints against theories containing phase transitions which would produce monopoles or domain walls, since in either case the production rate is so large that they completely disagree with observations of the universe's energy density. It is perhaps possible for a very late phase transition to produce acceptable entities of these types.

Cosmic strings turn out in some theories to be of just the appropriate mass to create density perturbations about which galaxies may form, suggesting a possible mechanism, and many studies have been made over the last few years of how cosmic string networks evolve, how matter accretes onto them and so on. A knowledge of which phase transitions might occur in the early universe would be needed to check the viability of such a theory, though there are many ways of testing this scenario as cosmic strings should affect pulsar timings, have characteristic gravitational wave spectra and may even be observable directly, e.g. through gravitational lensing.

Cosmic strings are not the only candidate for the density perturbations; dark matter is also a possible candidate. There is a critical density for matter in the universe; if the real density is above it the universe will later recontract back to a singularity in the future, below it and it will expand forever. Many theorists believe that the universe should be at or extremely near this density (particularly those who favour inflationary models - see later), but visible matter appears only to be about a tenth of this and indeed it can be shown that baryonic matter (protons and neutrons) cannot give more than about twenty percent of the critical density. Hence it is conjectured that there may be a large amount of unseen matter to raise us to the critical density; this has become known as dark matter. Particle theory provides many candidates for this, for example neutrinos may have a small mass, and there are so many neutrinos in the universe that even a mass of perhaps 20 eV would be

enough to explain the discrepancy. Other candidates are axions, or weakly interacting massive particles. The various types of dark matter can help to form density perturbations about which galaxies might form, but again a better knowledge of the particle theory is needed to provide input.

Perhaps the most fruitful area of interaction between cosmology and particle physics is that of inflation. Inflation is a mechanism, described below, which is much used to circumvent several problems with the standard cosmology. Most predominant of these are the horizon and flatness problems, first emphasised in detail by Guth.

The standard cosmology postulates homogeneity and isotropy, but the horizon problem is concerned with why this should be so. Look up in the sky at two points separated by, say, sixty degrees (in fact we can use a much smaller number). From each we can observe the microwave background radiation at its characteristic temperature of around three Kelvin, which indeed is roughly constant across the sky. But if we trace back the histories of the two points we are looking at, we find that light has not yet had time to get from one to another; that is, the two regions have never been in causal contact with each other. Hence there is no way that they have had an opportunity to reach thermal equilibrium, and therefore no reason why they should be at the same temperature. In fact, Guth showed that there is a huge ($\sim 10^{83}$) number of disconnected regions and no good explanation for their thermal equilibrium.

The second problem is the flatness problem. We know from direct observations that the universe has a density between about a tenth and ten times the critical density. However, the critical density is an unstable point; a universe above it will rapidly recollapse while in a universe below it the expansion is fast and the density rapidly falls to well below the critical density. In order for the universe to be so close to it today, it must originally have been phenomenally close (Guth estimates one part in 10^{55}). So again we have an extreme fine tuning problem.

The inflationary universe was suggested by Guth as a resolution of these two problems. In this scenario, the universe undergoes early in its history a period of very rapid expansion, usually taken to be exponential. During this phase, small areas which have been in thermal contact are expanded by huge amounts, their volume increasing by a factor of around 10^{90}. One such small area would now constitute the entire visible universe. Such an expansion thus solves the horizon problem. Also it is a natural consequence of this rapid expansion that the universe becomes very flat due to its huge size. Hence inflation can in principle solve the two problems described above.

That is all very well in principle, but we need a mechanism via which such an expansion could actually occur. This is provided by phase transitions in particle theories; during these a huge amount of energy is released which drives the rapid expansion. Many people have worked to try and produce realistic scenarios, with differing amounts of success; there are in fact many constraints on inflationary processes which must be obeyed. Some of these topics will be pursued in chapter four.

Inflation can also be useful in other circumstances. For example, it was stated earlier that theories in which monopoles are produced usually feature an unacceptable overproduction. In such cases, inflation can play the role of diluting this excess monopole density because of the huge expansion, and so provided the monopole production precedes inflation the monopole problem in some GUTs can be avoided. It can also be shown that because of quantum effects inflation will produce density perturbations, thus raising the hope that inflation can also explain galaxy formation. In general though one has to be careful because the density perturbations are several orders of magnitude too large, and often fine tuning is required to bring them down to acceptable levels.

Finally, it is worth considering how cosmology is affected by such theories as Kaluza-Klein, supergravity and superstrings. While those that have gone before only

affect the particle interactions, these theories, by trying to draw gravity into the general framework, actually modify the structure of the gravitational interaction. This occurs in two ways. Firstly, these theories usually have extra hidden dimensions, and cosmologically the effect of these can be important through their modification of the Einstein equations. Secondly, in the case of superstrings the actual gravitational Lagrangian is modified by higher order terms which change the equations of motion even classically. In fact, these higher order terms can be useful in aiding the construction of inflationary models. Cosmology can provide an opportunity for studying the validity of these modifications to the Einstein equations.

Having said all that about the use of particle physics to cosmological ends, it is worth making a few comments about what particle physics can gain from this interplay. In many situations, cosmology can provide very useful constraints on the construction of particle theories, because it allows access to events at energies well in excess of those which can be attained in current or forseable particle accelerators. Any particle theory with cosmological predictions at odds with observation can of course be ruled out.

An example of a useful constraint from cosmology is the setting of an upper limit on the number of neutrino flavours. The number of flavours affects the process of nucleosynthesis and it seems that unless there are five or less flavours observations cannot be explained. Since it is assumed that the number of neutrinos is the same as the number of families of quarks, this prediction tells us that there is a limit to the number of generations of particles allowed in a gauge theory. Cosmology can also provide upper limits on the masses of neutrinos, a limit which turns out to be of around the same order as that obtainable either by terrestrial or astrophysical experiments.

Cosmology can also provide restrictions on symmetry breakings. As mentioned above, certain symmetry breakings will produce vacuum defects such as domain walls. Since heavy domain walls certainly do not exist, any GUT phase transition

which would produce them is disallowed. Monopoles are a more serious obstacle; it can be shown via group theoretical methods that any series of breakings from a GUT group down to the standard model must at some stage produce monopoles. Hence for GUTs to be acceptable some mechanism, such as inflation, must dilute their huge overproduction.

Higher dimensional theories can also be constrained by cosmology. In general, in the early moments all dimensions in such a theory are of similar size; it is only later that a differentiation in size between them will occur. However neat a higher dimensional theory may be, if it cannot explain satisfactorily why its evolution leads to some large and some small dimensions then it must be rejected. At this time it is fair to say that in most cases the early dynamics of these models are so complicated that it is not known how these processes, particularly concerning the splitting in size, might occur.

To conclude this section, it is fashionable amongst authors to show a schematic diagram of the evolution of the universe showing the timings and energy scales. Figure 1.3 illustrates how the universe might have evolved given some of the ideas mentioned in this chapter, and should be read from the bottom up. (This diagram owes a lot to a similar one in [1].) In a few years several of these possibilities may have been confirmed or eliminated. On the other hand, the diagram may look completely different. Many of the features within it would have been absent ten years ago.

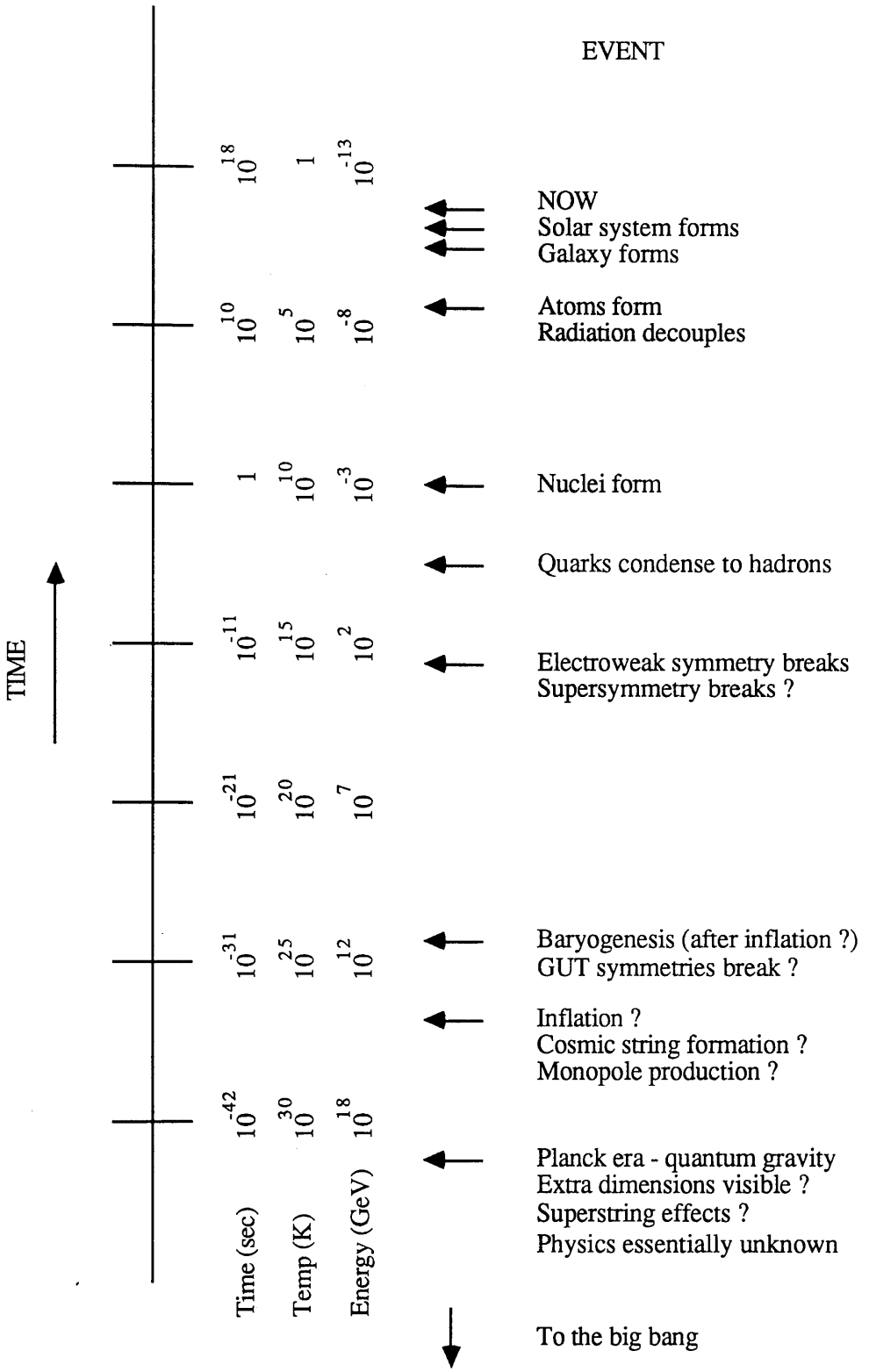

Figure 1.3 The history of the universe, as favoured in 1989.

(iv) Astrophysics and Neutron Stars

Having concluded our review of contemporary cosmology, it is time to turn to consideration of the other subject mentioned in the thesis title, astrophysics. Astrophysics is physics on a scale only slightly less grand than cosmology; it is the study of the various objects which reside within the universe. There are a whole range of objects observed which astrophysicists strive to understand. There is a wide variety of stars, from conventional hydrogen burning stars like our own sun, to the rapid evolutionary life of the red giant star, to the white dwarf remains at the end of stellar evolution. Then the theory of relativity provides us with more unusual configurations, expected to be found when stars collapse at the end of their evolutionary cycle, such as neutron stars and black holes, the birth of which may be heralded by novae or supernovae. At the extreme distances seen by modern telescopes, small objects called quasars radiate huge amounts of energy and remain a mystery. The study of all these objects falls into the realm of astrophysics.

All these objects have been observed by astronomers, with the possible exception of black holes for which the evidence remains circumstantial though convincing. For the most part, these stellar objects are well understood, with a solid knowledge of the evolution of stars being well known certainly up to the time when they have no more fuel to burn. When they reach this stage, they are effectively at the end of their lifetime as stars, and are expected to collapse to form one of the dense objects named above. The particular object formed depends for the most part on the mass of the star, though there is some dependence on the mechanism of collapse itself which is hard to determine. In this thesis we are predominantly interested in the collapsed objects thus formed, for it is they which have high densities and for which the notions of relativity are required for a proper treatment, while stars can be fairly well described using entirely Newtonian physics. Hence here a brief review of stellar collapse and the dense objects formed is provided; for more details the book by Shapiro and Teukolsky [2] is an excellent reference.

A star's lifetime comes to an end when it has no fuel left to burn. In its early years a star will be fusing hydrogen to form helium while near the end of its evolution it may become sufficiently dense that it can fuse these elements together to form yet heavier ones, such as carbon, oxygen, and ultimately even iron. However, iron represents the limit to how far this process can go - either breaking it into pieces or fusing anything with it requires an input of energy, so the star cannot use these processes to keep burning. At the end of its life, a star may be made from a central core of iron, surrounded by shells of successively lighter materials at radii where the density is too little to allow them to fuse, giving an overall structure somewhat like an onion. It has no fuel left, and its evolution takes a drastic turn.

A collection of atoms on their own will always tend to collapse gravitationally towards some common centre; in the case of a star this collapse is prevented by thermal pressure created by the burning of fuel. When the fuel runs out, this pressure is no longer present and so the star must collapse inwards to form a new object. White dwarfs and neutron stars are characterised by their very small size, because the only thing which keeps them from complete collapse is the pressure of degenerate electrons in the former case and of degenerate neutrons in the latter. In the case of a black hole, the original star was so massive that even these forces cannot prevent collapse, and the matter collapses completely to a singular point. The actual process of collapse is not of direct relevance here, only that collapse to one of these objects seems inevitable. Some models of collapse do exist, and it is even possible to construct models of stars which undergo supernova explosions at the end of their lifetime such as that observed in 1987 in the Magellanic Clouds. Unfortunately, the details of collapse can be very awkward and it may be hard to estimate how much matter collapses inwards to form the new object and how much is ejected by explosion mechanisms or thrown off by the rapid rotation induced as the matter collapses inward.

Here we shall focus our attention on neutron stars, which can be formed in the

collapse of objects of mass over perhaps five times the mass of our sun. Because of the uncertainties in the amount of matter thrown off, it is not well known which of these masses will lead to neutron stars and which to black holes. However, it is known that neutron stars can be formed because astronomical observations can actually detect them. In 1967, a group at Cambridge discovered a source of regular pulses of radio waves, with a period of around a second. Such sources were later given the name pulsars. Several explanations were proposed, but the only one accepted today is that pulsars are in fact rotating neutron stars, with the pulses generated by particles escaping along the axis of a strong magnetic field associated with the star. This explanation for the phenomenon arises because the pulses are rapid and remarkably evenly spaced, hence they must originate from a very small dense source. Further evidence is provided by the observation of a pulsar in the remnants of the 1987 supernova, where a neutron star would be expected to have formed.

Here we are mostly interested in the theoretical aspects of neutron star structure. These objects are dense enough to require general relativity to be taken into account, and this was first done by Oppenheimer and Volkoff in 1939. Because of the exclusion principle, neutrons have a long mean free path and are well described as a perfect fluid. In their model they used an equation of state for this fluid proposed by Chandrasekhar which describes non-interacting fermions in thermal equilibrium. What they discovered was that the class of neutron stars is parametrised only by the central density of the star, and further that there was a maximum mass (about 0.7 times the mass of the sun) for which stable neutron stars exist. This important observation remains a feature of more up to date models, though the maximum mass which can be obtained is higher.

The only real difference between this model and ones considered today is that much more complicated equations of state for the matter are used; these include many features over a whole range of densities, such as nucleon interactions, and the

neutron stars feature shells of different types of matter, but the details of these shall not interest us. These models are required over the Oppenheimer-Volkoff version because they allow a higher maximum mass, which is necessary as neutron stars of more than the sun's mass have been seen. A maximum mass of between 1.5 and 3 times the sun's mass is common in the wide range of models that exist now.

The aim in chapter five is to examine how the existence of an extra dimension, as advocated by several popular particle theories, might affect the structure of neutron stars. In our studies, we will restrict ourselves to looking at the Oppenheimer-Volkoff case, while always remembering that an accurate treatment would require a more sophisticated equation of state. The reasons for this are twofold. Firstly, this is done for simplicity to prevent any effects that we see being tangled up amongst those of a complicated equation of state, but more importantly it is done for reasons of consistency. The extra features we add - the effect of an extra dimension in chapter five and of adding an interacting boson field in chapter six - are introduced without consideration of any complex interactions which they might be involved in, and given this there is no good reason for taking such interactions into account in the neutron terms. Hence we will use the Chandrasekhar equation of state which corresponds to non-interacting neutrons, in the assumption that interesting effects here will generalise to a more realistic equation of state. This then forms the basis for our investigations.

(v) Scalar Fields and Boson Stars

Here we consider some rather more unusual stellar objects which might exist in our universe. These have a markedly different status from those which were discussed in section (iv) in that as yet they have not been observed by astronomers. Their position is instead that they are predicted as possible consequences of current particle theories, and they are examined on that basis. The best motivation for their study is in the possibility that the dark matter in the universe, if it does indeed exist,

may reside in heavy unconventional stellar objects rather than in the form of, for instance, free neutrinos or axions. Hence here we consider the possibilities for stars made from bosons rather than conventional fermionic stars such as neutron stars.

We shall primarily be interested here in what have come to be known as boson stars. Given the intense usage of scalar fields in cosmology, it is an interesting question to consider whether or not stars can be made from bosons in equilibrium with gravity; these are the bosonic analogue of neutron stars. It turns out that such objects can exist, with the gravitational attraction balanced by pressure forces which can be viewed as having their origin in Heisenberg's uncertainty principle. However, the treatment is slightly different to that of neutrons; for fermions the perfect fluid approximation is good and gives accurate results, but for bosons this approximation breaks down. Fortunately, in the case of the scalar field the treatment using the field itself is quite simple. It was shown that the class of possible stars is parametrised purely by the central value of the bosonic field, just as the class of neutron stars is purely determined by their central density. Overall, the results from the two cases are remarkably similar, with the boson stars also featuring a maximum stable mass which depends only on the mass of the scalar particle and on the strength of its coupling. One major difference though is that the boson field vanishes only asymptotically, though it does so exponentially quickly. A neutron star in contrast has a definite edge.

Original studies of boson stars concentrated on the simple case where the bosons do not interact with each other. It turned out that the stable configurations in this case are very light, which led to some waning in the interest in these objects. However, it was later shown that if the scalar field is self interacting, such as a Higgs particle in the standard model, then the interaction term is very important even if the dimensionless coupling is very small. This leads to configurations which have a higher maximum mass, allowing them to be at least of comparable size to fermionic stars.

There are other objects which can be made from scalar fields, in which we have no direct interest here; these have come to be referred to as Q-balls and non-topological solitons. These too are localised bosonic objects, but their existence derives from extra couplings which compete to localise the energy density, essentially by introducing surface and volume terms in the effective potential, and may require additional bosonic or fermionic fields. Gravity is not important in their construction. We shall therefore restrict ourselves to the simple couplings and take gravity fully into account.

(vi) Scalar Fields in Cosmology and Astrophysics

This section describes more specifically the work which is detailed in this thesis. As the thesis consists of several separate sections which in principle stand alone, detailed introductions are instead supplied at the start of the relevant chapters. The aim of this section is instead to provide an overview of the thesis and to discuss some common themes which appear therein, primarily the pervasive influence of scalar fields and their consequences in both cosmological and astrophysical contexts.

In recent years, scalar fields provided by particle theories have been leapt upon by cosmologists as a source of cures for all manner of cosmological ills. While it is fair to say that a large part of this is based upon the fact that the scalar field is by far the easiest such object to handle, it is also true that scalar fields have many special properties which justify the enthusiasm with which they are used. Realms of physics in which scalar fields play an essential part include inflation, where it is observed that the scalar field can conveniently provide a temporary cosmological constant, and cosmic strings, where flaws in the scalar field vacuum create massive string loops onto which matter may accrete to form galaxies. In a more peripheral role, scalar fields are also studied in other cosmological settings, where they often appear in the guise of extra dimensions such as those found in Kaluza-Klein theories and superstrings. Much examination is also made of the consequences of less visually

obvious fields, such as the light axion introduced to solve a difficult particle theoretical problem known as the strong CP problem, which in a role as dark matter may also help solve the mystery of galaxy formation. Even the possibility of stellar objects constructed from scalar fields, known as boson stars and non-topological solitons, has received much attention in the last few years.

Despite this attention, it must be remembered that as yet *no scalar field has been observed in nature* . This is not to say however that there are not vast numbers of candidates for them, and almost all physicists would believe in the existence of at least one. The most famous possibility is the Higgs boson, which may soon be observed at LEP and which is essential in the construction of the standard model and gives the origin of mass in the universe via symmetry breaking. Generalisations of the standard model to GUTs usually require further Higgs bosons for symmetry breakings at higher masses - these are popular for construction of inflationary models. Other candidates are the axion, mentioned above, and there also exist fundamental scalars in supergravity models. Finally, compact extra dimensions in higher dimensional theories are often formally equivalent to scalar fields. One of the main aims of particle cosmology is to provide evidence of the existence or non-existence of various scalar fields, providing a much needed alternative to the accelerator program which is unlikely to reach much higher energies than are available now.

This thesis is concerned primarily with investigating various effects of scalar fields, both in cosmology and astrophysics. The individual topics considered are for the most part unrelated, but various connections can be weaved between the constituent parts. Chapters two to four are concerned with cosmology. Chapters two and three follow the theme of cosmological solutions in a higher dimensional theory, based around a specific theory related to the low-energy limit of the superstring. Here the scalar field arises as a fundamental object; it is already present in the Lagrangian of the theory, and is known as the dilaton. Its effect on the equations of

motion in the model is noted; it damps chaotic motion on the way to the singularity and also affects the behaviour of the spacetime as it expands towards large sizes. In chapter four a completely different theme is chosen - an examination is made of a class of solutions giving a type of inflation known as power law inflation. In the most general case considered, the origin of the scalar field is not specified; it is merely assumed that it has a particular type of potential, one commonly found in many theories. Later on in this chapter a specific model is considered, where the scalar field corresponds to the size of an extra dimension, and it is shown in this context how to construct an inflationary model based on the ideas contained in this chapter.

A common idea to these three chapters is a consideration of an extra consequence of having a dynamical scalar field present in the theory; that the variation of the field will in general produce particles via its couplings to other fields in the theory. In each instance the effect of this is examined. The treatment in each of these chapters is slightly different, but in each case the particle production leads to terms resembling a viscosity term, as they tend to damp the motion of the scalar. This can have a major influence on the behaviour of the system as a whole, and also can provide some indication of how the model universes that we consider might evolve towards the one we observe today.

Chapters five and six move off on a different tack, by considering the influence of scalar fields on astrophysical objects. Chapter five looks at how the existence of fundamental scalar fields might affect the structure of astrophysical objects; the motivation here is in the idea that extra dimensions give formally the same equations of motion as we obtain by adding real scalar fields to conventional relativity. In the presence of compact astrophysical objects such as neutron stars, general relativistic effects become significant and so one might hope that the existence of extra dimensions would betray itself. Neutron stars are studied as a possible source of information about the extra dimensions. The analysis also holds for fundamental real

scalar fields, but in this case it is the extra dimensional interpretation that is potentially of the most interest.

Chapter six follows a similar line, only here the scalar field, now massive and self-interacting, is used to make up some of the substance of the star, rather than the picture of the star being affected by the different geometry caused by the extra dimension. The scalar field may now be complex or real; in the complex case the equilibria feature only one independent scalar field component. This is following the idea of boson stars, massive stellar objects constructed from bosonic particles, which has been given much attention recently. (It is also possible to construct a class of stellar objects known as non-topological solitons, but these are not considered here.) Here we consider the combination of both bosons and fermions in a stellar object, whereas previously only one or other was taken into account. The scalar field in this instance is imagined to be a fundamental scalar field of some characteristic mass; particle theory provides several candidates such as the heavy Higgs particle or the light axion which might fulfil this role. These combined Bose-Fermi stars generalise the concepts of both neutron stars and purely bosonic stars.

(vii) Some Notes on Conventions

Conventions used in this thesis follow those of Misner, Thorne and Wheeler [3]. In particular, the signature of the metric is chosen as (- + + +) , i.e. with the timelike direction given the negative sign (in extra dimensions add more plus signs). Unless stated otherwise in the text, natural units are used throughout with the speed of light, Planck's reduced constant and the gravitational constant all set to one. When required, these will be denoted by c, $\hbar$ and G respectively.

The metric will be referred to as $g_{\mu\nu}$, with the scale factors denoted a or r. Scalar fields are normally indicated by Greek letters; in particular ϕ and ξ are often used. Normally an overdot will mean a time derivative and, unless another meaning is obvious from the context, a dash will refer to a spatial derivative with the precise

variable of differentiation specified in the text. If a particular symbol is used frequently within a chapter, it is defined once and its meaning assumed thereafter; meanings do not carry between chapters except between chapters two and three which are the only chapters which follow on directly rather than being self contained.

Many of the equations in this thesis were derived or checked using the computer algebra program REDUCE [4], which proved invaluable in the manipulation of complex expressions.

Chapter 2

Cosmology of the Dilaton and H field from Superstring Theory

(i) Introduction : Cosmology and the Superstring

Superstring theory [5] (see also chapter one, section (ii)) has been proposed as a candidate for the much vaunted 'theory of everything' which has been one of the prime goals of particle theorists this century, and particularly over the past twenty years; that is, it provides a framework in which the four fundamental forces of nature may be unified. While it has been known for some considerable time how to unify the strong, weak and electromagnetic forces into a single theory, known as the 'standard model' [6], superstring theory is the first realistic attempt to also include gravity in its picture, and so for the first time many theorists are optimistic that the theory may be the ultimate description of matter. It is however true that superstring theory has a long way to go before it can be accepted as such a description, for there are many problems in relating the superstring theory of high energies with the universe we see around us today.

Interest was centred on superstrings following the important paper of Green and Schwarz [7] in which they showed that the superstring theory is plagued with anomalies associated with the gauge symmetry group, *unless* the symmetry group was one of only two very large groups, those known as SO(32) or $E_8 x E_8$. Hence for the first time there was actually a motivation for a particular choice of gauge group. Furthermore, the theory only worked if the number of space-time dimensions was ten, so again the superstring allows us to pin down the type of theory allowed. It was the existence of these two restrictions which led to the huge rush of theorists into the study of superstring theory around 1985.

[Note - It should be pointed out that since the work detailed in this and the following chapter was carried out, methods have been discovered by which string theories in dimensions other than ten can be constructed, and in particular there are some constructions in four dimensions [8]. These theories do however lose a lot of the elegance of the original superstring theories, and seem to have less phenomenological possibilities. It is fair to say however that the existence of superstring theories in a wide variety of dimensions, and with many possible gauge groups, removes a lot of the motivation for believing that one day superstring theory might provide the 'theory of everything' ; how do you choose from the wide range of possible string theories? The neatest theories still remain the original ones of Green and Schwarz.]

Given that the ten dimensional superstring is worth studying, there are many different areas which people have looked at over the past few years. The physics of the string theory itself has received much examination; to determine what kind of particles might appear as modes of the string, to analyse the cross sections of string-string interactions, to examine the symmetries of the string theory, to attempt to classify the types of string theory - the list is endless. Here we are interested instead in trying to see how the superstring might explain the universe around us today, a field known loosely as superstring phenomenology.

Clearly there is a lot of explaining to do. The most obvious drawback is that the string theory is ten dimensional, whereas we see only four dimensions. A solution to this problem is provided by the original Kaluza-Klein work on higher dimensional theories; what we do is postulate that the extra six dimensions are curled up to be very small, so that they are unobservable to us. The standard analogy here is that of a hosepipe; seen from a large distance it looks just like a one-dimensional line, but close up we see that at each point of the original line is in fact a small circle, and that the hosepipe is in reality two dimensional. This curling up procedure is known as 'compactification'. Mostly, attention has been focussed on what the physical

situation is after compactification, imagining a fairly static situation where the extra dimensions have already curled up in some way. Hence our universe already appears four dimensional. There is another advantage of compactification. The string theory features the colossal symmetry groups mentioned above, which have to be broken down towards that of the standard model if they are to explain everyday particle physics. Depending on the form of the internal space, the compactification itself will actually break some of the gauge symmetry due to non-trivial gauge configurations on the internal space, a process known as flux-breaking. One example of such a space is a Calabi-Yau space [9], which was much favoured in the early studies. In principle, complete knowledge of the compactification gives details of the low energy effective theory, and some authors have displayed specific models though never anything compelling.

In this and the following chapter we are interested in another aspect of the compactification problem, that of how it might actually have occurred. This is the point at which cosmology begins to interact with the superstring theory. Naturally, we are not going to be so ambitious as to try and analyse a compactification to some complex internal space as mentioned above; we are merely going to examine ways in which three of the spatial dimensions might become large while the other six remain small (around the Planck length). The picture we have therefore is one of evolution as the universe grows larger.

At early times, round about the Planck era, we expect that all the ten dimensions are on an equal footing and here the dynamics of the universe are essentially 'stringy'. The processes occurring at this stage are almost completely unknown. The universe continues to expand and falls to energies below the Planck scale; at this stage we are entering the realm where we can begin to comprehend what the string theory means in terms of an effective low energy field theory. The relevant field theory has been shown [10] to be an N=1 Supergravity theory in ten dimensions, much studied in recent years. Hence we are interested in seeing if there are

cosmological solutions in this theory, with additional restrictions from superstring consistency requirements, which lead to appropriate behaviour for compactification. We will also study various other solutions with regard to a particular model, the construction of which will be outlined in the next section. To outline this work, the remainder of this chapter is devoted to approximate analytic techniques having constructed a specific model. Chapter three then details the numerical approach to exact solutions of the relevant equations. Chapter three will also consider extensions to the basic scenario such as production of particles caused by time variation of the scalar field in the theory.

(ii) The 3-Spaces Model

In this section we construct a specific model within the context of which we shall discuss superstring cosmology. We take the bosonic Lagrangian, derived as a classical low energy effective field theory from the superstring, as being the basic quantity; it has been shown [10] that the low energy limit of superstring theory is the ten-dimensional supergravity theory as originally discussed in [11]. While cosmologists often concentrate purely on the scalar fields in a particular theory, and use them for purposes such as inflation, cosmic string formation and so on, we wish to be somewhat more general by considering the entire bosonic sector of the theory. This consists of three fields. There is the graviton which provides the gravitational interactions via the standard Lagrangian term, given by the scalar curvature. There is also a scalar field, usually referred to as the dilaton, which we shall refer to throughout as ϕ, and finally there is a three index antisymmetric tensor field, denoted $H_{\mu\nu\rho}$, which can also be written as a three form. When we are using the form notation we shall refer to it simply as **H**. The Lagrangian which we require is given by

$$\frac{1}{e}\boldsymbol{L} = -\frac{1}{2}R + \frac{1}{4}e^{2\phi}H_{\mu\nu\rho}H^{\mu\nu\rho} + \partial_\mu\phi\,\partial^\mu\phi \qquad (2.1)$$

where e is the determinant of the vielbein (equivalently $\sqrt{-g}$, where g is the determinant of the metric).

Here we are specifically neglecting extra effects coming from the superstring, such as additional R^2 terms in the Lagrangian, or actual 'stringy' effects. Such effects should only be important above or near the Planck scale, where we have no real knowledge of the processes which might occur. It is therefore natural that our attention is focussed on an era where the energies are somewhat less than this, where we can expect our Lagrangian to be valid. We also treat the Lagrangian as a classical field theory, since again quantum effects should be important mainly at Planck energies and above.

The following section is based on a construction by Henriques and Moorhouse [12], on whose paper the majority of this chapter is based. Further details can be found there. The basic idea now is that we use the **H** field to split the nine spatial dimensions into three spaces, each of dimension three, which we shall refer to throughout as 3-spaces.We achieve this by making the ansatz that **H** is given by

$$\mathbf{H} = h_1(t)\,\Omega_1 + h_2(t)\,\Omega_2 + h_3(t)\,\Omega_3 \qquad (2.2)$$

where Ω_i is the volume form on the i -th 3-space (and therefore necessarily a three form). It can be shown that this ansatz allows the equations of motion for **H** to be satisfied, and, provided the 3-spaces are of suitably simple topology (examples include 3-tori and 3-spheres), an additional integrability condition arising from the superstring is also satisfied [12].

This type of ansatz is in fact well known from earlier studies of compactification in supergravity theories; it is a generalisation of the Freund-Rubin mechanism [13] of compactification in eleven dimensional supergravity. That theory features a four form field, called **F**, and the Freund-Rubin ansatz is that this is proportional to the volume form on four of the eleven dimensions, in an analogous way to equation (2.2) above. Our ansatz is similar, though now in the ten dimensional theory with a

three form field, but it is more general in that the **H** field takes values on each of the 3-spaces, not just a particular one which we are trying to force to large sizes.

In traditional Kaluza-Klein fashion [14], we factorise the metric into separate scale factors on each of the three 3-spaces. Normally in Kaluza-Klein there is a simple two-way split into a metric on the four external dimensions we see today and a metric on the remaining internal dimensions, but again here we are slightly more general in splitting up the metric into a scale factor on each of the three 3-spaces. Our treatment also differs slightly in that we keep the time constant separate and introduce comoving coordinates so that the metric can be written as

$$ds^2 = - dt^2 + r_1^2 (t) \sum_{k,l=1}^{3} g^{(1)}_{kl} \, dx^k \, dx^l$$

$$+ r_2^2 (t) \sum_{k,l=1}^{3} g^{(2)}_{kl} \, dy^k \, dy^l + r_3^2 (t) \sum_{k,l=1}^{3} g^{(3)}_{kl} \, dz^k \, dz^l \qquad (2.3)$$

where the r_i are the scale factors associated with each of the 3-spaces and the g_{kl} are the metrics on them satisfying Einstein's equations. As mentioned above, not all choices of the metric will satisfy the integrability condition.

To guarantee that the equation of motion for the **H** field is satisfied, the $h_i(t)$ in equation (2.2) must satisfy the relation

$$h_i (t) = r_i^{-3} (t) h_i \qquad (2.4)$$

where the h_i are constants. Hence there is a characteristic value of h_i associated with each 3-space, which is conserved for all time, though of course we see from equation (2.4) that the actual size of the **H** field will reduce as the scale factor increases. The original value is an initial condition that would emerge from the Planck era.

We are now in a position, having coped with the ansatz on **H**, to write down

the equations of motion for the rest of the system, which will determine the dynamics. The equations will be for the three scale factors r_i, which will appear symmetrically, and for the dilaton field ϕ. These are obtained from the generalised Einstein equations, which are of course derivable via the variational principle from the Lagrangian (2.1), and from the equation of motion for the scalar field. In fact, we shall use the energy conservation equation to derive the equation for ϕ in a simpler, though equivalent, way. We shall not go into the details of the derivation here; these can be found in [12]. The equations for the system are found to be

$$\frac{\ddot{r}_i}{r_i} + 3\left(\sum_j \frac{\dot{r}_j}{r_j}\right)\frac{\dot{r}_i}{r_i} - \left(\frac{\dot{r}_i}{r_i}\right)^2 = e^{2\phi}\left(\frac{1}{2}\frac{h_i^2}{r_i^6} - \frac{1}{8}\sum_j \frac{h_j^2}{r_j^6}\right), \quad i = 1, 2, 3 \tag{2.5}$$

$$\ddot{\phi} + 3\dot{\phi}\left(\sum_j \frac{\dot{r}_j}{r_j}\right) = -\frac{1}{4}e^{2\phi}\sum_j \frac{h_j^2}{r_j^6} \tag{2.6}$$

$$3\sum_j \frac{\ddot{r}_j}{r_j} = -\frac{1}{8}e^{2\phi}\left(\sum_j \frac{h_j^2}{r_j^6}\right) - 2\dot{\phi}^2 \tag{2.7}$$

Equation (2.5) comes from the spatial Einstein equations, equation (2.6) from energy conservation and equation (2.7) from the time-time component of the Einstein equations (also from the Bianchi identities). These equations actually overspecify the system, since energy conservation is automatically guaranteed by the Einstein equations alone, so we have one redundancy. Notice that by substituting equation (2.5) into equation (2.7) we would obtain a first order equation, viewed as an expression for ϕ, explicitly given by

$$9\left(\sum_j \frac{\dot{r}_j}{r_j}\right)^2 - 3\sum_j \left(\frac{\dot{r}_j}{r_j}\right)^2 = \frac{1}{2}e^{2\phi}\left(\sum_j \frac{h_j^2}{r_j^6}\right) + 2\dot{\phi}^2 \tag{2.8}$$

and so we could discard equation (2.6) as being unnecessary. However, to preserve the symmetry between the r_i and ϕ we prefer to retain equation (2.6), which is second order in ϕ. If we do this, then we must impose equation (2.8) as an initial condition, but after that it is guaranteed that it is satisfied at all times by the other equations of motion.

Hence the four equations given by equations (2.5) and (2.6), coupled with the initial condition equation (2.8), give the dynamics of our model, and so we can now turn towards looking for solutions which are of cosmological relevance. The equations are coupled non-linear ordinary differential equations of second order in each of the four fundamental variables, so there are eight initial conditions required to completely specify the system. Having done this, we can examine which solutions exist. We will use two techniques to do this. Numerical work will be used to provide exact solutions, and the details of this will be given in chapter three. The remainder of this chapter will be concerned with approximate analytic methods that can be used, and which shall be seen to provide very useful intuition for analysis of the numerical work.

(iii) Chaos Damped by the Dilaton

We now consider approximate solutions to the equations of motion as described in the previous section. In a region where the potential terms are negligible (the potential terms are those in the equations of motion which feature h_i) we can solve the equations of motion by

$$r_i = a_i t^{p_i} \quad ; \quad e^{\phi} = a_4 t^{p_4} \tag{2.9}$$

where a_i and p_i are constants, and where the p_i must satisfy the additional constraint equations that

$$3 (p_1 + p_2 + p_3) = 1 \quad ; \quad 3 (p_1^2 + p_2^2 + p_3^2) + 2 p_4^2 = 1 \tag{2.10}$$

Notice that the second of these two constraints places an upper bound on the modulus of the p_i , and that the fact that there are two constraints on the four quantities implies that there are only two degrees of freedom for the p_i . It is the p_i that we will be primarily interested in; the a_i just correspond to a rescaling of the approximate solution.

Solutions of this type are very familiar from early studies of anisotropic cosmologies, initially by Kasner [15], and indeed we shall refer to a particular solution, with some specific values for the p_i , as a Kasner mode. In his studies, he used a metric (for normal four dimensional space) with a separate scale factor associated with each of the three spatial dimensions, and found that there was a solution identical to the first part of equation (2.9). (He, of course, had no scalar field.) There exist two constraint equations, analogous to equation (2.10); namely that the sum of the p_i should be one and the sum of their squares should also be one. This leaves one degree of freedom and we find, amongst other things, that the constraints force one of the p_i to be negative.

This scenario was revived in the late sixties by Misner [16,17] for his construction of the so-called Mixmaster model. He used the Kasner solutions as given above, and showed that, moving *backwards* in time towards an initial singularity, the spatial geometry would perturb the solution from one mode having Kasner indices p_i to another with indices p_i', where the p_i' are related in a specific way to the p_i . The idea at the time was that when one of the p_i is negative, light can circumnavigate the universe in the i-th direction. The switching between modes would allow light to traverse the universe in each successive direction, and hence solve the horizon problem (see introduction and [18]). This was one of the earliest attempts to solve this problem, but unfortunately it was later shown that the details of the switching between modes would not allow this scenario to work [19]. Currently, inflationary models are the standard way of solving the horizon problem. It should be pointed out that this work is still of relevance in terms of the very complicated

initial singularity it leads to, with switching of modes happening ever faster so that there is always an infinite number of switchings before any given time; this behaviour becomes chaotic [17,20]. It has been shown [19,21] that this type of singularity is very generic of anisotropic and inhomogeneous space-times, and the most general type of cosmological singularity may be to have Mixmaster behaviour at each point.

We find that our model can be analysed in exactly the same way as the Mixmaster model, and that very similar qualitative features arise. Here, we find that the potential terms (which we neglected in constructing the Kasner solutions), have the effect of perturbing us from one Kasner mode to another; in the Mixmaster model this role was played by spatial geometry terms. It is possible to find explicitly the iteration which gives us the new Kasner mode from the old one as we move *towards* the singularity.

In general, the potential terms may not remain negligible as we approach the singularity, because of their time dependence. Below we will consider the condition which allows a potential term to grow large; for now we assume that one of them does. We reorder the p_i so that it is the first potential term that is important while the rest are negligible. A careful choice of variables (details can be found in [12]) allows us to write the problem as a free particle moving towards a potential barrier. It will be reflected from this barrier, which corresponds to the transformation into the new mode. Solving this barrier problem leads to the iteration

$$p_1' = 1 + (p_1 - 1) \gamma \tag{2.11a}$$

$$p_i' = (p_i - (1 - 3 p_1 + p_4) / 4) \gamma \qquad i = 2,3 \tag{2.11b}$$

$$p_4' = - \frac{2}{3} + (p_4 + \frac{2}{3}) \gamma \tag{2.11c}$$

where

$$\gamma = 4 / (7 - 9 p_1 + 3 p_4) \qquad (2.11d)$$

This 'bouncing' from one Kasner mode to another will continue indefinitely towards the singularity, provided that there is always a potential term which becomes large as we approach the singularity. We have to reorder the p_i so that it is the first potential term that becomes large before reapplying the iteration. The spatial terms all go as t^{-2}, so we are looking for potential terms which grow faster than this. The condition for the i-th potential term to become large at small t can be seen from the equations of motion to be

$$3 p_i - p_4 > 1 \qquad \text{for } i = 1, 2 \text{ or } 3 \qquad (2.12)$$

There are many possible Kasner modes such that this condition is not satisfied by any of the p_i ; if the solution falls into one of these modes the potential terms will remain completely unimportant as we near the singularity and we will remain in the same mode all the way back. We therefore conjecture that the solution will bounce from one Kasner mode to another, and after a finite number of bounces it will fall into a stable mode and remain there. We note that in the absence of the dilaton field the situation is exactly as in the Mixmaster model; this is equivalent to setting $p_4 = 0$ in the iteration, and in particular in equation (2.12). Then the condition for instability is always satisfied by one of the p_i , so one potential term will always become large and we will get chaotic behaviour near the singularity. Hence it is the presence of the dilaton which is moderating the chaotic behaviour in the approach to the singularity.

To confirm our conjecture, a computer program was written to carry out the iteration and reordering. First of all a routine was designed to choose Kasner modes at random satisfying the constraints of equation (2.10). It is observed first of all that of this random selection, around about 40% are already stable under the criteria of equation (2.12). In a computer run simulating the behaviour of 50,000 initial Kasner modes, all were found to reach a stable mode after a finite number of bounces,

usually less than five. The highest number of bounces observed was 55 before reaching a stable state. Empirically, we conclude from this that the chaotic behaviour, of a type reminiscent of the Mixmaster model, is indeed damped out by the presence of the dilaton, and that only a finite number of oscillations will result during the entry to the singularity from a starting Kasner mode.

The analysis of the iteration by computer produces another important piece of information. First of all, we note that the iteration as shown has a single fixed point; that is, there is one mode which, under the iteration, would be mapped back to itself. This is given by the values

$$p_1 = p_2 = p_3 = \frac{1}{9} \quad ; \quad p_4 = -\frac{2}{3} \tag{2.13}$$

This point is actually on the border line between stability and instability since it has $3p_i - p_4 = 1$ for all i. Incidentally, it also has the smallest possible value of p_4. It is not clear from the arguments above whether or not this point is stable, but we note that even if it is iterated we finish in the same mode since it is a fixed point, so the stability question does not arise. Despite this, all the modes which are near to the fixed point are unstable, because if we decrease one of the p_i below 1/9, we have to increase another to stay consistent with equation (2.10). The same happens if we try to make p_4 nearer to zero.

What the computer simulations indicate therefore is that the fixed point is unstable, and so if the initial Kasner mode is 'near' to it (with respect to some metric), the mode will tend to drift away from it towards the stable region. If we start very close to the fixed point it takes a very large number of bounces to get to the stable region, and we can arrange for an arbitrarily high number of bounces by starting sufficiently close. This situation is represented in the schematic drawing below, figure (2.1). Here modes are represented by points in a plane, which is finite in size since the modulus of the p_i is bounded. That it is a plane is justified by the

fact that there are only two degrees of freedom; however, we do not have an explicit representation in terms of two independent coordinates which is in principle possible. Hence it should be remembered that the illustration is purely a schematic interpretation of the effect of the iteration.

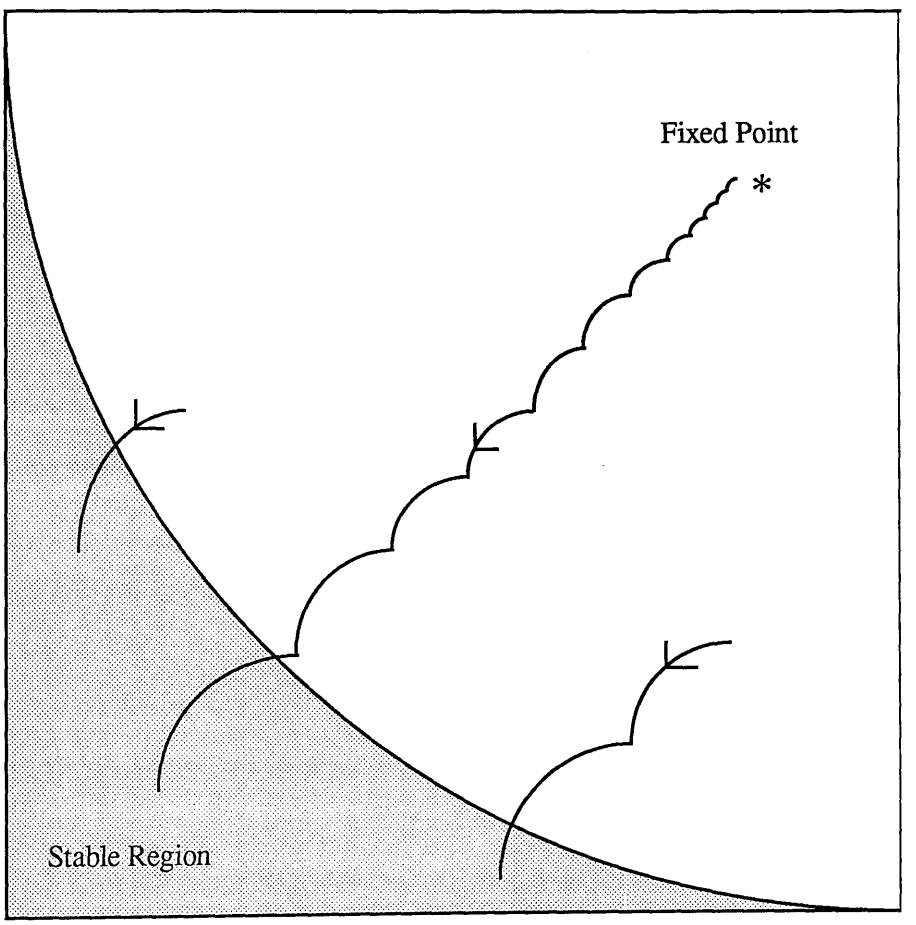

Figure 2.1 As we approach the singularity, the solution 'bounces' away from the fixed point, illustrated by a star, towards the large stable region.

(iv) Solutions Forward in Time

Having demonstrated that the bouncing terminates as we move towards the singularity, we now turn our attention towards the behaviour as we move forwards in time. Again we want to devote attention here to an analytic approach, with numerical work detailed in the next chapter, so once more we concentrate on the iteration as given by equations (2.11).

It can be shown that the iteration has a very special property, which is that if we act it twice on a given mode, *without reordering* , we return to the original mode; that is, denoting the iteration by **I** we have

$$\mathbf{I}^2 (p_1,p_2,p_3,p_4) = (p_1,p_2,p_3,p_4) \tag{2.14}$$

What must be remembered is the extra complication which is introduced by having to rearrange p_1, p_2 and p_3 each time so that it is p_1 which is associated with the unstable mode; the situation we have is therefore more involved than just the iteration itself, which is why computer simulation is a necessary tool. However, we can extract one vital piece of information from equation (2.14); the iteration is its own inverse,

$$\mathbf{I}^{-1}(p_1',p_2',p_3',p_4') = \mathbf{I}(p_1',p_2',p_3',p_4') = (p_1,p_2,p_3,p_4) \tag{2.15}$$

Now we have a different supplementary condition which gives the ordering of the p_i' before we iterate; it is determined by having the mode *after* the iteration satisfying the condition for instability $3p_i - p_4 > 1$. This condition ensures that we do get the inverse behaviour as we go forwards in time. It is not particularly surprising that the iteration is its own inverse when we consider the moving particle interpretation of the bouncing, because in this picture (details in [12]) the particle is moving perpendicular to the barrier. Hence the inverse is just obtained by reversing the particle path, which gives exactly the same situation as we had originally and hence

the same iteration formulae. We emphasise that it is the supplementary stability condition and necessary reordering which give rise to the results we observe.

We are now in a position to once again use computer simulation, this time to investigate what happens as we move forwards in time. The first observation we make, which is certainly not immediately obvious, is that under the iteration (i.e. backwards in time) all points in the stable region are images of points outside it. As we move forwards in time any point in the stable region will be mapped out of it; there are no modes which are stable as we move forwards in time and so in this direction Kasner oscillations will continue indefinitely. The other possibility, that there could have been modes stable in both directions, does not occur.

Given the lack of stable modes, we find that all modes are drawn towards the 'fixed point' mode given by equation (2.13), which is what we might expect from the analysis of behaviour towards the singularity. Hence the solution is behaving as though the fixed point is an attractor. We must emphasise that there is an important difference between this situation and the usual theory of attractors [22]. In the normal case, repeated application of an iteration takes a solution towards a point or set of points (e.g. a limit cycle). Here we have the added complication that there is the extra stage of reordering of the p_i ; hence the situation is more complex, and there is no obvious way to analyse the attractor further. We are therefore forced to treat the observation by computer that it is an attractor as an empirical fact. Figure (2.2) illustrates this behaviour, essentially the inverse of figure (2.1).

The physical significance of this attractor is that, provided our approximations remain valid, the solutions to the original differential equations at late times should tend to the fixed point Kasner mode, giving

$$r_i = a_i t^{1/9} \quad ; \quad e^{\phi} = a_4 t^{-2/3} \tag{2.16}$$

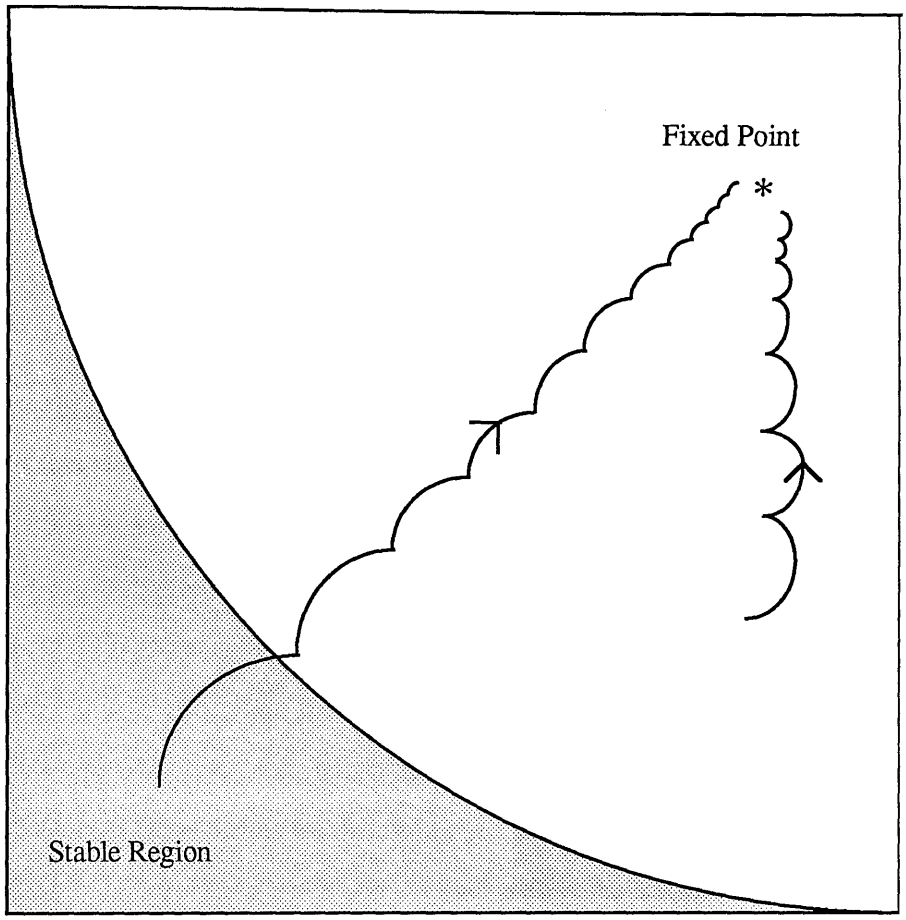

Figure 2.2 Moving forwards in time, all modes are drawn to the fixed point

The validity of our approximations will be considered in the next chapter, where numerical work will be utilised to investigate the accuracy of the results that we have obtained here. Discussion of what these results mean will also be reserved until the next chapter, where the tie up between these analytic methods and the exact numerical solutions will be exhibited.

Chapter 3

Numerical Solutions to Superstring Cosmology, and the Effect of Particle Production

(i) The Need for Numerical Simulation

In this chapter we continue the theme of chapter two, but shift the emphasis from approximate analytic techniques to using numerical simulation as a means of obtaining solutions to the field equations given by equations (2.5) and (2.6), with an initial condition constraint supplied by equation (2.8) as described in the previous chapter. Numerical solution has the advantage that we are able to deal with the complete equations, and we no longer have a need to neglect potential terms in some circumstances. These results are therefore intended to complement the analytic ones described in the previous chapter, and we shall see that the analytic results give us an ideal framework within which to explain the full numerical results.

The main reason for wishing to see numerical results is that it will indicate how good the approximations which were made to obtain the analytic solutions are. Amongst other things, we want to see whether the Kasner structure of the solutions and the bouncing from one mode to another is a genuine effect or just an artifact of the approximations that we made. We shall find out that the picture of modes bouncing from one to another is indeed a good one, and in the numerical simulations we shall be able to clearly identify the progression of Kasner modes. The exact results also cast light on the actual bouncing itself, about which little information can be extracted via the iteration picture as described in chapter two. Numerical simulation also allows us to test the variation of the solutions under a wide range of differing initial conditions.

A description of the numerical techniques used is given in appendix one, where

the setting up of a sample program based on a problem from a later chapter is given. Numerical simulation is a common theme throughout this thesis; here the equations are somewhat more complex than those discussed in, for instance, chapter four, but the method of solution remains the same in all cases, with use being made of library routines on the physics department mainframe IBM. These routines feature stringent internal accuracy requirements.

In this chapter, section (ii) will describe the setting up of the problem and a discussion of which initial conditions should be investigated, concluding with an investigation of behaviour as we move backwards in time towards an initial singularity. Section (iii) then continues with an examination of the types of solution as we move forwards in time; this is the main theme of this chapter which is concerned primarily with examining cosmologically relevant solutions to the equations of motion. Here the nature of the 'fixed point' as described in chapter two, section (iv) is elucidated and the long term behaviour categorised. Section (iv) continues in the same theme examining a slightly different model, where the **H** field only takes values on one 3-space.

The remainder of the section is concerned with extending the basic model by considering the effects induced by introducing a simple model of particle creation. Section (v) sets up the basic motivations and formalism for this, and then sections (vi) and (vii) examine how it affects the solutions found earlier. Ultimately, section (viii) concludes the chapter with a summary of the results obtained in chapters two and three, with some conclusions based on the contents of these chapters.

(ii) Towards the Singularity

For convenience, it is useful to make a redefinition of the scalar field before embarking on the numerical work. This is done to bring out more clearly the analogies between the structure of the equations for the r_i and the dilaton. By making the substitution $\xi = e^{\phi}$, we can write the equations of motion (2.5) and (2.6) in the

form

$$\ddot{r}_i + 3\left(\sum_j \frac{\dot{r}_j}{r_j}\right)\dot{r}_i - \frac{\dot{r}_i^2}{r_i} = r_i\xi^2\left(\frac{1}{2}\frac{h_i^2}{r_i^6} - \frac{1}{8}\sum_j \frac{h_j^2}{r_j^6}\right) \quad , \quad i = 1,2,3 \qquad (3.1)$$

$$\ddot{\xi} - \frac{\dot{\xi}^2}{\xi} + 3\xi\left(\sum_j \frac{\dot{r}_j}{r_j}\right) = \frac{1}{4}\xi^3\left(\sum_j \frac{h_j^2}{r_j^6}\right) \qquad (3.2)$$

with the constraint equation (2.8) becoming

$$18\left(\sum_j \frac{\dot{r}_j}{r_j}\right)^2 - 6\sum_j \left(\frac{\dot{r}_j}{r_j}\right)^2 - 4\left(\frac{\dot{\xi}}{\xi}\right)^2 = \xi^2\sum_j \frac{h_j^2}{r_j^6} \qquad (3.3)$$

When the equations are written in this way the analogy between r_i and ξ which leads to the Kasner mode structure can clearly be seen. Notice however that when the right hand side of equation (3.3) is no longer assumed to be zero this term prevents an exact Kasner relationship from holding.

This last point is important when we come to consider which initial conditions are sensible to supply to the integration; equation (3.3) tells us that we cannot start in an exact Kasner mode. However, in regions where the potential term is small, i.e. well away from a bounce point, a slight perturbation out of a Kasner mode will satisfy equation (3.3) and be a valid initial condition. Hence for now our initial condition philosophy will be to choose a random Kasner mode and perturb it slightly to satisfy the initial condition equation (precisely, we shall perturb the initial value of the derivative of ξ to do this). It should also be pointed out that equation (3.3) provides a useful cross check on the simulation; we can check during or after the simulation to see if it is still satisfied, since we only impose it initially and the equations of motion themselves should preserve it.

The simulations demonstrate that the initial condition philosophy is reasonable,

and further that the picture provided by the analytic methods of chapter two is a very good one. We see Kasner behaviour (best exhibited in log-log graphs where power law solutions appear as straight lines) which does indeed satisfy the constraints of equations (2.10) on the power law exponents, and also the bouncing from one Kasner mode to another can clearly be seen. It is observed that the bouncing from one mode to another is a very sudden event (this is best seen in the simulations forward in time - see next section), which is a good indication that the assumption that the potential terms are usually unimportant is correct. The initial condition philosophy is also justified by the simulations, because in tests where wildly non-Kasner initial conditions are supplied, though still in accordance with the initial condition constraint equation (3.3), the system either falls rapidly back into Kasner behaviour or in other cases proves unstable, with singularities rapidly forming which suggests that the initial conditions are inappropriate.

Figure (3.1) shows a sample simulation of the approach to the singularity. In this case the h_i, one associated with each 3-space as described by equation (2.4), are each set to one third. These values are not of any particular significance, as shall be discussed in the next section. Here the system executes one Kasner bounce before entering the singularity, at which two 3-spaces tend to zero size and one to infinite size while the 9-volume decreases smoothly to zero. The scales of the graph are in natural units. That the singularity is not at zero on the time axis is merely due to the choice of initial time in the simulation; because the equations do not depend on time explicitly we can always add a constant to the value of time, and so the origin of the time coordinate should be shifted to coincide with the singularity.

The simulations also confirm the conjecture of chapter two, section (iii) that the presence of the dilaton will bring the Kasner oscillations to an end after a finite number of bounces; that is, the dilaton effectively damps out the chaotic behaviour near the singularity. Such an effect is also present in conventional relativity; there Belinsky and Khalatnikov [23] observed that a scalar field could end the Kasner

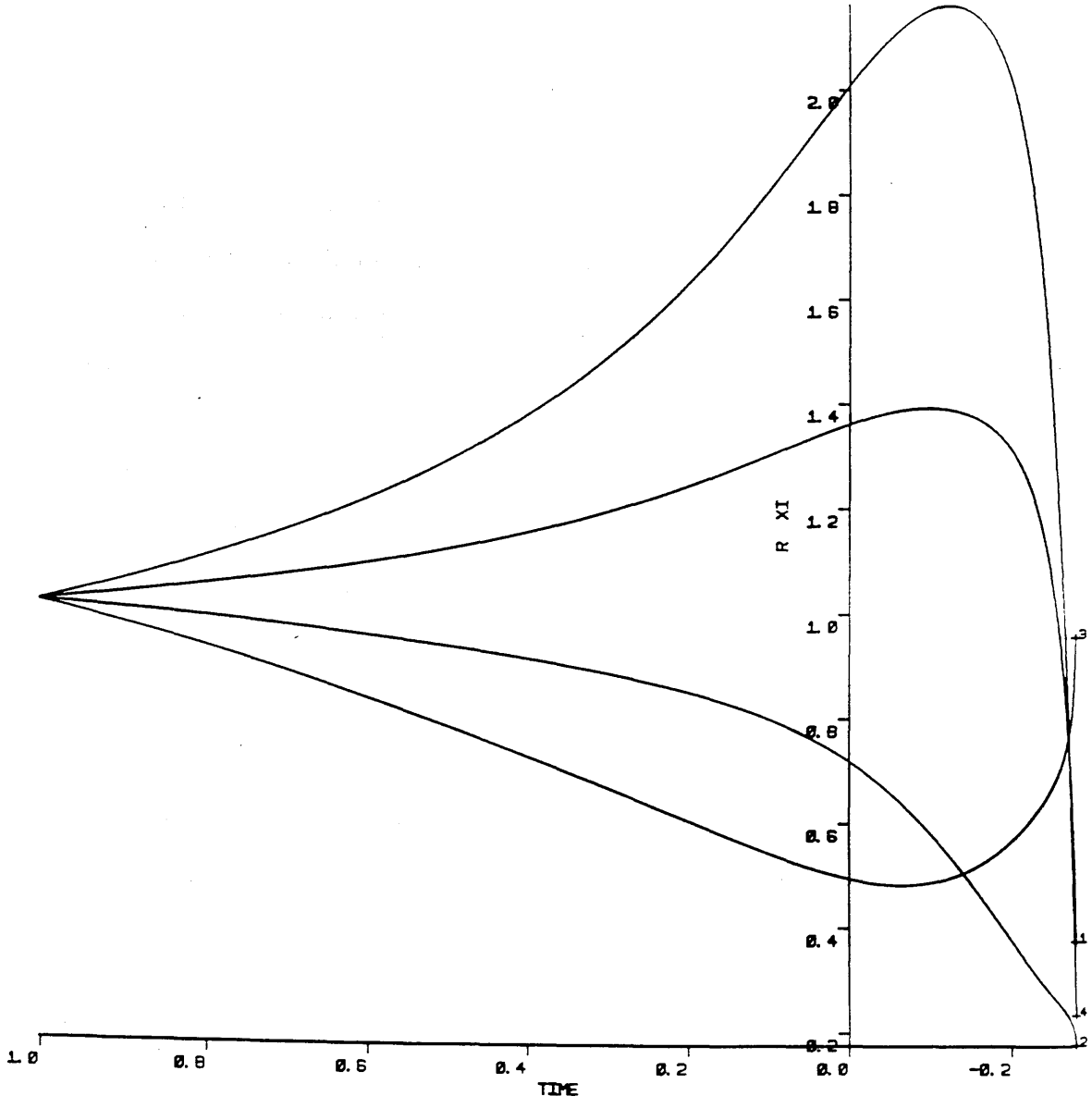

Figure 3.1 This graph shows the approach to the singularity, with the three h_i set equal to one third. The lines marked 1,2 and 3 are the sizes of the three 3-spaces, and the line marked 4 is the value of the ξ field ($\xi = e^{\phi}$ where ϕ is the dilaton field). The scales are in natural units.

oscillations, though in their case the spatial geometry caused the bouncing between modes whereas in our case it is the potential of the **H** field which performs this function. In the absence of a scalar field, it has been shown by several authors [24,25] that chaotic behaviour only exists when the number of spatial dimensions is less than ten, and Barrow and Stein-Schabes [26] have observed that in Kaluza-Klein models with extra dimensions incorporated as a direct product chaos does not occur.

(iii) Forwards in Time : The 'Fixed Point' Solution

We now move to a consideration of solutions forward in time, with a view to examining the cosmological relevance of the types of behaviour that we find. The groundwork for this has been described in chapter two, section (iv) by means of examining the iteration forwards in time, where it was demonstrated by computer trials that any initial mode is drawn towards the 'fixed point' at $p_i = 1/9$, $p_4 = -2/3$. As before, we use numerical simulation to test the validity of this picture (summarised in figure (2.2)) and also to study the bounce mechanism itself.

Here it is worth giving further consideration to the matter of the initial conditions, in the light of the apparently large number of free parameters which have to be set. These can be listed as

(a)	h_1 , h_2 , h_3	These give the values of the **H** field on the 3-spaces and determine the strength of the potential.
(b)	p_1 , p_2 , p_3 , p_4	The Kasner indices chosen for the initial conditions.
(c)	a_1 , a_2 , a_3 , a_4	The initial size of the 3-spaces and the dilaton field.
(d)	t	The initial value of the time parameter.

In fact we have far fewer degrees of freedom than it appears, partly because the equations have several scaling invariances and partly because it turns out that the long term behaviour of the solutions is for a large part independent of the precise choice of initial conditions. In particular, the initial choice of Kasner mode has no

qualitative effect on the short term behaviour or on the approach to the singularity, and no effect whatsoever on the long term behaviour. This was demonstrated by running batches of simulations with different random initial Kasner modes; in the short term the solutions are similar and in the long term become identical, due to the presence of the 'fixed point' as an attractor. The initial choice of the time variable also does not matter, as the equations do not depend explicitly on time, and so it can always be rescaled if necessary.

The number of initial conditions required is further reduced by observing that equations (3.1) to (3.3) are invariant under a rescaling of the form

$$r_i \to c_i r_i \ , \ \xi \to c_4 \xi \ , \ h_i \to \frac{c_i^3}{c_4} h_i \qquad (3.4)$$

where the c_i and c_4 are constants. This means that we can explore the space of all possible solutions by fixing either all of the a_i or all of the h_i and varying the other; we can then rescale the solutions as required. The strategy which turns out to be most fruitful is to fix the h_i (we choose the value one third, as quoted in section (ii) on the approach to the singularity) and merely vary the scaling of the initial conditions. Because of the non-linearity of the equations, this is potentially a non-trivial thing to do, but as we shall see the presence of the 'fixed point' attractor simplifies considerably the situations which we must consider.

Given these values for the h_i , we find that the long term behaviour of the solutions is exactly that predicted by the 'fixed point' picture obtained via the iteration. This occurs regardless of the magnitude of the initial conditions, determined by the a_i . This again justifies the analytic work, and we are easily able to see the progression from one Kasner mode to another. Figure (3.2) illustrates what happens as we move forward in time a little; we can see that the system executes several bounces and also that it is heading towards a configuration where each of the three 3-spaces is expanding with the same power law, that of the 'fixed point'

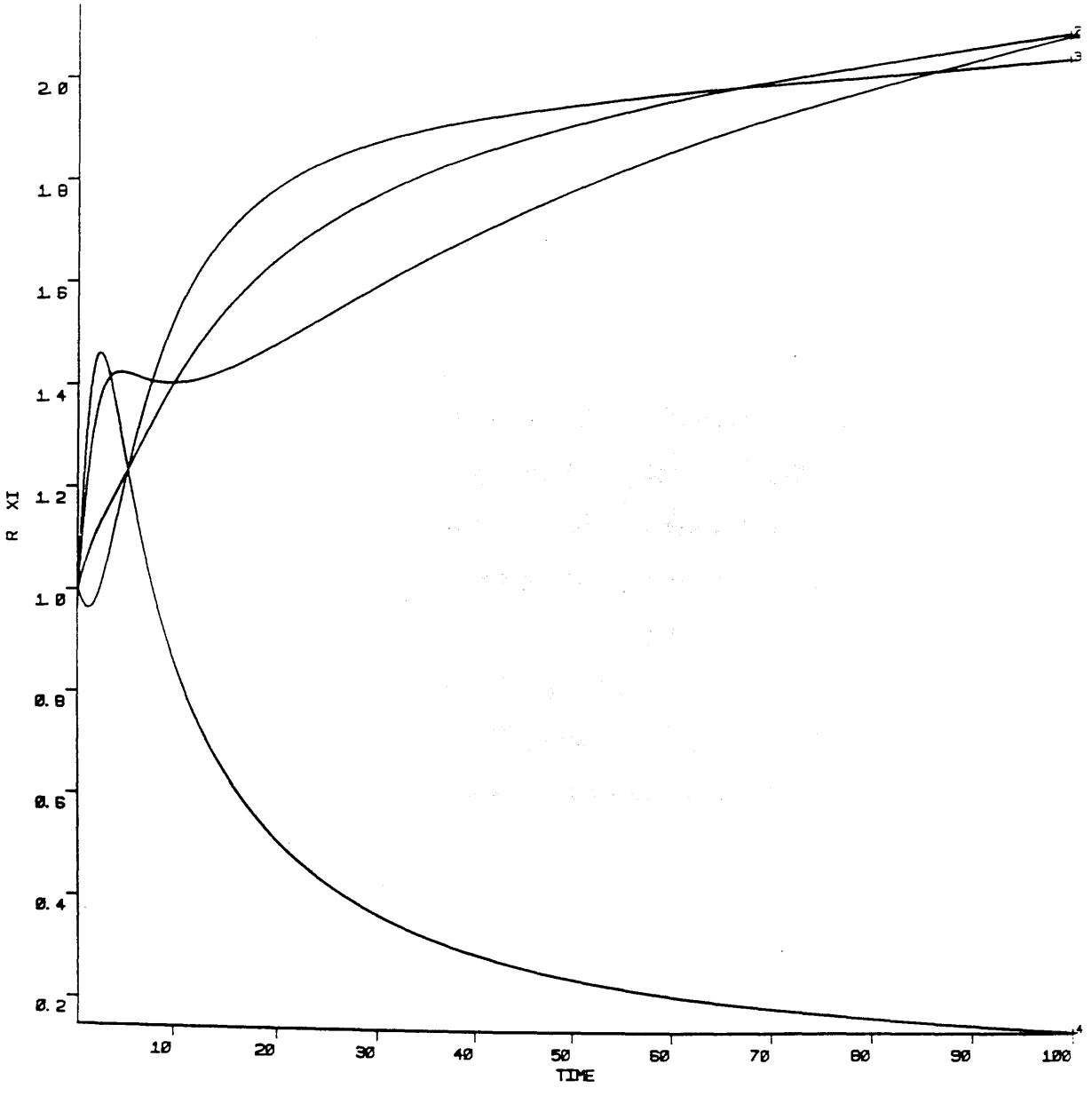

Figure 3.2 This graph shows the short term behaviour as we move away from the singularity (i.e. forwards in time). The system can be seen to execute several bounces. The sizes of the 3-spaces remain about the same, while the ξ field falls rapidly off to zero. Again the h_i are set equal to one third.

solution. The ξ field drops off rapidly towards zero; its power law heads towards minus two thirds.

Further investigation yields some more information; if all the h_i are equal then not only do each of the r_i tend towards the same power law, but also they tend towards the same magnitude as well, as seen in figure (3.3). This figure shows the development over a longer timescale than figure (3.2), and also the axes in figure (3.3) have been chosen to be logarithmic. The advantage of this is that Kasner modes appear as straight lines in such a graph, and we can now see clearly how the solution stays in one Kasner mode for a while, and then is very suddenly perturbed into another. Again here we see that we tend towards a power law of one ninth, and also we can see that despite the differing initial sizes of the scale factors they tend towards each other. This represents a natural damping of anisotropy within the model which is inherent within the bouncing mechanism.

We can now take advantage of the scaling laws of equation (3.4) to say that all solutions, even with different h_i , are of this form with the scale factors multiplied by different fixed constants, because we can rescale each of the h_i to one third and by a simultaneous rescaling of the r_i according to equation (3.4) we will obtain the same solutions. Figure (3.4) shows this in action; one of the h_i is given a different value but we just obtain the same asymptotic solutions with the associated scale factor multiplied by a constant, so that it tends to a fixed multiple of the others. These results rule out the possibility that there will be a dynamical separation in the sizes of the 3-spaces occurring in a model where the **H** field takes values on each of the spaces, unless perhaps if additional features such as curvature or particle production are taken into account. We refer to this set of solutions as the 'fixed point' solution; this is taken to include the whole class with any rescalings that might be required.

It is observed that the 'fixed point' solution is very nearly an exact solution of the full equations of motion *including* potential terms, and is in fact the only Kasner mode with the correct power law properties to do this. It cannot however be an exact

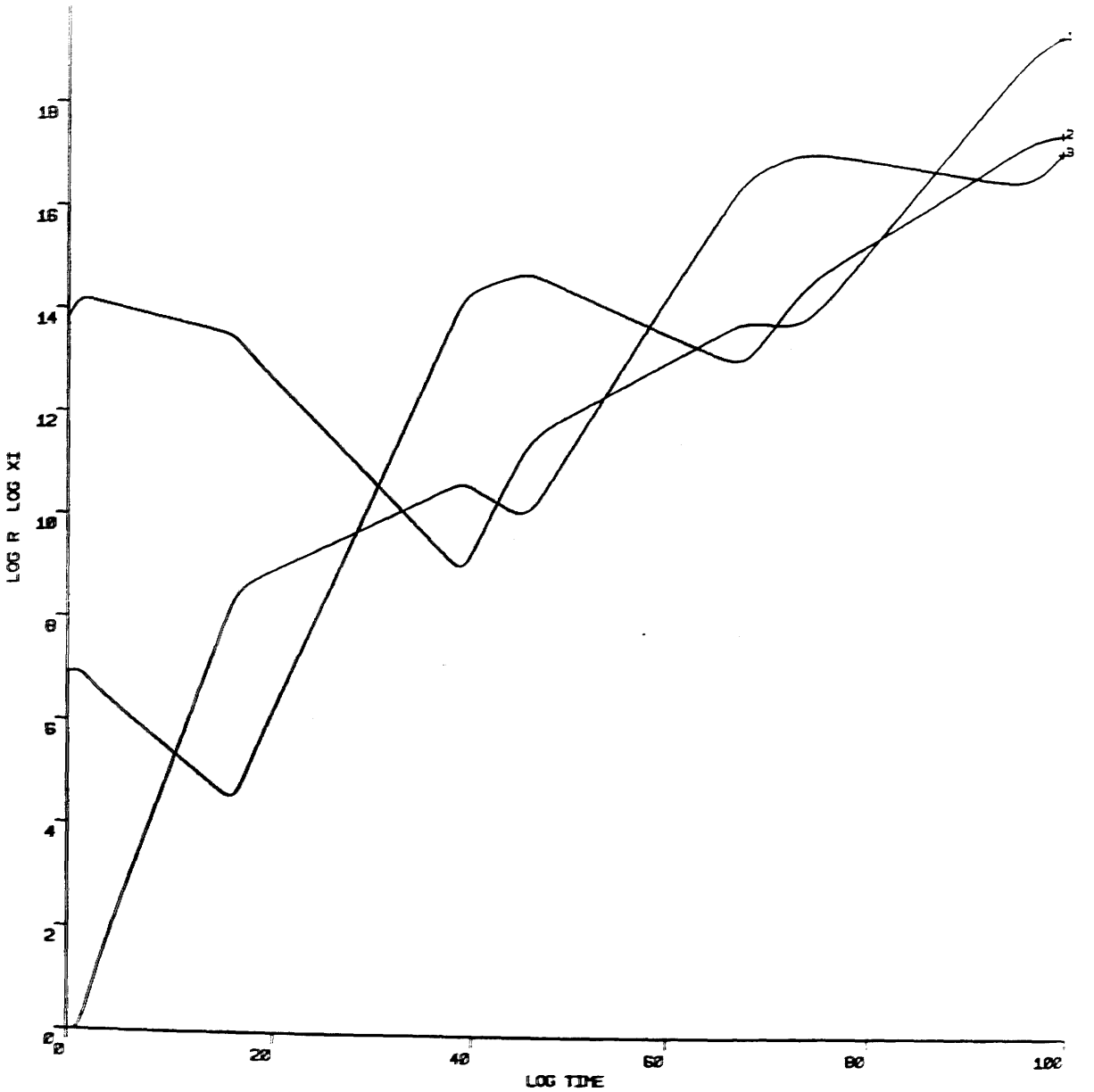

Figure 3.3 This graph illustrates the long term behaviour, with each of the h_i equalling one third. The graph is of log r_i against log t. On this graph, therefore, Kasner modes appear as straight lines. Here we can clearly see a succession of bounces, all of which occur sharply. The solutions all tend to the 'fixed point' Kasner mode (gradient one-ninth on this graph), and in addition they all tend to the same size even though they have differing original magnitudes. The ξ field is omitted from this plot for clarity; it decreases rapidly in the 'fixed point' configuration.

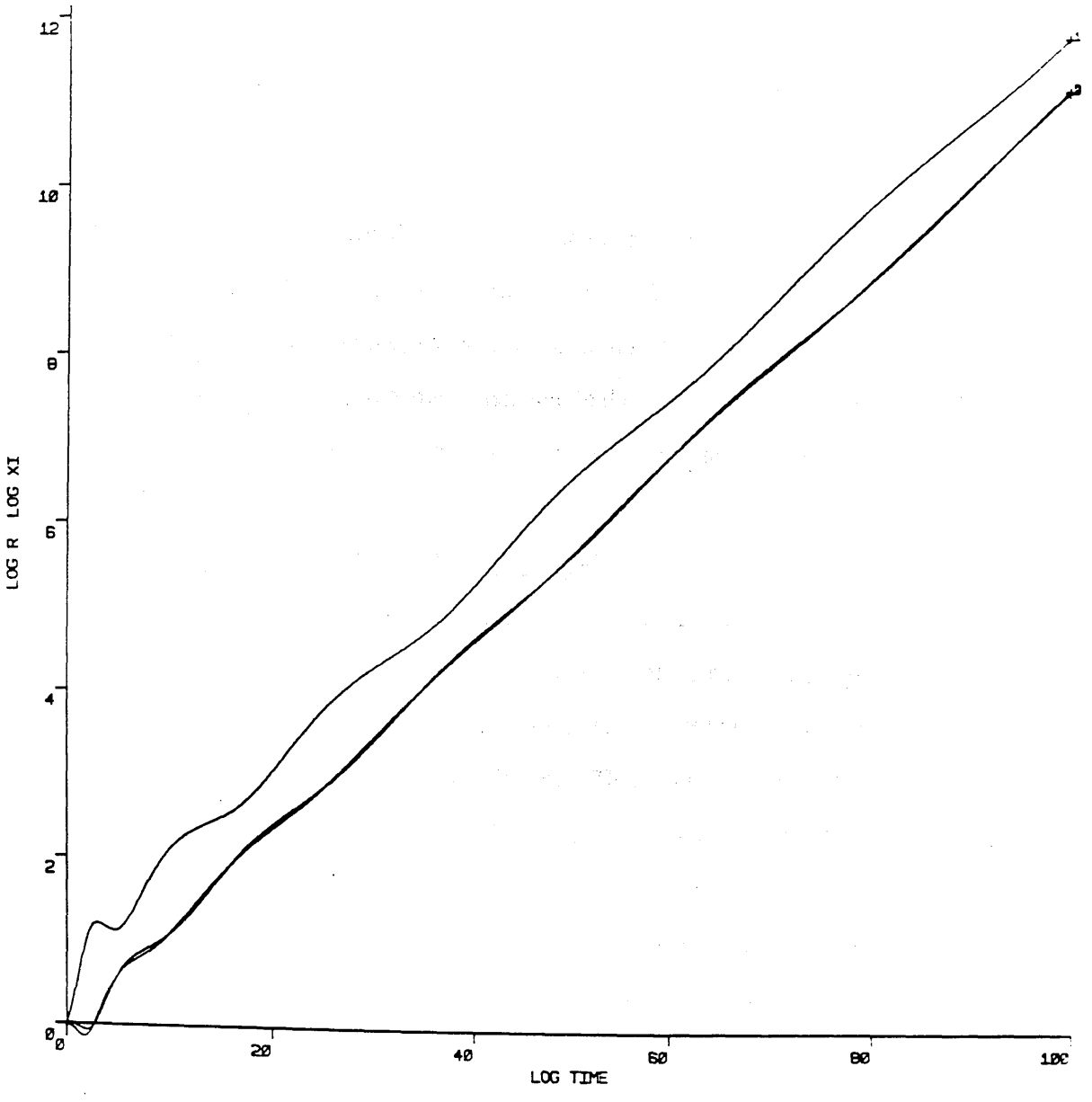

Figure 3.4 This graph again shows the long term behaviour on logarithmic scales. Here the h_i have been set to be different; we have $h_1 = 1$ and $h_2 = h_3 = 0.1$. Again we see the 'fixed point' behaviour at large times. One of the spaces now finishes larger than the others by a fixed multiple (recalling these are log scales); this is completely explained by the scaling laws in the light of the behaviour seen when the h_i are set equal and the r_i varied.

solution because there are no coefficients a_i which consistently satisfy both the equations of motion and also the additional initial condition constraint equation (3.3). The long term solution appears from simulations to be the 'fixed point' solution with a small oscillatory perturbation superimposed upon it; clearly this combination can give an exact solution. It is clear from these results that while they exhibit an interesting Kasner structure, we shall have to look elsewhere if we are to obtain solutions corresponding to compactification. In the next section we shall consider a slightly amended model where the **H** field arises only on one 3-space.

(iv) The **H** Field on One 3-Space

In this section we consider a model where the **H** field arises on only one 3-space. This corresponds in our formalism to setting h_2 and h_3 equal to zero. Formally then, the remaining 6-space is being regarded as two 3-spaces but the case where it forms a unitary 6-space is subsumed. This can be viewed as rather natural in the sense that the **H** field is arising spontaneously on its minimum possible number of dimensions, it being a 3-form. Theories resembling this have been investigated by Freund and others [13,27]. These indeed give the same formal equation of motion for **H** as we have, but , besides the absence of a varying dilaton field in the theory of Stein-Schabes and Gleiser [27], without considering the extra restriction imposed by the superstring integrability condition, as discussed in [12]. We find solutions which have different overall properties to those in the references mentioned above.

In this model we find solutions which are the most promising that we have as regards compactification; the **H** field is seen to drive one space to large sizes while the other two spaces remain of the Planck scale, exactly as one would require from a sensible compactification. The reason why we can now find solutions different to those of the previous section is that the scaling laws described by equation (3.4) no longer hold and we do not have the freedom to rescale the initial conditions. The

iteration as described in chapter two also breaks down in the case where there are vanishing h_i .

A computer simulation of this model is shown in figure (3.5). As in the 'fixed point' case we find that the solutions are fairly independent of the initial conditions which we impose, but in this case we find that the lack of an attractor means that there is no precise long term solution. The first 3-space expands in power law fashion with a power law exponent of around one half, and as initial conditions are varied it can shift between extremes of about 0.45 and 0.55 as power law behaviour. The other spaces also have power law behaviour, but with much smaller exponents, and they stay around the Planck scale relative to the first 3-space. They may be increasing or decreasing slowly; in figure (3.5) each of the second two 3-spaces is decreasing slowly in size.

It should be pointed out that although this mechanism gives a good separation in size between the 3-spaces, we do not have a rapid enough increase in the size of the first space to provide power law inflation, which requires as a minimum that the scale factor increases faster than t, so that the space itself expands faster than the horizons within it. This failure is a fairly generic feature of Kasner-like models, because of the presence of the constraint that the sum of the power laws equals one (with some normalisation, perhaps), such as in equation (2.10). It is also worth noting that the contribution of **H** to the right hand side of Einstein's equations diminishes with r_1^{-6} (where r_1 is the radius of the expanding space); that is, it diminishes as t^{-n} with n around 3. Thus any residual cosmological term from the **H** fades rapidly away once **H** has performed the function of differentiating the three 3-spaces.

In conclusion, this model provides a possible way of producing a differentiation in the sizes of the 3-spaces in the early universe, with one 3-space growing to macroscopic sizes and the other two remaining at around the Planck scale. However, it is fair to say that this model remains far too simplistic to make any particular claims

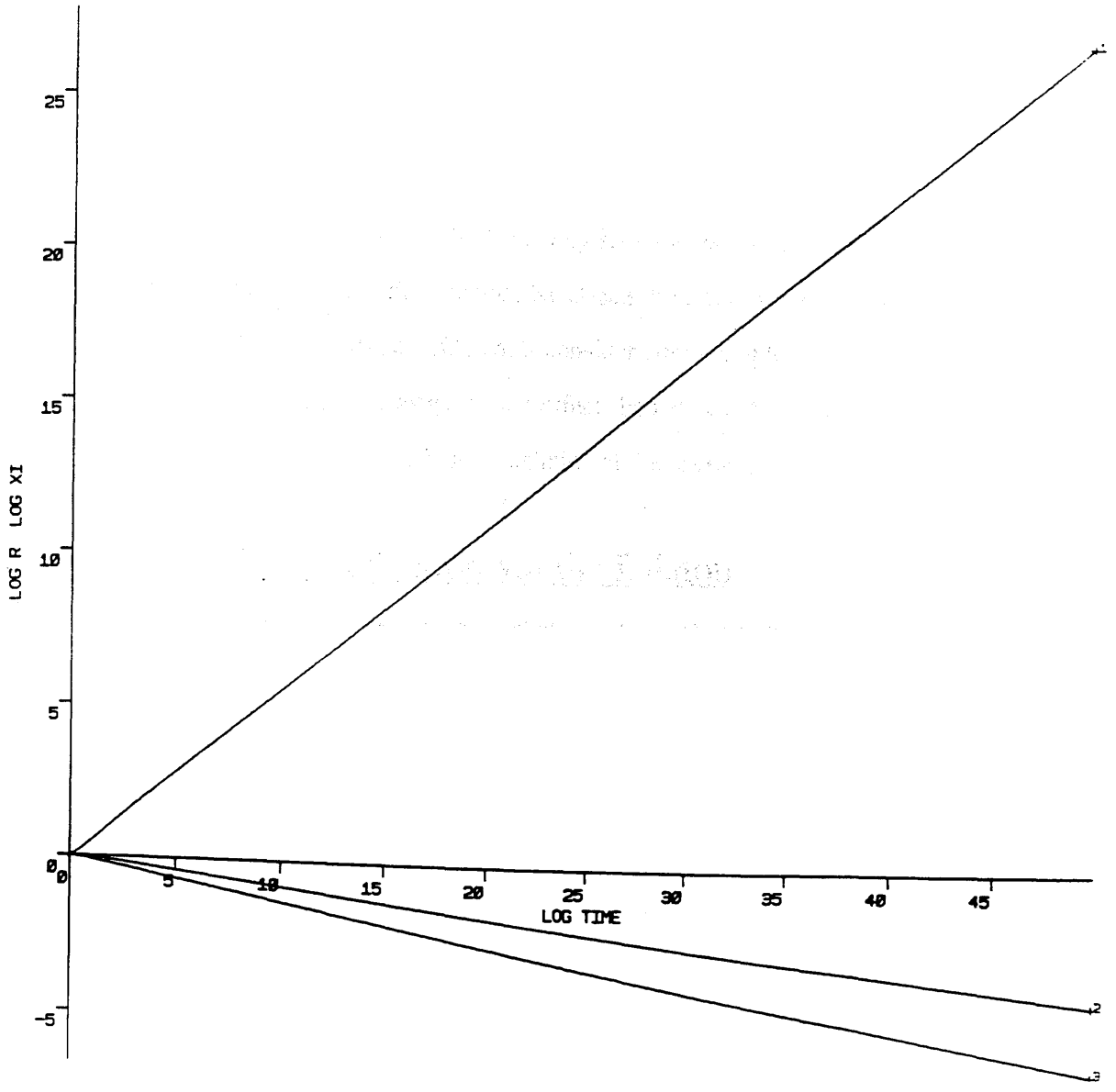

Figure 3.5 Again on log-log axes, this graph is a simulation of the situation where the **H** field sits on one 3-space; i.e. $h_1 = 1$ and $h_2 = h_3 = 0$. Here we see solutions corresponding to compactification type behaviour, with the first space growing large and the others remaining near the Planck scale. Roughly speaking, $r_1 \sim t^{1/2}$, independently of the initial conditions.

about the mechanism or to draw any observational predictions from. It also precludes the possibility of inflation while these terms are the only dominant ones around; for more generality a consideration of other degrees of freedom in the theory should be embarked upon. In the following sections, we make some short steps along this road by considering the possible effects of particle production induced by the variation of the inflaton. We shall consider some simple model versions of particle production and investigate their effects both on the 'fixed point' solution of section (iii) and the 'compactification' solution of this section.

(v) Particle Production via the Dilaton

It is clear that the bosonic Lagrangian cannot be an accurate description of the universe for all times; later on, other processes must come into play which bring us into the traditional four dimensional Friedmann universe. We shall consider here one possible mechanism which might bring us closer to this scenario, by taking into account the production of particles by the time variation of the dilaton field. Within the context of the full field theory, we expect there to be many couplings of the dilaton to the other fields, including the fermionic ones, in the full theory. The variation of the scalar will provide interactions and we can expect that these would produce fermionic particles (we do not need to consider bosons, as they are taken into account already by our field theory approach). Representing the fermions by field theory is very difficult, but fortunately the fluid description of fermions is very good when there are large numbers, so we can represent the production of particles by the flow of energy into a perfect fluid. Considerations of this type have been made by, amongst others, Albrecht, Steinhardt, Turner and Wilczek [28] in the context of particle production at the end of inflation as the inflation-causing scalar field oscillates about the minimum of its potential. Particle production also features prominently in chapter four of this thesis, though the work there is not directly related to that of this and the previous chapter.

The full supergravity Lagrangian of the theory we consider has many scalar-fermion couplings, to particles of both spin 1/2 and spin 3/2; however, to actually calculate the decay rate (which would in principle give the exact form of the particle production equations) would be extremely difficult and time consuming. An alternative view, that the calculation should be done within the context of the underlying string theory itself, would also be a prohibitively difficult proposal. However, following [28], we note that the rate of production should depend only on ϕ and its rate of change, so we can consider general forms of the decay rate. The aim here is to see if the effect of particle production does not depend sensitively on the exact form of the particle production terms. This is analogous to the notion in inflation studies that the phenomenon of inflation should occur for a wide range of generic potentials rather than require some specific fine-tuned potential - the cosmic no hair conjecture. We specify that the energy of the particle production should go into a ten dimensional relativistic perfect fluid, with energy density ρ and pressure p obeying an equation of state $p = \rho/9$. The important quantity shall be the rate of energy flow from the scalar field into the particle fluid, which we shall denote throughout by Δ.

As discussed above, we are interested in trying out various generic forms for Δ. Perhaps the most natural choice for this is that Δ should be proportional to the square of the time derivative of ϕ. This is because the overall scale of ϕ should be unimportant, and the square appears because we expect the particle production to be independent of the sign of the variation of ϕ. This choice, which can be written

$$\Delta = \alpha \dot{\phi}^2 \tag{3.5}$$

where α is some constant, is that which was made in reference [28]. We have also considered more general forms of Δ, for example

$$\Delta = \alpha \dot{\phi}^2 \, f(\phi) \tag{3.6}$$

where α is again a constant and f is some function of ϕ. Several choices of f were investigated, but it is found that ϕ always remains close to one and so for most obvious choices (exponentials, logarithms, polynomials etc.) this generalisation seems to have little effect. A further variation is to try different powers of the derivative, for instance

$$\Delta = \alpha \dot{\phi}^4 \tag{3.7}$$

This results in a lengthening of the time scale of the effect of particle production, but does not seem to affect the final outcome. In any of these cases amending α changes the magnitude of the energy density ρ but again the qualitative behaviour stays unchanged. Hence, in what follows, we shall report on the effect of particle production using equation (3.5) with α set equal to one.

We apply the particle production scenario to both the 'fixed point' and 'compactification' solutions that we obtained in sections (iii) and (iv). To do this we have to extend the equations, not only so that they contain the energy transfer term given by Δ but also by adding the energy-momentum terms appropriate to the fluid which must now be consistently absorbed into our scenario. The equations are altered from equations (3.1) and (3.2) to give

$$\ddot{r}_i + 3\left(\sum_j \frac{\dot{r}_j}{r_j}\right)\dot{r}_i - \frac{\dot{r}_i^2}{r_i} = r_i \xi^2 \left(\frac{1}{2}\frac{h_i^2}{r_i^6} - \frac{1}{8}\sum_j \frac{h_j^2}{r_j^6}\right) - \frac{1}{9} r_i \rho \quad , i = 1, 2, 3 \tag{3.8}$$

$$\ddot{\xi} - \frac{\dot{\xi}^2}{\xi} + 3\dot{\xi}\left(\sum_j \frac{\dot{r}_j}{r_j}\right) = \frac{1}{4}\xi^3 \left(\sum_j \frac{h_j^2}{r_j^6}\right) - \frac{\Delta \xi}{2\dot{\xi}} \tag{3.9}$$

that is, there is an extra contribution to the right hand side of the r_i equations from the pressure terms (here reexpressed using the equation of state), and there is an extra contribution to the ϕ equation as energy is removed from it into the radiation

fluid. To these we add the continuity equation expressing energy conservation for the radiation fluid which is

$$\frac{d\rho}{dt} + \frac{10}{3}\rho\sum_{i=1}^{3}\frac{\dot{r}_i}{r_i} = \Delta \qquad (3.10)$$

This completes the set of equations which are now soluble for ρ, r_i, and ϕ. We imagine the particle production mechanism as being 'switched on' at one Planck time; before this we have no understanding of what might be occurring and so we do not wish to extrapolate the particle production into this region. The simulations are then started at one Planck time in a perturbed Kasner mode, as before in accordance with the initial condition equation. We set the initial fluid energy density to be zero. This puts us in a position where we can examine how particle production affects our earlier scenarios. For simulation, the derivative of ξ on the denominator of the last term of equation (3.9) is cancelled with one in Δ to avoid a removable singularity when the derivative of ξ equals zero.

(vi) Particle Production and the Fixed Point

We have observed in section (iii) that when the **H** field is present on all three 3-spaces there is a solution which is unique up to a rescaling of the scale factors - the 'fixed point' solution. When we incorporate the particle production mechanism of the previous section into this scenario, we find that it alters the Kasner structure of the system in the following way. The production of particles is found to completely damp out the variation in the ξ field after a while so that it settles down to a constant value of order one, rather than the 'fixed point' behaviour which has $\xi \sim t^{-2/3}$. This is very much as one would expect from the idea that energy is removed from the scalar field into the radiation fluid, and shows that the other possibility - that the attractor might have been strong enough to defeat the particle production effects and retain a varying ξ field - does not occur.

Because the ϕ field is damped out, the 'fixed point' solution is no longer a stable solution of the system. What we find instead is that again the r_i tend to equal sizes, but this time with $r_i \sim t^{1/3}$. There is an original burst of particle production, but this is then diluted by the expansion of the space and so we find that $\rho \sim 0$ except at very early times. Figure (3.6) illustrates a sample simulation of this model, where once more log axes clearly show the power law behaviour of the r_i. It can be seen that after a while ξ assumes a constant value, here around 0.7, while ρ remains near zero (this graph shows $(\rho+1)$ to enable it to be shown on the log axes). In fact on these scales we cannot see any particle production at all, but on smaller scales the initial production is visible and is rapidly diluted away by the expansion of the space, just as in conventional cosmologies. We again observe several oscillations of the r_i before reaching the asymptotic state.

We can gain some understanding of this situation by noticing that we can find an exact analytic solution to the full equations under the assumptions that

$$r_i \rightarrow r\,, \qquad \xi \rightarrow c\,, \qquad \rho \rightarrow 0 \tag{3.11}$$

where r is some function and c is a constant. Then we can find a unique power law solution which is

$$r = A\,t^{1/3} \tag{3.12}$$

where A is a constant which is uniquely determined from the value of the constant c, the long term value of the ξ field. The predictions of this solution are in excellent agreement with the numerical results, which suggests that the solution of equation (3.12) is an attractor for the system, though we have no proof of this. Certainly it indicates that the limits given by equation (3.11) hold, at least asymptotically.

These results are however not favourable in terms of gaining a sensible compactification solution; the hope that particle production might freeze one of the

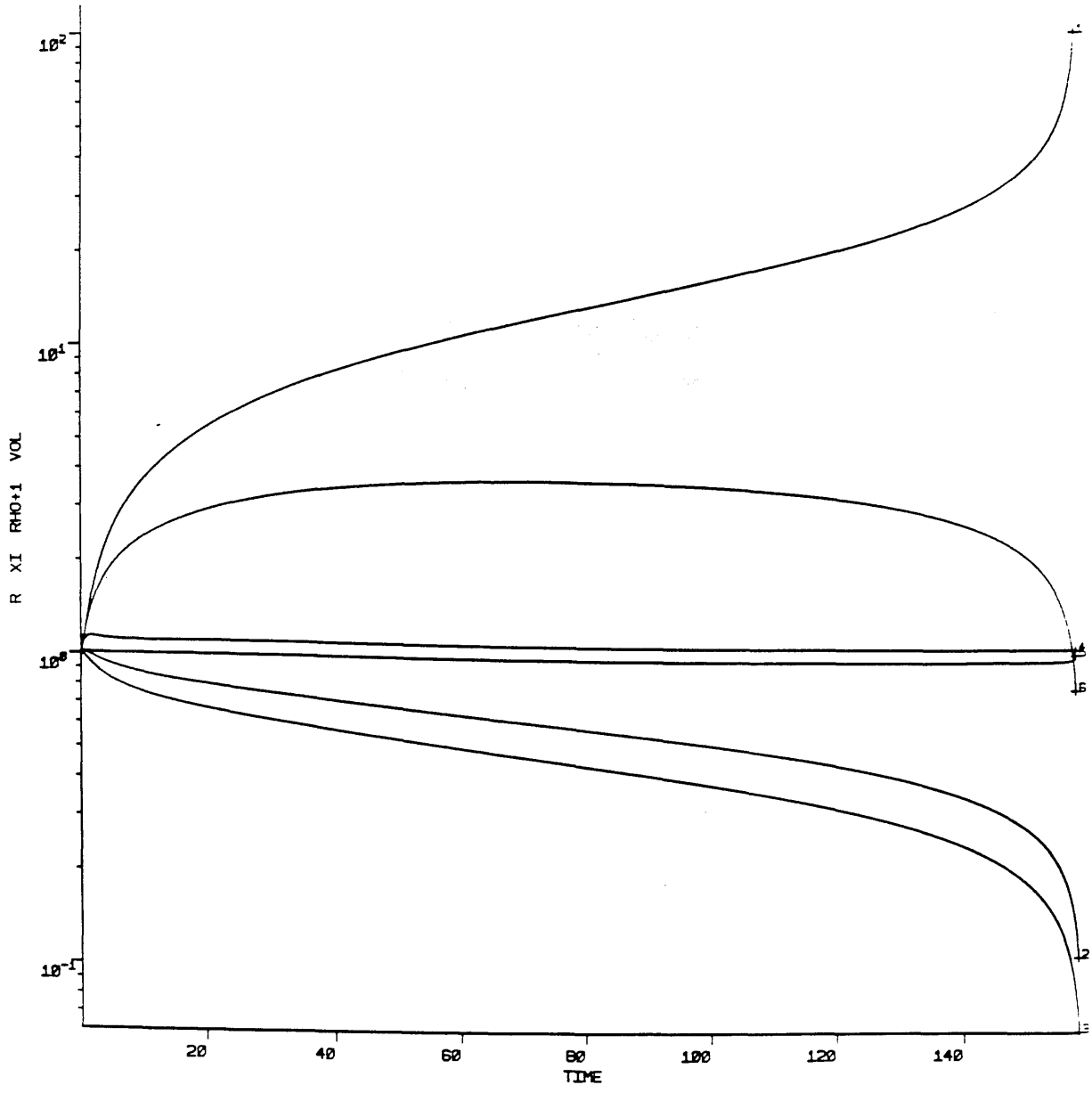

Figure 3.6 This graph shows how particle production affects the 'fixed point' solution, here with all the h_i set equal to one third. The solution is perturbed out of the old 'fixed point' solution into a mode where $r_i \sim t^{1/3}$, after executing some bounces. In the region after $t = 10^3$ the ξ field stabilises to a constant value and we can get an approximate analytic solution. The line marked 5 is equal to $\rho + 1$ (to enable it to appear on log scales). Hence $\rho \sim 0$ throughout the simulation.

3-spaces in an expanding mode does not appear to be realised. We are very much in the same situation as section (iii), where, since the particle production via the dilaton affects each 3-space in the same way, each 3-space expands at the same rate and we have no differentiation in size between them.

(vii) Particles and the Compactification Solution

We now move on to investigating the addition of particle production to the compactification scenario of section (iv). Here we find that particle production has a more drastic effect than it has on the 'fixed point' scenario; the effect of adding particle production is to induce a second singularity where the 3-space containing the **H** field shoots off to infinity while the other two tend rapidly to zero. Figure (3.7) indicates how this occurs, where we can see r_1 becoming large and the others small. Again ξ is effectively damped out by the particle production, and once more ρ has very small values except near the two singularities. This graph also indicates the proper volume of the universe at each point in time (actually, it is the cube root which is plotted). We see that the volume increases smoothly to a maximum and then decreases back towards zero, which it attains at the singularity. This behaviour indicates that we are indeed dealing with a true singularity, and that it is not an artifact of the numerical methods used.

The actual lifetime of the universe is determined by the value of α in equation (3.5), which determines the strength of coupling between the dilaton and the matter fields. By selecting a very small value of α, we can extend the lifetime of the universe with a corresponding drop in the radiation energy density; this also allows a larger differentiation in the sizes of the 3-spaces.

We can in fact specify the behaviour close to the second singularity more precisely; it is given by

$$r_i \sim (t_1 - t)^{p_i} \qquad (3.13)$$

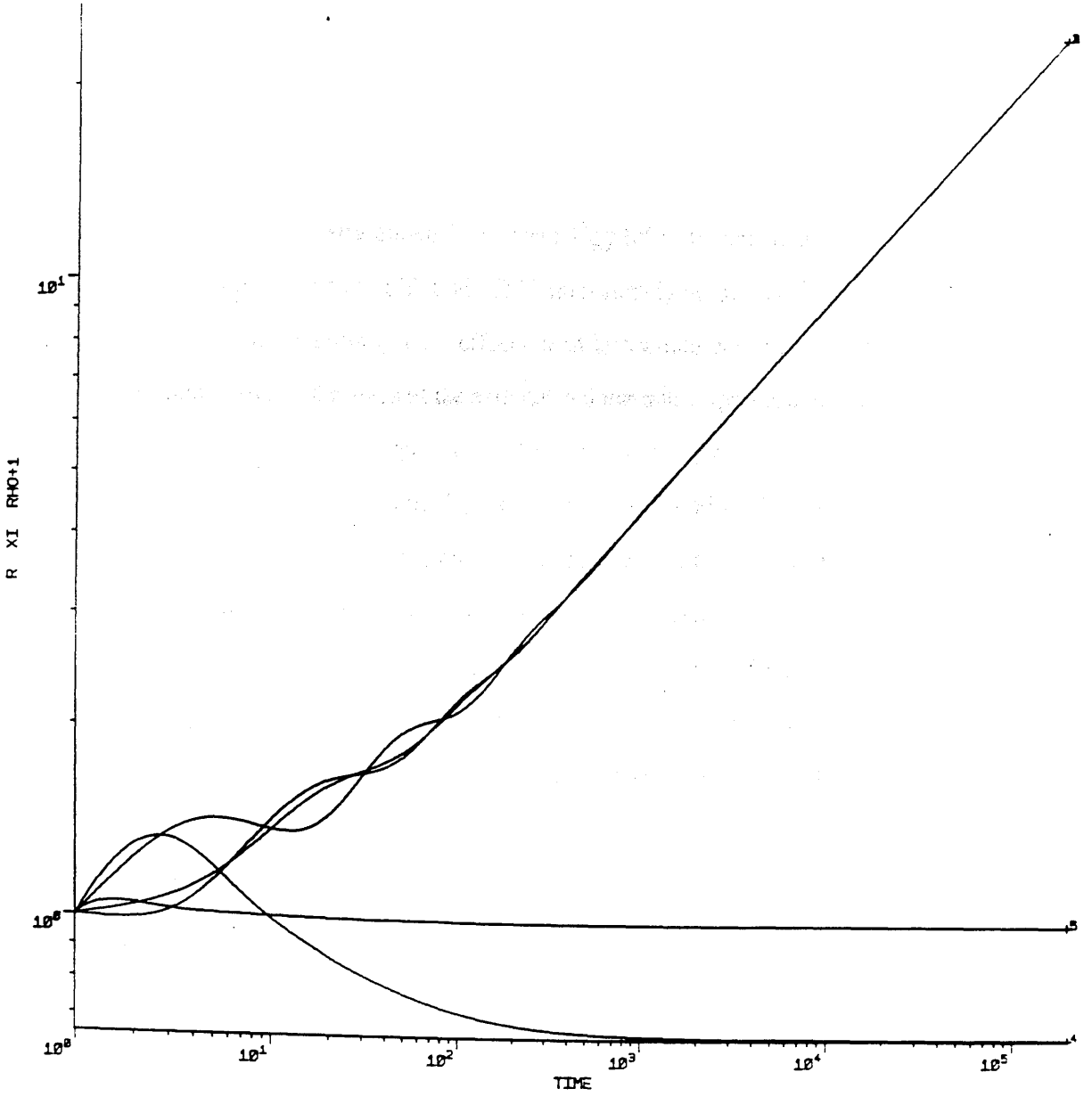

Figure 3.7 This graph shows how particle production affects the situation with the **H** field on one 3-space. We encounter a singularity with r_1 going infinite and the others tending towards zero. Once more the energy density (line 5) remains near zero, except near the singularity. Line 6 shows $r_1r_2r_3$ (i.e. the cube root of the total volume), showing that the volume increases and then decreases smoothly as we enter the singularity.

where t_1 is the time of the second singularity. Hence the second singularity is also of Kasner type; it appears that the effect of particle production becomes negligible on the approach to the second singularity. Such a situation has cropped up several times in investigations of extra dimensional cosmology [29]. If some quantifiable effect could be found which cut off figure (3.7) immediately before the singularity (e.g. some unknown quantum gravity effect), then this would certainly lead to a large separation between the sizes of the external and internal 3-spaces, and in addition it would also provide an extremely rapid inflationary phase in the external space. (Inflation of this type, given the name pole-law inflation, has received some consideration recently [30]). However, at this stage no authors have been able to come up with satisfactory arguments, even of a hand-waving type, as to how the cut off near the singularity might be realised. A more likely scenario is that long before the singularity is reached the approximations of our model would break down, perhaps because of increased fermion density with associated interactions and back reactions, leading to different phase in the evolution of the universe, in such a way that the problem of the singularity is never realised in a practical cosmology.

(viii) Summary of Chapters Two and Three

Finally, we summarise the work described in chapters two and three and catalogue the various types of behaviour found in the models examined. Within the context of a model where the **H** field is used to split the nine spatial dimensions of superstring into three three-dimensional spaces, we have examined two specific models. Firstly, a model in which the **H** field takes values on each of the 3-spaces is investigated and then a model where the **H** field arises solely on one 3-space, its minimum possible number of dimensions.

In the first of these cases, it can be shown by approximate analytic means that there exists an unusual type of attractor governing the iteration which takes us from one Kasner mode to another, arising from a slight generalisation to the conventional

theory of attractors in that the various parameters, here the p_i, must be rearranged between each application of the iteration. By numerical methods, it can be shown that this attractor is indeed realised when we consider the complete set of equations, and that because of this the long term behaviour in this instance is essentially unique up to rescaling independent of the values the **H** field may take. The behaviour is such that each 3-space has power law behaviour with exponent one ninth, which is certainly not useful when we come to consider compactification. We refer to these solutions as the 'fixed point' solution, a notation intended to cover the entire class including rescalings. This model therefore will not lead to the desired separation in sizes between the 3-spaces unless further effects are taken into account, for example the influence of fermions.

The second model, with the **H** field on one 3-space, gives a more satisfactory compactification scenario. The first space, on which the **H** field has arisen, is driven to large sizes with behaviour as t^n where $n \sim 1/2$, while the other two remain comparable to the Planck scale. This also has the benefit that the residual contribution to the cosmological constant from **H** falls off as t^{-6n}, and so will be unobservable at present times. Hence it appears that this mechanism can provide a mechanism for the differentiation in sizes between external and internal dimensions as the universe evolves, though the model is far too simplistic to take into account the true nature of compactification. There one would be interested in the specific nature of the internal space (for instance it may have a very complicated topology) which gives much of the structure of the effective field theory in four dimensions that we see today. Again we would also wish to consider a more general theory, with fermionic and gauge degrees of freedom, before coming to any definite conclusions as regards this model.

In the second half of chapter three, we went on to consider a generalisation of the model in which some provision is made for fermions, by assuming that they can be represented by a radiation fluid. Sample couplings were then introduced between

this and the dilaton field to see what effects might arise; the true couplings are in principle derivable from the underlying theory but are very difficult to calculate, so we prefer instead to use various generic forms of the coupling. These couplings will lead to the production of fermionic particles from the scalar field, and the effect of this on our two scenarios was investigated.

In the 'fixed point' case, little qualitative change is made; the scalar field is now damped out and the 3-spaces increase with a slightly different power law, but the rate of increase of the three remains the same, which again is unfavourable for compactification. Hence particle production appears unable to freeze a single 3-space in an expanding mode. The effect on the compactification solution is somewhat more drastic, in that it induces a second Kasner singularity where one 3-space tends to large sizes while the other two become small. This could be favourable if some effect could terminate this behaviour near to the singularity, since it would give rise to a large differentiation in the sizes of the three spaces, but it seems unlikely that anything can be said concerning possible mechanisms which might do this. Instead, it is simpler to consider that the assumptions of the model break down well before the singularity, perhaps due to inadequate treatment of fermions etc. If the scalar-fermion coupling is small, a large differentiation can still be obtained, as in section (iv) without particle production, well away from the singularity so with a small amount of particle production this scenario could still be effective for compactification solutions.

Chapter 4

Power Law Inflation with Exponential Potentials

(i) Introduction : Why Power Law Inflation?

Since the pioneering work of Guth [18] in 1981, followed up and improved by Albrecht and Steinhardt [31] and Linde [32], and since then by many authors [33], inflation is now regarded as the standard solution to such long-standing cosmological problems as the horizon and flatness problems [18]. It is also used as a solution to the related question of why the universe should appear so homogeneous and isotropic, and also that of excessive monopole production in a huge range of grand unified theories [34]. While much effort has gone into the examination of ways of implementing inflation within the context of modern particle theories, these models have in general remained somewhat unsatisfactory because unnatural fine tuning of parameters in the underlying particle theory is required to ensure that the induced inflation satisfies several cosmological constraints and also provides a satisfactory amount of inflationary expansion.

The standard method for implementing inflation is via a scalar field, often called the inflaton and which we shall refer to throughout as ϕ, moving in some appropriate background potential which is in principle determined from some underlying particle theory. A potential much used in early studies is the Coleman-Weinberg potential [35], which arises in symmetry breaking scenarios in, amongst others, grand unified theories, and this was the context in which many of the earlier inflationary models were constructed. In these constructions, the scalar field rapidly comes to dominate the energy-density of the universe, and this energy then drives a rapid expansion in the universal scale-factor. In the original inflationary scenarios this expansion would

be exponential, mimicking de Sitter space. This is because when the scalar field moves very slowly, so that the potential is almost constant and the variation of the scalar negligible, $V(\phi)$ appears in the field equations exactly as a 'cosmological constant' term and de Sitter space, giving exponential expansion, is a good approximate solution. Unfortunately, fine-tuning is required to create a potential sufficiently flat to allow this slow scalar field motion. The expansion is later halted by the scalar field falling into the minimum of its potential, after which the scalar terms become negligible in the field equations and we move into the conventional Friedmann-Robertson-Walker universe.

Though exponential inflation is the simplest to arrange, there is no known potential arising from particle theories which exhibits the necessary fine-tuning to lead to a satisfactory inflationary model of this type [36]. This has led to the examination of a wider class of inflationary theories, with the realisation that any rapid expansion of the scale factor, not necessarily exponential, can solve the cosmological problems mentioned above. These models are known as generalised inflationary models [37]. To cause inflation, the key property is that the universe itself must expand faster than the horizons within it, which of course travel at the speed of light. This means that regions which appear causally separated now may have been in causal contact in the pre-inflationary universe, and so had the opportunity to become thermalised. This can explain the homogeneity of the universe as observed today. (Of course, there is no breach of causality in this expansion; it is space itself which is expanding faster than the speed of light, not anything moving within it.)

In this chapter a special case of these generalised inflationary models will be considered - that of power law inflation. In power law inflation, the scale factor a(t) of the universe obeys the relation

$$a(t) \sim t^{p} \tag{4.1}$$

where p is some constant which will be determinable from the field equations. Since the horizon volume increases as t^3, and the proper volume as $a^3(t)$, clearly p must be greater than one for inflation to occur. Ideally p should be significantly greater than one to satisfy various cosmological constraints, a point which shall be discussed in section (iv) with regard to the construction of a specific model. As p becomes large, the inflation begins to become indistinguishable from conventional exponential expansion.

In this chapter, both analytic and numerical methods will be used in an examination of power law solutions in various situations. First the simple case of an exponential potential for the scalar field will be examined; this is not meant to be a realistic model, but rather is treated as an example where exact analytic solutions can be found. This will supply useful intuition for more realistic cases which are considered later, where potentials arising from particle theories are investigated. These are approximately exponential at some values of ϕ, and numerical work shows behaviour close to that which is expected on the basis of the analytic solutions. Numerical simulation is necessary to find the true solutions in these cases, especially where the potentials differ significantly from the exponential form.

In power law models, the scalar field does not move extremely slowly during the inflation as in exponential inflation, and so the effect of the variation of the scalar field must be taken into account. This variation will lead to the production of particles. Perhaps surprisingly, this leads to an enhancement in the efficiency of the inflation by increasing the value of the power law exponent p in equation (4.1) above. This behaviour is examined numerically with the simple exponential potential and then implemented in a more realistic setting using a potential motivated by particle physics. The various constraints present are examined in some detail and the construction of a specific inflationary model of this type is outlined.

(ii) An Exact Solution and the Need for Numerics

It is well known [38,39] that power law solutions of the form of equation (4.1) can be found when the energy density of the universe is completely dominated by a scalar field ϕ having an exponential potential of the type

$$V = V_0 \exp (- \lambda \phi) \tag{4.2}$$

where V_0 and λ are constants which ultimately should be determined from some underlying theory of the scalar field interactions. λ turns out to be a very important parameter, and as notation throughout this chapter λ will be taken to mean the coefficient in the exponential potential. It transpires that the types of solutions obtained depend on the value of λ. Potentials of this type are common in higher dimensional theories such as Kaluza-Klein and also supergravity / superstring models after dimensional reduction has been applied [38,40,41].

To obtain analytic solutions we take space-time to be spatially flat Robertson-Walker with metric given in isotropic coordinates by

$$ds^2 = - dt^2 + a^2(t) \ (dx^2 + dy^2 + dz^2) \tag{4.3}$$

It is also possible to consider spaces of non-zero curvature, but here we will only consider the simplest case since the main aim is to work towards the construction of a more realistic theory. The Einstein equations and the equation of motion for the scalar field (also obtainable via energy conservation) then give

$$\left(\frac{\dot{a}}{a} \right)^2 = \frac{1}{6} \dot{\phi}^2 + \frac{1}{3} V_0 \exp (- \lambda \phi) \tag{4.4}$$

$$\ddot{\phi} + 3 \left(\frac{\dot{a}}{a} \right) \dot{\phi} - \lambda V_0 \exp (- \lambda \phi) = 0 \tag{4.5}$$

Power law solutions of these equations have been given previously by several

authors, but a more general exact solution than has appeared before is given by

$$a = a_0 t^p \qquad \text{where } p = \frac{2}{\lambda^2} \tag{4.6}$$

$$\phi = \frac{2}{\lambda} \ln \left(\sqrt{\frac{\lambda^4 V_0}{2(6-\lambda^2)}}\ t \right) \tag{4.7}$$

It is clear from equation (4.7) that this solution only exists when $\lambda^2 < 6$. If $\lambda^2 > 6$ then other techniques are needed; here numerical simulation will be used to examine what happens in this situation. The solution above generalises the solutions first offered in Barrow [39] and then Burd and Barrow [42]. Their solutions have the unsatisfactory feature that they only exist when λ and V_0 are related by a specific equation, which is unlikely to be realised in any naturally arising problem where they come directly from an underlying theory. In fact, as we shall see later, there are strong constraints on V_0 which will prevent it from being related to λ in the required way. The solution above also demonstrates that the constants t_0 and ϕ_{c0} in Yokoyama and Maeda [43] are not integration constants as they claim but are in fact uniquely determined by the equations of motion of the system. The only true integration constant in this solution is a_0.

It is of course clear that the solution given in equations (4.6) and (4.7) is not a general solution to the equations of motion, since the solution has only one constant of integration while a general solution would be expected to have at least three. Since the system is non-linear, it is therefore not immediately clear that this solution will have any physical relevance, because the initial conditions for the inflationary era will probably not obey the equations (4.6) and (4.7). In such non-linear systems, it is usual for the initial conditions to dictate the types of allowable solutions. However, in this case, it has been shown by Halliwell [38] that the equations of motion can be reduced to a plane autonomous form by a transformation to conformal

time in the metric. A plane autonomous system, in this context, is one where the equations can be written with the second derivatives of α and ϕ with respect to some choice of time variable depending only on the first derivatives of α and ϕ, and not the values of α and ϕ themselves. When this happens, the system can be analysed using phase portraits and Halliwell was able to show that power law solutions are attractors for all initial conditions in a flat universe when $\lambda^2 < 6$. He did not, however, give an explicit form of the solution as given above.

The knowledge that the power law solution is an attractor means that the above solution should be relevant as a long term solution; regardless of the initial conditions one would expect the solution to asymptotically approach (4.6) and (4.7) for sufficiently late times, provided λ is in the required range. It has been confirmed by numerical simulation, using the same techniques as described below, that this is exactly what happens, with the transition into the power law mode occurring very rapidly. Notice that the power law exponent of the long term solution is independent of the value of V_0, though the magnitude of V_0 does decide how quickly we reach the attractor solution. Figure (4.1) shows a sample simulation with $\lambda^2 = 2$.

While this analysis is clear cut for $\lambda^2 < 6$, we have not yet discovered anything about the case where λ is not in this range, because the exact solution as given above no longer exists. This case is in fact of particular interest, because, as we shall see later, the potentials which arise in more realistic theories tend to have values of λ^2 in excess of six. As well as the exact solution failing here, the phase plane analysis of the system gives no definite result either, so we need to use other techniques to find out what types of solution we can have. Here we will use numerical simulation with a range of possible initial conditions to study this case. Appendix 1 gives more details about the numerical techniques; this problem is employed as an example of the numerical integration methods used throughout this thesis.

The results of the simulation show that the behaviour of the system is completely different when $\lambda^2 > 6$. Instead of arriving in an asymptotic power law

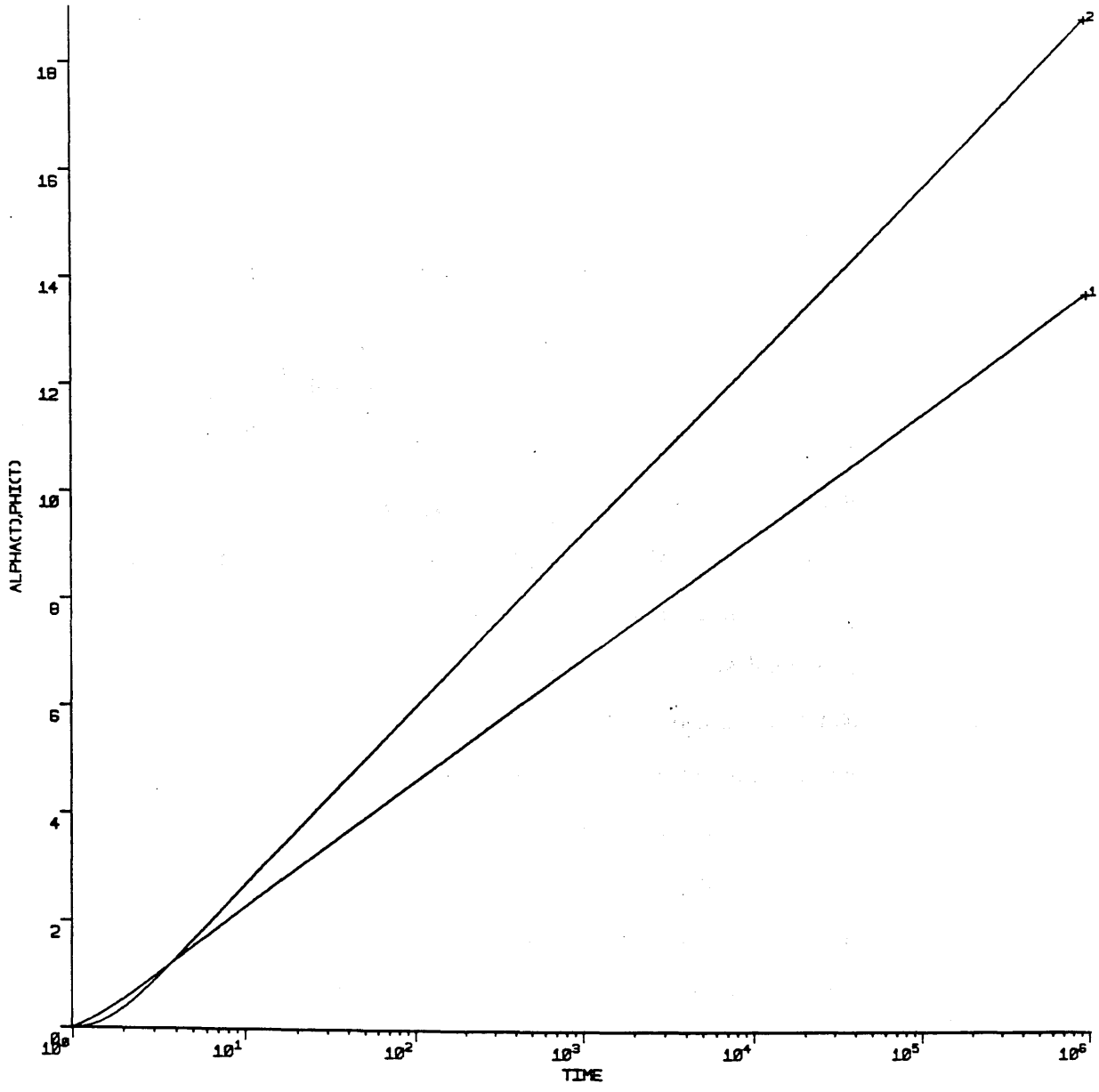

Figure 4.1 This graph, with $\lambda^2 = 2$, demonstrates by use of a logarithmic time axis that solutions do indeed follow the exact solution given by equations (4.6) and (4.7). The line marked 1 gives α, the log of the scale factor, while that marked 2 gives ϕ. The gradient can be used to obtain the power law exponent of the inflation. In addition, this graph also indicates the speed with which the attractor acts.

solution of the type (4.6), where the power law exponent p varies with λ, we find that we have exactly the same asymptotic solution for any λ with $\lambda^2 > 6$. This can be described by the equations

$$a = a_0 t^{1/3} \tag{4.8}$$

$$\phi = \phi_0 + \sqrt{\frac{2}{3}} \ln(t) \tag{4.9}$$

where this time both a_0 and ϕ_0 are integration constants. Again the value of V_0 does not affect the long term behaviour of the scale factor. The relevance of this solution is that it is the unique exact solution to the equations of motion when the potential term is neglected completely. It turns out that when we have a large λ, which corresponds to a steep potential, the rapid fall of the potential does indeed lead to the potential energy becoming negligible and so we find solutions which asymptotically approach equations (4.8) and (4.9). Figure (4.2) illustrates this with $\lambda^2 = 8$.

This notion can be made more precise by examining how the potential and kinetic energies are related in the exact solution for low λ. The calculation shows that for the solution of (4.6) and (4.7), the ratio of potential to kinetic energy is constant in time and is given by

$$\frac{\text{potential energy}}{\text{kinetic energy}} = \frac{6 - \lambda^2}{\lambda^2} \tag{4.10}$$

Because this ratio is constant, the potential terms are never completely negligible in the case $\lambda^2 < 6$, which explains why the solution in the absence of the potential terms is not relevant in this case. We can however see the trend that as λ^2 approaches six the ration starts to become very small until at $\lambda^2 = 6$ it is equal to zero. For large λ, although (4.10) of course no longer applies, it is easy to see that it is possible for the potential terms to become completely unimportant.

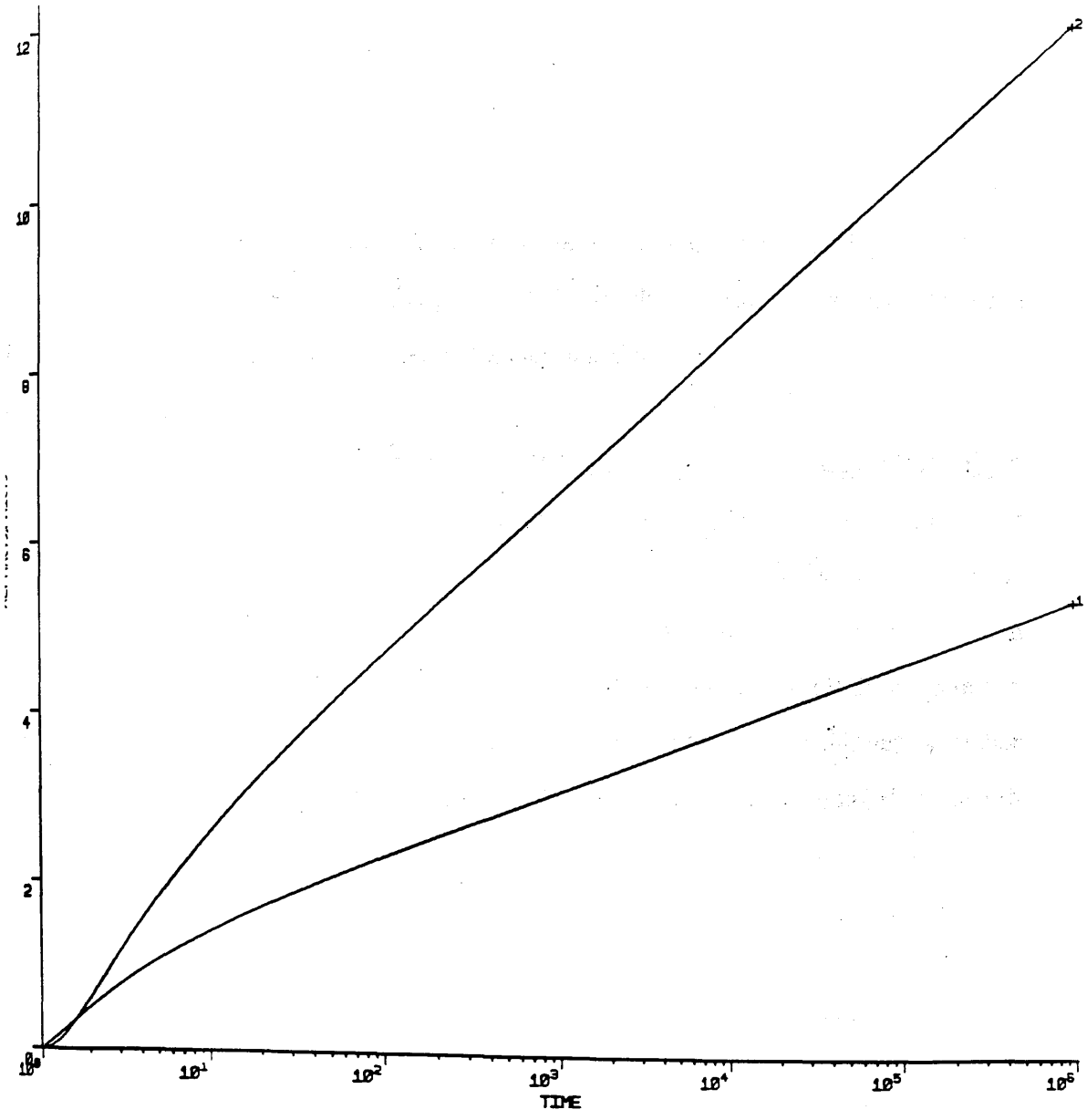

Figure 4.2 This graph (lines marked as in figure 4.1), with $\lambda^2 = 8$, shows the type of solution obtained when the exact solution no longer exists. Again we get power law behaviour, and from the gradient, we see that the solution behaves as if $\lambda^2 = 6$. This is true for any value of $\lambda^2 > 6$.

The effect of scalar fields with these exponential potentials is also of interest in the case of anisotropic cosmologies. We shall not however study this extension here as the theme of this chapter is instead to study the effect of viscous forces - see the next section. A phase plane analysis of such models along the same lines as Halliwell [38] is given in [42], and this analysis shows many of the general features that we have seen in the isotropic case.

(iii) Viscous Forces and the Enhancement of Inflation

In exponential inflationary models, it is a common assumption that the time variation of the scalar field can be neglected during the inflation. In general, the potentials required for such inflation are very flat, to ensure that the inflation lasts sufficiently long, and the scalar field does indeed roll down them very slowly. As has been emphasised by Yokoyama and Maeda [43], this approximation is no longer such a good one when we have an exponential potential, since then the scalar field can fall with an appreciable speed. This means that we have to consider the possible consequences of a time-varying scalar field for the equations of motion of the system.

Recalling that the scalar field is originating in some particle theory, possibly higher dimensional, there will be many couplings of the scalar field to other fields in the theory. When the scalar field varies, these couplings will lead to the production of particles, a process which will transfer kinetic energy away from the scalar field to supply the energy necessary for the creation of these particles. This will damp the motion of the scalar field; we shall therefore refer to these as viscous forces. Hence the equations of motion must be modified to include a viscous term. We assume that the particles produced can be represented by a radiation fluid; this can describe photons and also relativistic fermions, which is reasonable at the high temperatures of the early universe. An extra equation of motion, describing the time evolution of the radiation fluid, must also be included in the system. These particle production

scenarios are familiar from studies of particle production at the end of conventional inflation ([28,44] and chapter 3 of this thesis), where the scalar field oscillates about the global minimum of its potential and exactly the same mechanism comes into play.

For now, we shall introduce a viscosity term C_v on phenomenological grounds. Later on we shall discuss what form it should take; clearly it is in principle determinable from a knowledge of the underlying particle theory, but in practice the best we can hope for is a reasonable approximation. By applying Einstein's equations and the continuity equations for the system expressing energy conservation, the enhanced equations of motion taking viscosity into account are given by the system

$$\ddot{\phi} + 3\,\dot{\alpha}\,\dot{\phi} + \frac{dV}{d\phi} + C_v\,\dot{\phi} = 0 \tag{4.11}$$

$$\dot{\alpha}^2 = \frac{1}{6}\,\dot{\phi}^2 + \frac{1}{3}V + \frac{1}{3}\,\rho_{rad} \tag{4.12}$$

$$\dot{\rho}_{rad} = -4\,\dot{\alpha}\,\rho_{rad} + C_v\,\dot{\phi}^2 \tag{4.13}$$

Here $\alpha(t) = \ln a(t)$, and ρ_{rad} is the energy density of the radiation fluid. These equations are equivalent to those given in [43]. Compared with (4.4) and (4.5), we see that the ϕ field equation has picked up an extra term which looks like a viscous damping and the equation for the scale factor has an extra contribution because of the energy density of the radiation. There is a new equation for the energy density, which shows that it is diluted by an expansion of the space, but that energy is fed into it from the varying scalar field. These equations do not at this stage rely on a particular choice for the potential V, but in practice the choice of C_v will depend on the precise form of the potential. Hence these equations will also be relevant later when we consider potentials which are not exactly exponential.

We need a form for the viscosity coefficient C_v . Yokoyama and Maeda point

out that a physically reasonable assumption is that it should be proportional to the effective mass of the inflaton, which is the root of the potential's second derivative; that is

$$C_v = f \sqrt{\frac{d^2 V[\phi]}{d\phi^2}} \tag{4.14}$$

where f is a phenomenologically introduced constant. They also perform a perturbation calculation which backs up the choice of this form.

As a precursor to examining power law inflation caused by a potential arising from a particle theory, we examine how viscosity affects inflation with the exponential case. This situation was analysed, again by phase plane analysis, by Yokoyama and Maeda [43]; however, once again the analysis is only valid in the region $\lambda^2 < 6$ (λ having the same meaning as previously, given by equation (4.2)). When we have an exponential potential, the viscosity coefficient takes on the particularly simple form

$$C_v = f \lambda \sqrt{V} \tag{4.15}$$

A transformation of time variable as before gives a plane autonomous system, and it can be shown that not only do power law solutions remain as attractors, but in addition the viscosity gives an enhancement of the power law exponent, p in equation (4.1). Hence power law inflation is rendered more viable by the introduction of viscosity.

As in the previous section, we are really going to be interested in the case which arises in most physical theories, that of $\lambda^2 > 6$. Again we resort to numerical simulation to investigate this; this method has the advantage also that it is easily generalised to potentials which are not of an exponential form, whereas in such cases the phase plane technique will not be applicable and so we will not be able to obtain

any information in this way. It also allows a clearer elucidation of the fate of the radiation energy density.

Firstly, the simulation is used to confirm the analytic work of Yokoyama and Maeda. It is seen that the enhancement of the exponent in the power law inflation does occur, and by using a wide variety of initial conditions it is confirmed that these solutions are attractors with the power law behaviour always apparent at large times. The larger the value of f in equation (4.15), the greater the enhancement of the power law. Further, it is observed that the radiation energy density is always quickly redshifted towards zero by the rapid inflationary expansion of the space. This means that the scalar energy density remains the dominant contribution to the equations of motion, as is required to gain inflationary solutions. This behaviour of the radiation energy density also occurs for $\lambda^2 > 6$.

When we examine the case of large λ by numerical simulation, we find that the solutions are very similar in type to those for $\lambda^2 < 6$. We continue to have power law solutions as attractors and there is still an enhancement in the power law exponent which becomes greater as f is increased. Since the natural power law without viscosity in these cases is smaller, a larger value of f is required in order to give a satisfactory amount of inflation. There is one major difference in these solutions now that we have viscosity included; whereas before there was exactly the same attractor solution, given by equations (4.8) and (4.9), whatever value of λ^2 greater than six we had, now the larger values of λ give smaller power law exponents in a manner reminiscent of the small λ case. Table 4.1 below gives some sample values of the power law exponent p when λ^2 and f are varied.

λ^2 \ f	0	1	2	5	10
2	1.00	1.57	2.84	5.26	9.38
6	0.33	1.01	1.49	2.90	5.30
8	0.33	0.90	1.31	2.35	4.48
12	0.33	0.77	1.08	2.05	3.69

Table 4.1 Power law exponent varying with λ^2 and f

The first column of this table, which is the viscous-free case, is easily explained by means of the solutions of section (ii). The other columns show how the enhancement increases as the value of f goes up, and gives a guide to what value of f might be required in order to obtain a satisfactory amount of inflation. Notice that for large λ the viscosity must be quite large. The size of the power law exponent which is required by cosmological constraints is discussed later in this chapter. Figure (4.3) shows a simulation with $\lambda^2 = 8$ and $f = 5$; this can be compared with the simulation illustrated in figure (4.2), in which there is no viscous damping.

A few comments are useful to conclude this section. The first is to emphasise that viscosity is not just an *ad hoc* addition designed only to make the inflation more efficient; it is a definite physical effect which must be taken into account in construction of these models. Secondly, it may at first sight seem strange that viscosity does improve the efficiency of the inflation in this way. However, it is important to realise that it is the potential energy and not the kinetic energy of the scalar that is driving the inflation; hence, by slowing the fall of the inflaton down the potential the viscosity is actually helping the inflation. Finally, it is worth noting that the purely exponential potential is unsatisfactory as a complete model of inflation; in this model the inflation is eternal as there is no minimum of the potential for the

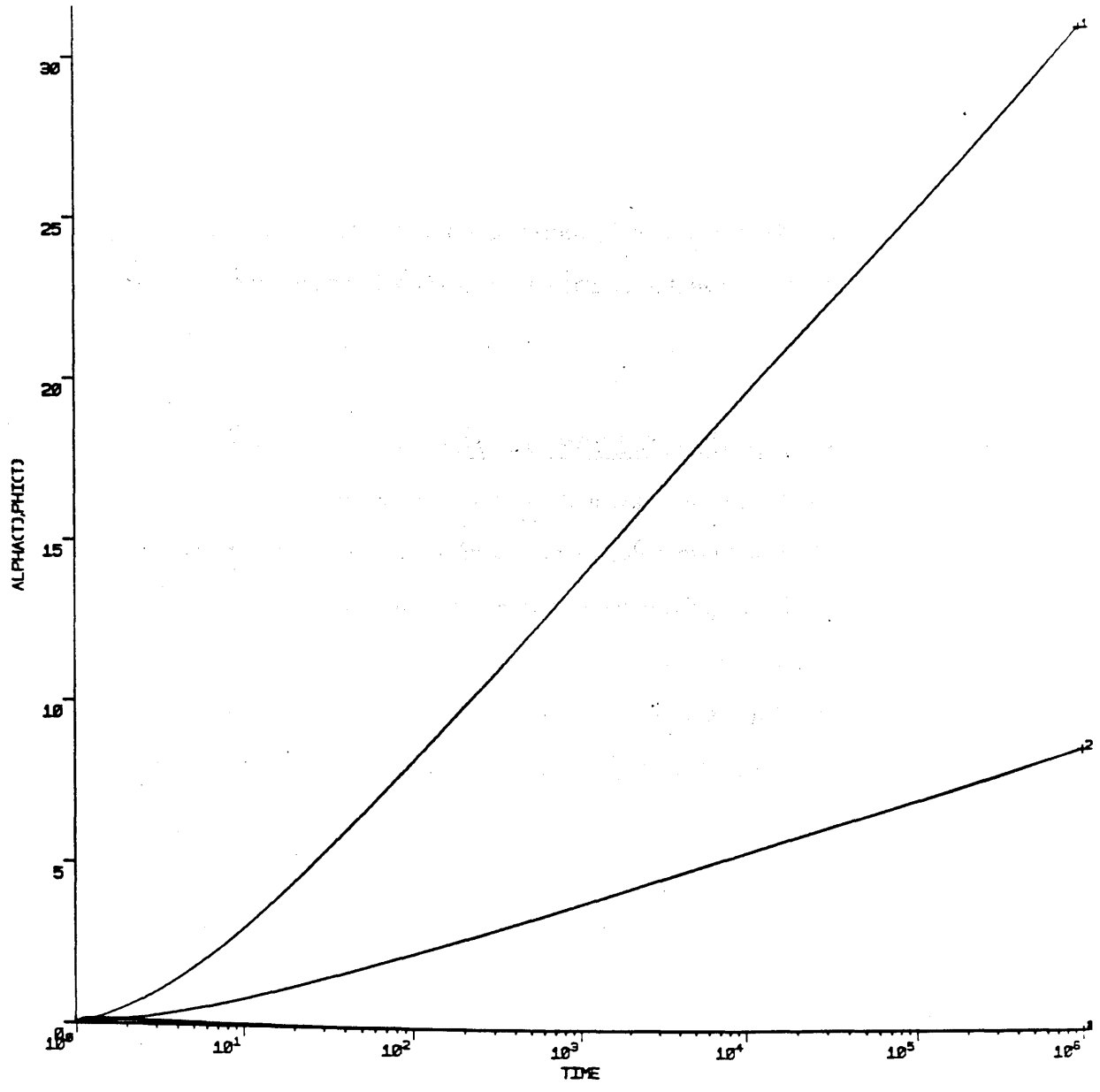

Figure 4.3 This graph demonstrates the effect of adding viscosity to the situation of figure 4.2. Once more $\lambda^2 = 8$, but we have now introduced viscosity with a coefficient f = 5. This can be seen to enhance the power law obtained, with the exponent now over 2.5 rather than 0.33. Notice that α is now given by the top line. The line marked 3 gives the energy density, which drops rapidly towards zero.

scalar field to fall into. A more realistic model would have a potential which has a minimum into which the scalar field would finally fall, bringing the inflationary era to an end. Further, this potential should be at $V[\phi] = 0$ so that the scalar field today gives a vanishing contribution to the cosmological constant. The next section will extend this work to consider just such a potential and how to use it in an inflationary scenario.

(iv) Towards a Realistic Power Law Inflation Model

In this section, we demonstrate how the ideas of the preceding sections can be incorporated into the construction of a more realistic power law model. This model is based around a potential which comes from an underlying particle theory and which satisfies the criteria mentioned at the end of the previous section. Here we will consider the various cosmological constraints on power law inflation in order to see whether or not a successful model can be arranged, and we shall also see how the presence of the attractor solutions, as described above, means that we do not have to worry about the particular form of the initial conditions supplied to the scenario. The construction here is not meant to be interpreted as a complete inflationary scenario; rather, it is an outline of how one might go about implementing such a model and also shows how the introduction of viscosity substantially improves the viability of these models.

The theory which we consider here is what is called the Salam-Sezgin model [45]. This model consists of an N=2 supergravity theory (that is, there are two supersymmetry charges) formulated in six space-time dimensions, and then compactified on a two-sphere in order to give a four dimensional theory. While this is certainly not a complete theory giving a correct particle spectrum in the four dimensional reduced theory, it is a useful theory to study because of its simplicity as compared to the more complicated supergravity theories such as the ten dimensional theory obtainable as a low energy effective field theory to the superstring. Further,

much of the behaviour in this theory can be expected to be rather generic of these sorts of higher dimensional theories, since the forms of the potentials are very similar in all these theories [46], and because of this its cosmological behaviour has received considerable attention in recent years [41,47].

We follow in part here an original calculation of the potential in this theory by Halliwell [47]. Given a particular ansatz for compactification, where the Maxwell field takes on a magnetic monopole configuration over the extra dimensional two-sphere, he showed that the system is equivalent to two scalar fields moving under an effective potential in a standard Friedmann cosmology. The details of this can be found in [47]; a rough description of what happens is the following. The higher dimensional theory is given two scale factors, one associated with the external space and one with the internal two sphere, and in addition has a single fundamental scalar field. When we go to the dimensionally reduced theory, we have to conformally rescale the external and internal metrics to ensure constancy of the gravitational 'constant', and it is also convenient to make other redefinitions. The final upshot is that the three variables of the six dimensional theory given above become the scale factor of the four dimensional theory and two scalar fields moving under an effective potential determined via these transformations. The important feature for our considerations is that the effective potential has exponential regions which might allow the scenarios of the previous sections to be implemented.

(Note - There are small differences between the forms of the potential we have and those given by Halliwell. This is because a different normalisation of the scalar fields has been used - the scalar fields in both of Halliwell's papers [38,47] are equivalent to ours divided by $\sqrt{6}$. This accounts for differences in the potentials and brings the equations of motion into the same form.)

We call the scalar fields in the theory ξ and ϕ, and continue to refer to the scale factor as a with the definition $\alpha = \ln(a)$ for convenience.The equations of motion are just equations (4.11) to (4.13), with an extra equation similar to (4.11) for the ξ field

and with extra ξ field terms in (4.12) and (4.13) mimicking the ϕ terms. The potential in which the scalar fields move is given by

$$V = \frac{1}{18} e^{-\sqrt{2}\xi} \left(e^{-\sqrt{8}\phi} - 2 e^{-\sqrt{2}\phi} + 1 \right) \tag{4.16}$$

which can also be rewritten as

$$V = \frac{1}{18} e^{-\sqrt{2}\xi} \left(e^{-\sqrt{2}\phi} - 1 \right)^2 \tag{4.17}$$

It is clear that there are two separate exponential potentials here; the ξ field has a purely exponential potential of the form of the previous section, while the ϕ part of the potential behaves like an exponential potential for sufficiently negative values of ϕ. We now examine ways of implementing power law inflationary scenarios using this potential.

First, we give brief consideration to the ξ field, though in fact ultimately we shall find that it is the ϕ field which is better adapted to our purposes. The form of the ξ part of the potential, a single term multiplying $V[\phi]$, is a general consequence of the scale invariance of the classical theory [46]. This is is a feature of many theories of this type [46], and means that the potential does not have a global minimum in the ξ direction; essentially we have the same situation as discussed at the end of section (iii). This makes the construction of an inflationary scenario harder as we need a means of bringing the inflation to an end. Halliwell [47] has considered a model where the ξ field induces inflation which is brought to an end by the ϕ field falling into its global minimum at $\phi = 0$, at which point the entire potential vanishes. This is making use of the observation that the power law behaviour does not depend on V_0 in equation (4.2). In his model without viscosity, this does not actually allow a working inflationary scenario to occur, since the ξ potential has $\lambda^2 = 2$ which leads to a power law exponent of exactly 1. However, we can see from the results of

section (iii) that viscosity can improve this into a viable scenario; indeed we see from table 4.1 that not much viscosity is required to do this. In practice, however, it is probably impossible to obtain a sensible working scenario. This is because it is hard to see how it can be arranged for the ϕ field to fall into the minimum and end the inflation only after sufficient inflation has occurred but before any cosmological constraints are violated (excessive inflation can run into problems with overly large density perturbations), unless an extreme fine tuning of initial values was imposed. This possibility for inflation will not be considered any further here and we shall avoid scenarios which depend on sensitive use of both scalar fields because we will always expect these fine tuning difficulties.

For the rest of this chapter we consider an inflationary scenario using the ϕ field to provide the necessary energy density. It has been emphasised by Gibbons and Townsend [46] that the scale invariance of the classical theory, which leads to the form of (4.16) as described above, will not survive into the quantised theory, and they claim that in the full quantum theory there is likely to be a minimum in the ξ direction while the form of the the ϕ potential should remain unaffected. We therefore consider a situation where the ξ field falls into this minimum early in its evolution; the ξ field then drops out of the equations and we are left just with the ϕ field moving in a potential given by

$$V = V_0 \left(e^{-\sqrt{8}\,\phi} - 2\, e^{-\sqrt{2}\,\phi} + 1 \right) \tag{4.18}$$

Figure (4.4) illustrates the general shape of this potential, with V_0 set at one. In practice, the actual value of V_0 depends on the height of the minimum in the ξ direction, which is unknown, but in practice that this is not as important as one might think since the earlier analysis has shown that the magnitude of V_0 does not alter the power law exponent during inflation. There are however constraints on V_0 from cosmological observations; in particular the requirement that density

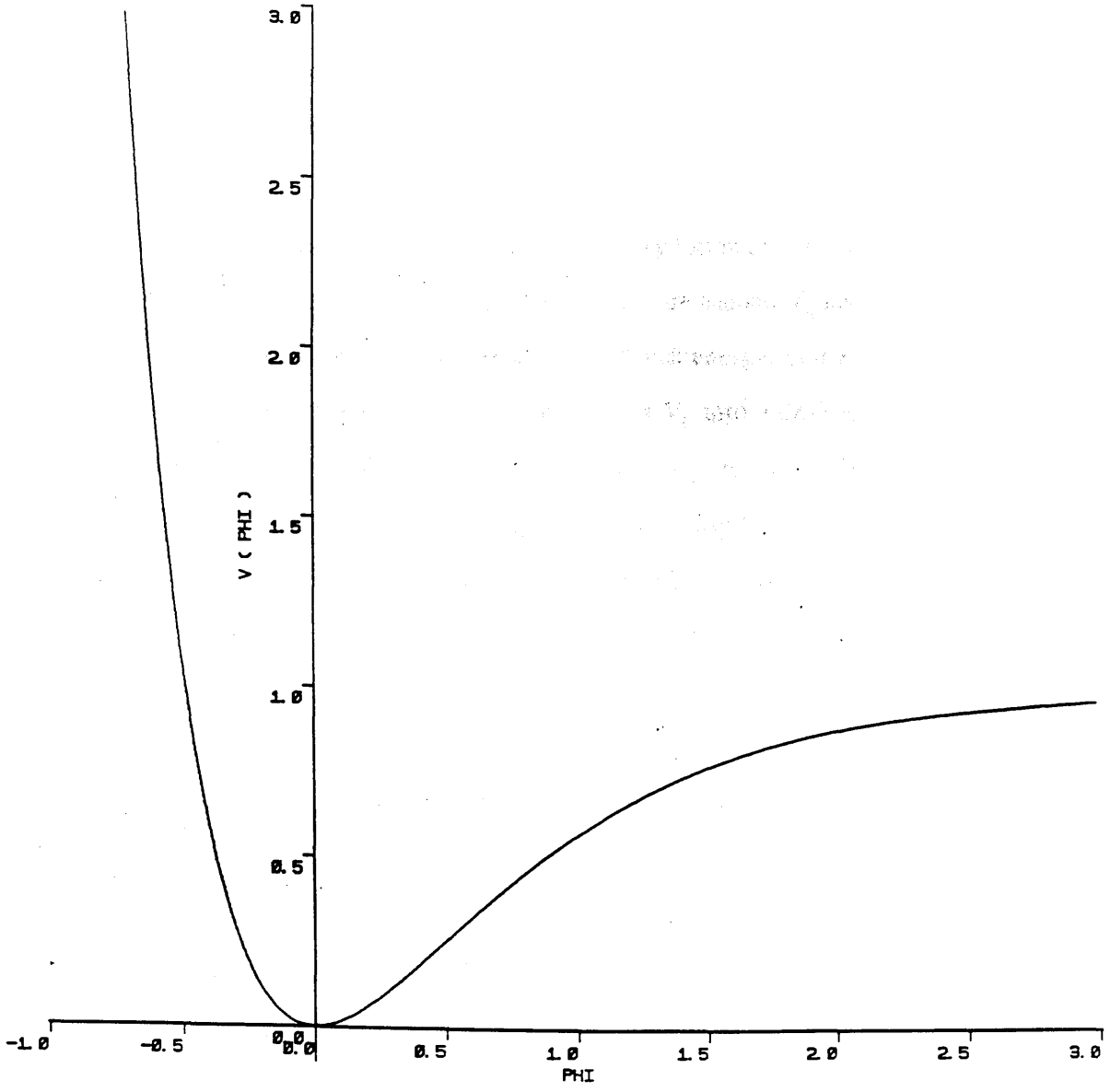

Figure 4.4 This figure shows the shape of the potential in equation (4.18) in the ϕ direction. for negative ϕ it is effectively exponential, but it features a global minimum where the potential energy is zero. The coefficient of the potential has been set to one for this diagram.

fluctuations caused by inflation should be small implies that V_0 should roughly be in the range from 10^{-13} to 10^{-15} in Planck units [48]. (This constraint is weakened if we only require that these perturbations be unobservably small, rather than of an appropriate size for some specific role such as galaxy formation. In this case we only have an upper bound for V_0 .) In fact, we shall require a small V_0 later since we do not wish to consider energies in excess of the Planck energy. Some fine tuning of model parameters may be needed in order to get V_0 into a desirable range. For numerical work, we will find it convenient to absorb V_0 into the potentials.

Here we consider a different possibility for inflation from that considered by Halliwell in [47] by taking advantage of the ϕ potential as given by equation (4.18), which is very well adapted for the construction of an inflationary scenario. We will start by allowing the ϕ field to take on a negative value (the motivation for this is considered later); when $\phi << 0$ the potential is exponential to a very good approximation, with an exponent $\lambda = \sqrt{8}$. As we have seen, this would normally not allow sufficient power law expansion, but the introduction of viscous effects will enhance the power law exponent with the possibility of a satisfactory amount of inflation. This potential has a global minimum at $\phi = 0$, at which point the potential also vanishes, and we can expect that the scalar field should fall into this minimum to bring the inflation to an end.

We now numerically examine the dynamics of this model. The relevant equations are still (4.11) to (4.13), where we now use (4.18) as the expression for the potential. The appropriate form for C_v comes from putting this potential into equation (4.14), and gives the expression

$$C_v = 2 f \sqrt{V_0 \left(2 e^{-\sqrt{8}\,\phi} - e^{-\sqrt{2}\,\phi} \right)} \qquad (4.19)$$

where f is the same phenomenologically introduced constant as before. This again has the appropriate form for an exponential potential with $\lambda = \sqrt{8}$ when $\phi << 0$, so

we can expect the work of section (iii) to be applicable here.

We now have the complete set of equations for the system, but before we can proceed we have to supply initial conditions for the variables in the equations; that is, for α, ρ_{rad} and both ϕ and its first derivative. The hope is that by making a sensible physical choice of these we will find a working inflationary scenario; this hope is well justified since in section (iii) we showed that inflationary solutions are attractors and hence the initial conditions should not be of major importance.

We first note that the initial value of α is irrelevant, and so nothing is lost by setting it initially to zero. The solutions are unaffected by adding a constant to α, since they only involve α's derivative, so we can always normalise it if required. Adding a constant to α corresponds to multiplying the scale factor by an arbitrary constant. What is relevant to our scenario is not α, but rather the amount of inflation obtained, Z, given by the ratio of the final to the initial scale factor

$$Z = \frac{a_{final}}{a_{initial}} = \exp (\alpha_{final} - \alpha_{initial}) \qquad (4.20)$$

to which we shall give more consideration to later. The simulations also demonstrate that the initial value of the radiation energy density, ρ_{rad}, does not matter; during the inflation, despite constantly being fed energy from the scalar field variation, the expansion of the space is so rapid that the radiation density is red-shifted towards zero, just as in conventional inflation. Its affect on the dynamics is therefore negligible during the inflationary phase, and we can safely set its initial value to zero. Similarly, because the inflationary mode is an attractor, whichever initial value the derivative of ϕ is given we rapidly reach the power law inflation phase, so once more we are free to set its initial value to zero.

Hence the only initial value we need worry about is that of the ϕ field itself. This clearly is going to be a very important quantity, since the position on the potential, illustrated in figure (4.4), where the scalar field starts will determine how

far it has to fall to reach the potential minimum, and hence how much inflation will occur. To resolve the horizon and flatness problems, an inflation factor Z of at least e^{70} is required [18], so we must have a sufficiently negative initial value of ϕ to allow this. Such an initial condition is allowed, and indeed expected, in the chaotic inflation scenario of Linde [49]. In this picture, we postulate that as the universe cools down from Planck energies, we can expect that thermal and quantum fluctuations will cause different regions of the universe to have a whole spectrum of different values of ϕ with varying energies up to the Planck energy. In this context, this means that we can expect to find values for the scalar field anywhere in the potential such that its potential energy does not exceed the Planck energy, and so it is the value of V_0 which determines the actual range of ϕ allowed. Note that V_0 is in Planck energies. We will find that when V_0 is small, we can have a ϕ value sufficiently negative to allow adequate inflation to occur (this is again taking advantage of the power law exponent not depending on V_0). This is not a serious constraint in the sense that, as remarked earlier, there are already cosmological constraints forcing V_0 to be very small.

There is now one remaining quantity to be determined - the value of the viscosity coefficient f in equation (4.19). This can in principle be determined from the underlying theory via the coupling of the scalar to other fields, but in practice this is prohibitively difficult. The choice of f is important since, as is seen from table (4.1), its value decides how much the power law exponent is enhanced by during the inflation. Here we give some consideration to what value of the power law exponent might be required.

The power law exponent affects the type of density perturbations which are generated by the inflation. This spectrum is given by

$$\frac{\delta\rho}{\rho} \sim k^{-1/(p-1)} \qquad (4.21)$$

where ρ is the density, k the wave number and p the power law exponent. For large p, this spectrum becomes indistinguishable from the scale invariant Harrison - Zel'dovich spectrum obtained in conventional inflation, which has no dependence on the wave number and agrees well with actual observations. However, as p becomes smaller the unconventional spectrum may be in violation with observations. Notice that this objection is only valid if we are trying to use these perturbations to form galaxies. If we are using some other mechanism to form galaxies, such as cosmic strings for instance, then we would only require that the inflationary density perturbations are unobservably small, and there would be no constraint from their actual spectrum. It is worth noting that while just now there is no working scenario with both inflation and cosmic strings, due to problems with the reheating temperature being insufficiently high to allow a post-inflationary cosmic string producing phase transition [50], recent work [51] indicates that they may not be completely incompatible as has been suggested in the last couple of years.

Another effect relating to the power law exponent is that of the maximum reheat temperature after inflation [37]; that is, the temperature to which the final oscillations of the scalar can raise the matter in the universe. When p = 2, a maximum reheat temperature of 10^8 GeV is allowed which contradicts or is only marginally in agreement with baryogenesis models (the maximum reheat follows from purely energetic arguments, and so cannot be circumvented in a particular model). At p = 2.5 , the maximum reheat of around 10^{11} GeV is sufficiently high that this should pose no problems. It is also possible to get round this constraint if baryogenesis is provided by a process happening at much lower energies than standard GUT models; such an example is provided by anomalous electro-weak baryon production [52], which occurs at around the electroweak phase transition at 100 GeV. If such a model is viable (at this time no working model has been demonstrated satisfactorily), then clearly the reheating constraint can also be avoided.

To be on the safe side, we shall assume conventional baryogenesis and require

a power law exponent of around 2.5 or more. The analysis of exponential potentials in section (iii) with $\lambda^2 = 8$, as seen in table (4.1), indicates that such a power law can be obtained with a viscosity coefficient of around five or more. While it is hard to be definite, a first order perturbation calculation [43] shows that f is related to the number of scalar decay modes, and that in the supergravity model where the number of such modes is high, a value of f around five is not an unreasonable estimate.

We now have accumulated all the information necessary to arrange for our inflationary scenario. Numerical simulation is used to find out what happens given the initial conditions as specified above with values of f around five. It is discovered that by setting the original value of ϕ at about -20 a sufficiently large amount of inflation occurs, and as ϕ is made more negative the inflation factor Z increases. Figure (4.5) shows a sample simulation which outlines the main features of the solutions. This simulation is carried out with f equalling six, which gives a power law exponent of around three.

The evolution can be seen to be characterised by three different stages in the evolution of the universe. At first, the initial conditions supplied are not in a power law configuration, in general. The first stage of the evolution then is the transition into the power law state from these initial conditions, with the actual duration of this stage depending on how far from the power law state they are. It is reassuring, given our complete ignorance of which values the fields may have when they emerge from the Planck regime, that the power law state is found to be an attractor for all initial conditions.

The second stage is the power law expansion itself. In figure (4.5) the time axis is logarithmic, so when we plot α the power law solution appears as a straight line (and further, we can establish the power law exponent from the gradient of this line to show agreement with the work of section (iii)). During this phase the scalar field is falling down an effectively exponential potential under the action of viscous forces, but it is observed that the energy density of the particles produced by these

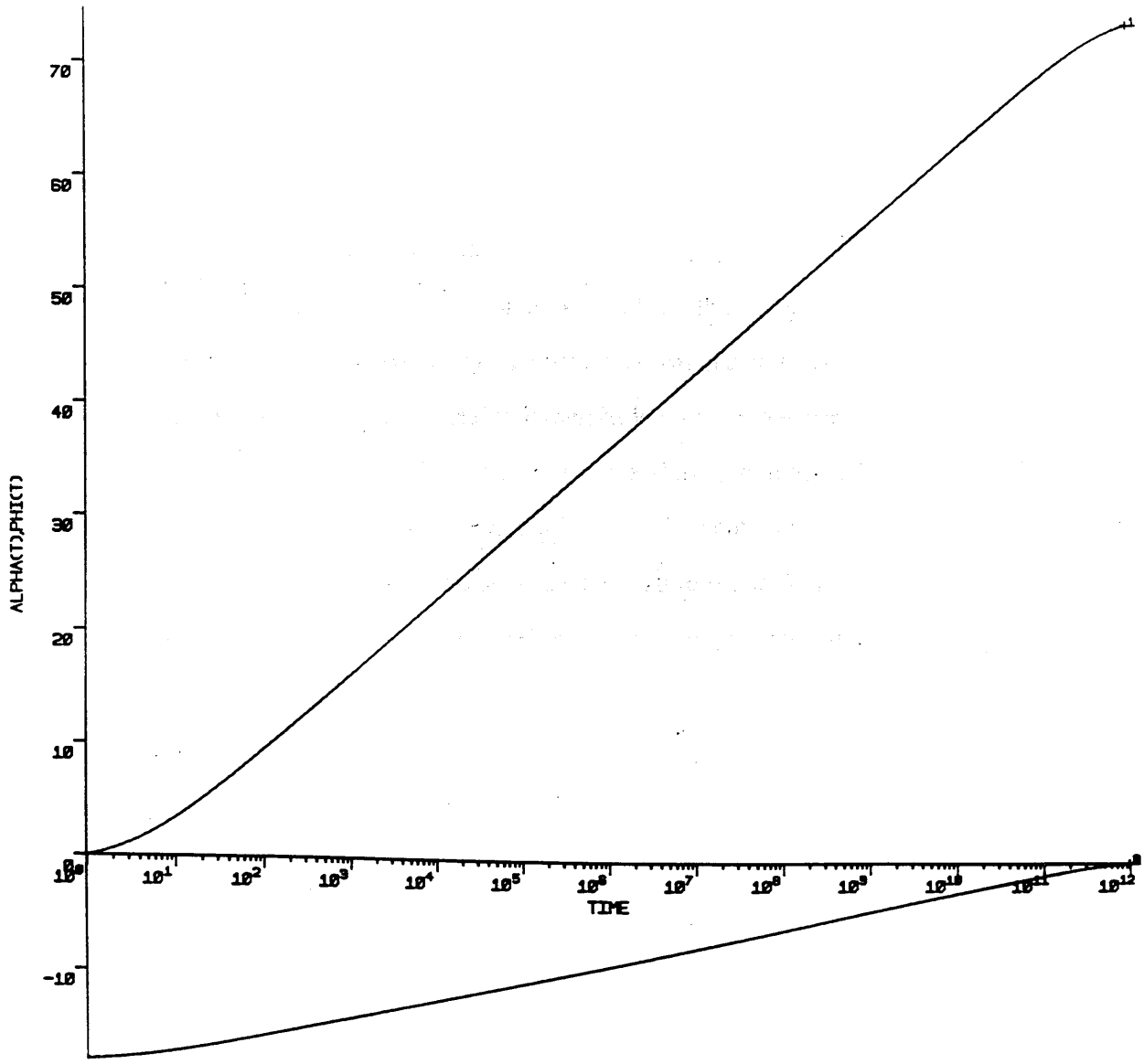

Figure 4.5 This shows a sample numerical simulation using the potential in figure 4.4. The ϕ field starts with a negative value and falls towards the potential minimum at $\phi = 0$. The top line is the log of the scale factor. Here the viscosity coefficient has been set at six, giving a power law exponent of around three. From equation (4.20) we can see that the inflation factor exceeds e^{70}, giving a satisfactory amount of inflation. The three phases in the evolution - approaching the power law solution, power law inflation, exit from inflation - can be clearly seen.

forces falls because of the rapid expansion of the space, and so they do not affect the dynamics. The duration of this inflationary phase is entirely determined by the initial position of ϕ in the potential, since it is the distance through which it must fall that determines the amount of inflation.

When it approaches the minimum we reach the third stage in the evolution; we no longer have an approximately exponential potential and the power law evolution comes to an end. The scalar field will then be in a situation exactly as that found in conventional inflation models; it will oscillate about the minimum, still under the influence of viscosity (in conventional inflation, it is only here that the viscosity is important), and will reheat the universe back up to higher temperatures. Here, as discussed earlier, the maximum reheating temperature, which depends on the power law exponent, is easily high enough to allow conventional baryogenesis models to take place, though in general never sufficiently high to allow the reformation of post-inflation cosmic strings. This last point is a failure common to all types of inflation at the moment, even with fine tuned potentials. Finally, when reheating is complete, we expect the scalar field terms to drop out of the equations of motion to play no further cosmological role, leaving us in a conventional Friedmann universe.

(v) Summary

The work described in this chapter can be summarised as follows. In section (i) the motivation for the study of exponential potentials is outlined and power law inflation is described. Section (ii) gives an exact solution exhibiting power law behaviour when we have the simple case of an exponential potential, and it is in addition demonstrated that the solution types depend on the range of values of the parameter λ in the potential - the solutions for $\lambda^2 > 6$ being of a different type to those with small λ. The solution given by equations (4.6) and (4.7), while only valid when $\lambda^2 < 6$, is more general than those which have previously appeared in the literature. In section (iii) the importance of the viscosity effects arising from particle

production are considered, and by numerical techniques are shown to enhance the power law exponent during inflation; this includes the cases $\lambda^2 > 6$ where analytic work by earlier authors is not valid. This is an important point because we find that in cases where the potential arises from an underlying particle theory λ tends to lie in this range. The variation of the power law exponent at various values of λ is examined as the amount of viscosity is varied.

Finally, in section (iv) an outline is made of how to construct an inflationary model consistent with cosmological observations in cases where a particle theory leads to a potential of approximately exponential type. Here numerical simulation is the only practical technique due to the complicated forms of the full potentials. A new method is demonstrated of gaining inflation from the potential derived in the Salam-Sezgin model given by equation (4.18), and it is demonstrated that viscosity makes the model more viable; in the absence of viscosity the power law exponent would not be great enough to induce inflation. Because we have shown that the power law solution is an attractor, inflation occurs for a wide range of initial conditions. In this sense inflation is rather generic in these kinds of theory. For some ranges of these initial conditions we may obtain unsatisfactory models due to such things as density perturbations, but we have shown that an appropriate choice of initial conditions can avoid this. The amount of inflation obtained is determined by the initial position of ϕ in the potential, and if ϕ is sufficiently negative adequate inflation occurs to solve the horizon and flatness problems. Suitable initial conditions would be expected, along with a range of others in different regions of the pre-inflationary universe, in the chaotic inflation scenario, so one of these original regions could today constitute the observable universe. The considerations of the model building are more general than the specific case of the Salam-Sezgin model which we consider here; it should be possible to construct an inflationary model following these outlines in many of the particle theories which give rise to approximately exponential potentials.

Chapter 5

Extra Dimensions, Neutron Stars and Gravitational Collapse

(i) Introduction : Neutron Stars and Extra Dimensions

In the last ten years there has been a proliferation of particle theories which rely on the existence of extra hidden spatial dimensions for a consistent formulation, such as supergravity theories and superstrings. All these theories have as a distant ancestor an idea of Kaluza that by incorporating an extra dimension into general relativity the equations of general relativity coupled to Maxwell's equations of electromagnetism can be obtained [53]. This was the first hint that interactions could be viewed as being caused by the geometry of extra dimensions.

Of course, we do not observe these extra dimensions around us today, but this potential worry is alleviated by the realisation that the extra dimensions must be very small, of the order of the Planck scale. This renders them unobservable at the energies obtainable in experiments which can currently be carried out; an accelerator circumnavigating the galaxy would be required to reach energies which might reveal these dimensions, clearly not a practical arrangement! This introduces the question of how one might go about testing the existence of these dimensions. As we have already seen in earlier chapters, one way of testing the predictions of such theories is by cosmological observations; at very early times we would expect all the dimensions to be of comparable size and then the effect of the extra dimensions might perhaps become important. The process of compactification, where all but three of the spatial dimensions remain small, may also provide a characteristic signature of higher dimensional theories.

Unfortunately, we are not yet in a position where such observations can tell us

much about these theories; also the theoretical standing is such that we do not have a clear idea of what one would look for as evidence. Because the earliest eras of the universe are not directly observable, we must rely on relic evidence such as the microwave background, the abundances of light elements, the gravitational wave spectrum from the big bang and other such things to tell us of the processes that went on when extra dimensions were important. What would be more useful would be to find events which are directly observable and which might tell us something about extra dimensions. With this in mind, we turn to a consideration of astrophysical objects.

For the sake of simplicity, we shall from here on consider the simplest extra dimensional theory - the original one of Kaluza and Klein [53] of which a brief review is given below. The results can be expected to generalise to extra dimensional theories beyond this one, though the details of how to deal with a more complicated internal space such as those expected in superstring theories are not clear. We shall capitalise on the well known fact that in the spherically symmetric case this theory becomes formally equivalent to conventional four dimensional general relativity coupled to a real scalar field.

In the simplest Kaluza-Klein theory, with one extra dimension and known as abelian Kaluza-Klein because its internal space has an abelian symmetry group U(1), one can show that the five dimensional metric can be split up into a four dimensional metric satisfying the four dimensional Einstein equations, a 4-vector which can be identified with the vector potential of electromagnetism, and a scalar field obeying the Klein-Gordon equation. This split is performed as follows, where γ_{mn} is the metric of the five-dimensional theory and $g_{\mu\nu}$ is that of the four dimensional subspace on which the four dimensional Einstein equations will hold. (Throughout, Greek indices will be used on the four dimensional manifold and Latin ones otherwise.) To do this we must assume that the metric does not depend on the coordinate of the extra dimension, on which more shall be said shortly. We get

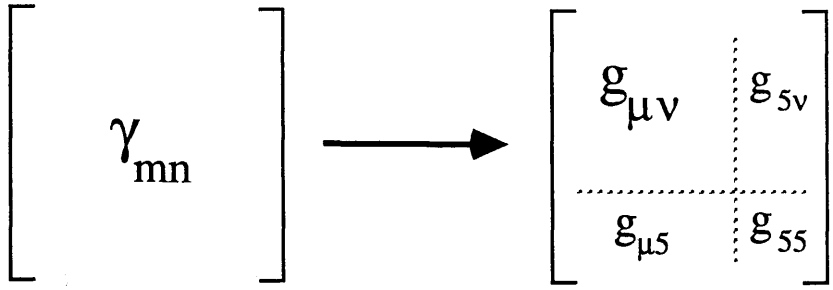

where the g_{mn} are obtained from γ_{mn} via the following relationships.

$$g_{\mu\nu} = \gamma_{\mu\nu} - \frac{\gamma_{\mu 5}\,\gamma_{\nu 5}}{\gamma_{55}} \tag{5.1}$$

$$g_{\mu 5} = \frac{\gamma_{\mu 5}}{\gamma_{55}} \tag{5.2}$$

$$g_{55} = \gamma_{55} \tag{5.3}$$

Since the metrics are symmetric, $g_{\mu 5}$ and $g_{5\nu}$ give the same 4-vector and they correspond to A_μ , the electromagnetic potential. g_{55} is often rewritten via the relation

$$\sigma = \ln\left(\sqrt{g_{55}}\right) \tag{5.4}$$

where σ now behaves as a scalar. In order to ensure that the gravitational constant truly is constant, we have to make an additional conformal transformation of the effective four dimensional metric, by defining

$$g^{*}_{\mu\nu} = e^{\sigma} g_{\mu\nu} \quad \left(= \sqrt{\gamma_{55}}\; g_{\mu\nu}\right) \tag{5.5}$$

If there is more than one extra dimension the internal metric, here given just by g_{55}, must also be conformally transformed.

It was mentioned above that for this construction to work the five dimensional

metric must not depend on x_5, which at first seems an unnatural requirement. It was first noticed by Klein that this becomes natural if the extra dimension is taken to be a very small circle at each point, giving a hypercylindrical spacetime. In fact, because the coupling of electromagnetism is related to the size of the extra dimension, the theory *requires* that the extra dimension should be small. This then justifies the use of the splitting given by equations (5.1) to (5.5), which is viewed as giving an effective theory valid when we are at energies sufficiently low that we cannot excite higher dimensional modes.

We are now in a position to consider solving the equations of the higher dimensional space-time. In keeping with studies of objects such as black holes in conventional relativity, we must impose some symmetry requirements on the problem to make it tractable. The notion of spherical symmetry will be applied, which leads to the Schwarzchild geometry in relativity. Under this assumption, the metric can be cast in diagonal form, so the electromagnetic contributions, which come from the $g_{\mu 5}$ component, all vanish. It can be shown that when the five dimensional Einstein equations are applied to this metric, the equations are formally exactly equivalent to a real massless scalar field minimally coupled to gravity; that is, they match the equations coming from the Lagrangian

$$L = \frac{\mathbf{R}}{16\pi} - \frac{1}{8\pi}\partial_\mu\phi\,\partial^\mu\phi \tag{5.6}$$

We shall for convenience use the scalar field formalism when we derive the basic equations, while always remembering that the main motivation resides in the higher dimensional case. The relations above allow us to determine the five-dimensional solutions from those of four dimensions plus a scalar.

Studies by most authors into higher dimensional solutions have concentrated on the notion of the black hole solutions in Kaluza-Klein theories, including those with the electromagnetic potential non-vanishing. The first attempt to categorise such

solutions in the abelian case was made by Chodos and Detweiler [54], who found a three parameter class of solutions, where the parameters can be viewed as being mass, electric charge and scalar charge, and investigated their causal structure. This class was extended by Gibbons and Wiltshire [55] to a fourth parameter, a magnetic charge, which saturates the set of static, spherically symmetric, asymptotically flat black hole solutions. A more comprehensive approach based on sigma model techniques was carried out by Breitenlohner, Maison and Gibbons [56], which also gives consideration to the generalisation of existence and uniqueness theorems from general relativity. Belinsky and Ruffini [57] found a class of axisymmetric solutions with rotation, but it remains unclear how to construct the most general solution of this type. Notice that not all these solutions correspond to what one normally considers to be a black hole; some have singular event horizons or wormhole like topology. Another variant on these solutions is the 'Kaluza-Klein monopole' configurations of Sorkin [58] and Gross and Perry [59] which exist due to the possibility of inequivalent topologies in the asymptotic boundary conditions.

While these solutions offer a lot of insight into the spacetime structure of higher dimensional spacetimes (in particular these solutions can have a global structure differing vastly from the Schwarzchild or Reissner-Nordstrom solutions, especially with respect to their singularities), they have yet to prove useful in allowing one to investigate the astrophysical consequences of Kaluza-Klein theories. This is mainly attributable to the extreme difficulty in observing black holes and obtaining details about their structure. Hence here we wish instead to investigate the effect on more easily observed objects, neutron stars, which in their manifestation as pulsars have been observed for over twenty years by astronomers, and about which far more information is known. An excellent review of the status of the theory and observation of neutron stars is provided by Shapiro and Teukolsky [2], and the study of pulsars has gained a new impetus from the recent observation of a pulsar as a remnant of the supernova SN 1987a in the Magellanic clouds. Neutron stars are

well adapted to our purposes since they are of sufficient density that their description must be made through the notions of general relativity; this means that we may hope that the alterations made to relativity by the incorporation of the extra dimension might be important.

In order to set up a model of neutron star structure, the most important choice that must be made is that of the equation of state. This determines the properties of the matter from which the star is made. Many different equations of state have been employed, applicable over differing density ranges, and an extremely detailed treatment may also allow for interactions between particles [2]. Here we shall evade such complexities, and consider the very first neutron star model, as devised by Oppenheimer and Volkoff [60] in 1939.

Their treatment revolves around an equation of state first derived by Chandrasekhar [61], which describes non-interacting fermions in thermal equilibrium. While this does not include interactions, it turns out that the results which can be obtained from it are very representative of those of more complicated equations of state. The equilibrium configurations are parametrised purely by the central density of the star. Of particular interest amongst the properties is that there is a maximum total mass at which stable neutron stars can exist, with extremely high central densities leading to more compact objects of lower total mass. This phenomenon, present in all equations of state, can be treated as the best theoretical evidence that black holes should exist in the universe, as presumably they are the only equilibrium configuration available to the higher mass objects. It turns out that the maximum mass in the Oppenheimer-Volkoff case is too small, at about seven-tenths the solar mass, to explain several neutron stars which are known to have masses of around one and a half times the sun's mass. (The masses of neutron stars in binary systems are fairly easy to measure.) More complicated equations of state are seen to have maximum masses sufficiently high to allow such stars. (Incidentally, the requirement of causality alone guarantees a maximum neutron star

mass independent of the details of the equation of state at extreme densities [62].) While this certainly rules out Oppenheimer-Volkoff as the complete theory, it is still very useful for study because of its inate simplicity, and we shall use it in the assumption that any interesting properties will generalise to more complicated equations of state. This is also done for reasons of consistency; since we are neglecting any explicit interaction terms involving the scalar field (or extra dimension) it makes sense to also ignore such terms among the fermions alone. It also has the advantage that any extra features we introduce will not be concealed by an already complex theory. We shall pay particular attention to the way we describe the fluid in the five dimensional theory.

In addition to the maximum mass question, we shall also be interested in the nature of the spacetimes which exist as exterior solutions to the neutron stars. When we describe the neutron fluid in an essentially five-dimensional manner, we find that we are *forced* into having the extra dimension varying in size, which corresponds to a scalar charge which is not allowed in the black hole solutions. This leads to an exterior metric which differs from the conventional Schwarzchild one, though it approaches it at large distances from the star.

Section (v) in this chapter considers a slightly different aspect to this problem - that of gravitational collapse itself. Such a problem can only be solved analytically under many simplifying assumptions even in general relativity, but again this turns out to include many of the features found numerically in more complicated models. The general relativistic model is generalised to the Kaluza-Klein case where, surprisingly, it can still be solved exactly. As we shall see, however, there are problems with the exterior solution due to the lack of a Birkhoff's theorem in Kaluza-Klein theories. The model treated is that of a sphere of pressureless dust, with no forces to keep the particles apart even at close distances, which collapses uniformly to a point while retaining an imposed spherical symmetry. The general metric pertaining to this problem can be found, a procedure much simplified by the

use of a convenient coordinate system.

(ii) The Equations of Stellar Structure

Here we derive the equations of stellar structure, from which our analysis shall be made. We assume from the outset that we are looking for equilibrium states; that is, there is no time dependence in the metric. We also restrict ourselves to the case of a static, spherically symmetric star, which allows us to cast the metric into a diagonal form. We shall use the scalar field formalism here for convenience, denoting the scalar field by ϕ. Under our assumption of staticity ϕ will depend only on the radial coordinate r. ϕ roughly corresponds to the exponential of the size of the extra dimension, as can be seen by equation (5.4). The metric can be written as

$$ds^2 = -B(r)\, dt^2 + A(r)\, dr^2 + r^2 (d\theta^2 + \sin^2\theta\, d\psi^2) \tag{5.7}$$

We have contributions to the energy-momentum tensor from both the neutrons, represented by a perfect fluid, and from the scalar field. We shall leave consideration of the equation of state for the fluid until later. For the fluid, we have energy momentum tensor

$${}^{n}T^{\mu}_{\nu} = (\rho + p) U^{\mu} U_{\nu} + p\, \delta^{\mu}_{\nu} \tag{5.8}$$

while for the scalar field we have

$${}^{\phi}T^{\mu}_{\nu} = g^{\mu\rho}\, \partial_{\nu}\phi\, \partial_{\rho}\phi - \frac{1}{2}\delta^{\mu}_{\nu}\, g^{\rho\sigma}\, \partial_{\rho}\phi\, \partial_{\sigma}\phi \tag{5.9}$$

where in each case the superscript preceding the T indicates which contribution to the energy-momentum tensor is being considered, and where U^{μ} is the fluid 4-velocity vector.

There are several equations that these quantities must obey; they must satisfy the

Einstein equations, the continuity equations expressing energy conservation in the system, and the equation of motion of the scalar field. These equations are not all independent, since the Einstein equations automatically guarantee energy conservation, but the equation of energy conservation turns out to be a simpler one. We shall begin by deriving it.

Energy conservation is expressed by the equation

$$T^{\mu}_{\nu;\mu} = 0 \tag{5.10}$$

where the semi-colon indicates a covariant derivative. In the metric given by equation (5.7), the total energy-momentum tensor from equations (5.8) and (5.9) can be written as

$$T^{\mu}_{\nu} = {}^{n}T^{\mu}_{\nu} + {}^{\phi}T^{\mu}_{\nu} = \begin{bmatrix} -\rho & 0 & 0 & 0 \\ 0 & p & 0 & 0 \\ 0 & 0 & p & 0 \\ 0 & 0 & 0 & p \end{bmatrix} + \frac{\phi'^{2}}{2A} \begin{bmatrix} -1 & 0 & 0 & 0 \\ 0 & 1 & 0 & 0 \\ 0 & 0 & -1 & 0 \\ 0 & 0 & 0 & -1 \end{bmatrix} \tag{5.11}$$

Applying equation (5.10) to this tensor, using the metric of equation (5.7), we can obtain the energy conservation equation

$$\frac{d}{dr}\left(p + \frac{\phi'^{2}}{2A}\right) + \frac{1}{2}\frac{B'}{B}(p+\rho) + \frac{\phi'^{2}}{2A}\left(\frac{B'}{B} + \frac{4}{r}\right) = 0 \tag{5.12}$$

which reduces to the well known Oppenheimer-Volkoff equation in the case of a non-varying scalar field.

The equation of motion for a massless scalar field in curved spacetime is given by the expression

$$\nabla \phi = \frac{1}{\sqrt{-g}} \partial_\mu (\sqrt{-g}\ g^{\mu\nu} \partial_\nu \phi) = 0 \tag{5.13}$$

Here ϕ depends only on r, and we can use the metric to write this as

$$\frac{d}{dr} \left(r^2 \sqrt{\frac{B}{A}}\, \phi' \right) = 0 \tag{5.14}$$

which ultimately gives the equation of motion as

$$\phi'' = \frac{\phi'}{2} \left(-\frac{4}{r} - \frac{B'}{B} + \frac{A'}{A} \right) \tag{5.15}$$

Substituting this into equation (5.12) we find that all the scalar terms drop out, and the energy conservation equation just becomes the standard Oppenheimer-Volkoff equation

$$p' = -\frac{1}{2} (p + \rho) \frac{B'}{B} \tag{5.16}$$

This is easily recognised as a consequence of the fact that the scalar field equation of motion itself is sufficient to guarantee its energy conservation.

This leaves us to derive the Einstein equations. These are of course given by

$$R_{\mu\nu} - \frac{1}{2} g_{\mu\nu} R = 8\pi T_{\mu\nu} \tag{5.17}$$

where we have set G = 1. By taking the trace, we can rewrite this as

$$R_{\mu\nu} = 8\pi g_{\mu\rho} T^{\rho}_{\nu} - 4\pi g_{\mu\nu} T^{\rho}_{\rho} \tag{5.18}$$

where the first term has also been slightly rewritten for convenience. This gives the Einstein equations where $T_\mu{}^\nu$ is given by equation (5.11). The Ricci tensor

components for the metric are well known (e.g. see [63], page 178); the only non-vanishing components are R_{rr} , R_{tt} , $R_{\theta\theta}$ and $R_{\psi\psi}$. From rotational invariance, the two angular terms give the same equation, leaving a set of three independent equations which are

$$-\frac{1}{4}\frac{A'B'}{AB}+\frac{1}{2}\frac{B''}{B}-\frac{1}{4}\left(\frac{B'}{B}\right)^2+\frac{B'}{Br}=4\pi A(\rho+3p) \tag{5.19}$$

$$\frac{1}{4}\frac{A'B'}{AB}-\frac{1}{2}\frac{B''}{B}+\frac{1}{4}\left(\frac{B'}{B}\right)^2+\frac{A'}{Ar}=8\pi\phi'^2+4\pi A(\rho-p) \tag{5.20}$$

$$-\frac{1}{A}+\frac{A'r}{2A^2}-\frac{B'r}{2AB}+1=4\pi r^2(\rho-p) \tag{5.21}$$

While these three are independent of each other, they are not independent of the energy conservation law of equation (5.16); this gives us the option of ignoring one of these four equations. It is fruitful to make some manipulations first.

Our aim is to write this as a first order system in A, B, p and ϕ'. This can be done because we can use the redundancy in the above equations to eliminate the B'' terms. First we concentrate on A and B. By taking the combination

$$\frac{(5.19)}{2A}+\frac{(5.20)}{2A}+\frac{(5.21)}{r^2} \tag{5.22}$$

and rearranging we can obtain the equation

$$A'=8\pi A^2 r\rho-\frac{A^2}{r}+4\pi A r\phi'^2+\frac{A}{r} \tag{5.23}$$

Similar manipulations lead to an equation for B' which is

$$B'=8\pi AB r p+4\pi B r\phi'^2+\frac{AB}{r}-\frac{B}{r} \tag{5.24}$$

We discard the remaining relation which it is possible to obtain from the three Einstein equations in favour of the Oppenheimer-Volkoff equation.

We can see from equation (5.14) that it can immediately be integrated to obtain a solution for ϕ' in terms of an arbitrary constant, and this expression could be placed in equations (5.23) and (5.24). However, instead of doing this, we wish here to generalise the model to include a source term which we shall call S for the scalar field, which may be a function of position. The reasons for doing this and the specific choice of the source term shall be discussed later; for now we shall just treat this as an enhancement to the model. This alteration does not alter the form of equations (5.23) and (5.24), which remain completely general. They do however affect the scalar equation of motion which becomes second order in ϕ (though effectively only first order in ϕ' as ϕ does not appear explicitly in the equations), and also the energy conservation law which now includes a scalar source term.

The scalar equation of motion becomes

$$\nabla \phi = \frac{1}{\sqrt{-g}} \partial_\mu (\sqrt{-g}\ g^{\mu\nu} \partial_\nu \phi) = S \qquad (5.25)$$

from which the generalised equation of motion is

$$\phi'' = A S + \phi' \left(-\frac{A}{r} - \frac{1}{r} + 4\pi A r (\rho - p) \right) \qquad (5.26)$$

while, from equation (5.12), we see that the energy conservation equation can be written, substituting in equation (5.24) for B', as a first order equation for p which is

$$p' = -\frac{1}{2} (p + \rho) \left(8\pi A r p + 4\pi r \phi'^2 + \frac{A}{r} - \frac{1}{r} \right) - \phi' S \qquad (5.27)$$

This gives us the complete set of equations, which are equations (5.23), (5.24), (5.26) and (5.27).

There are two things worth pointing out about this set of equations. First of all, ϕ does not appear explicitly, so the system is really completely first order in the variables A, B, p and ϕ', with ρ determined from p via an equation of state. The second important thing is that, although the equations are very non-linear and coupled in a complex manner, they are actually linear in B, so that we are always free to scale B up or down as desired by a multiplicative constant, exactly as if the equations were linear. This will be important when we consider what the appropriate choice of boundary conditions is.

Having our basic equations, we must now supply an equation of state to relate pressure to density. As described in the introduction, we shall take the Chandrasekhar equation of state as used in the original Oppenheimer-Volkoff model. This equation of state is given in parametric form with parameter t, and for a given t we have the expressions

$$\rho = K (\sinh t - t) \tag{5.28}$$

$$p = \frac{1}{3} K (\sinh t - 8 \sinh \frac{t}{2} + 3t) \tag{5.29}$$

where K is a constant given by

$$K = \frac{m_n^4}{32\pi^2} \tag{5.30}$$

when expressed in natural units with m_n the neutron mass. Because the equation of state is in this parametric form, it is convenient to change the variable of integration to t by employing the chain rule. Hence in our integrations we replace equation (5.27) with

$$t' = \frac{3}{K(\cosh t - 4\cosh\frac{t}{2}+3)}\left[-\frac{1}{2}(p+\rho)\left(8\pi A r p + 4\pi r \phi'^2 + \frac{A}{r} - \frac{1}{r}\right) - \phi' S\right] \tag{5.31}$$

where p and ρ are understood to be given by equations (5.28) and (5.29) as functions of t.

The only remaining matter is the choice of the source term S. This is included because we are interested in the five-dimensional viewpoint when it comes to the physics of these equations. The form of the source term is determined by the choice of fluid description in the five-dimensional theory, since this tells us how matter affects the extra dimension. It was shown in [14] (which also provides a very good survey of the relationship between the four and five dimensional interpretations) that the requirement that the fluid appears perfect in four dimensions does not lead to a unique five-dimensional fluid description, and hence our choice of S is not unique. Three possible values of S are $8\pi (p - \rho) / 3$, $8\pi p / 3$ and zero; these correspond to a straight generalisation of the four dimensional fluid description to five dimensions using equation (5.8), a slight modification to this with an anomalous pressure in the fifth dimension and a standard four dimensional fluid description respectively [14]. Following [14], we shall concentrate on these as a representative sample of possibilities. Setting S equal to zero is appropriate when we are taking the scalar field interpretation and corresponds to no coupling between the scalar and the matter. The other two options are of greater interest to us here as they correspond to a genuinely five-dimensional fluid description, where the matter affects the geometry of the extra dimension. Because of the special nature of the extra dimension, the anomalous fifth dimensional pressure in the second of these expressions is not necessarily a reason for discounting this fluid description [14].

The final thing we must do is consider the boundary conditions which are appropriate for our model. In particular we are interested in solutions which are non-singular at the origin, and it turns out that this is quite a powerful restriction on the possible solutions, with the entire solution space spanned by varying the central density of the star exactly as in Oppenheimer and Volkoff. By expanding each of the quantities in a Taylor series at the origin, we obtain restrictions from each of the

equations of motion. Some of these are obvious from the requirement of spherical symmetry alone, which demands the vanishing of derivatives at the origin, but they come out naturally from the equations. We find that near the origin we must have

$$A = 1 + \frac{8\pi}{3}\rho_0 r^2 + \ldots \tag{5.32}$$

$$B = b_0 + 4\pi b_0 (p_0 + \rho_0) r^2 + \ldots \tag{5.33}$$

$$\phi' = \frac{1}{3} s_0 r + \ldots \tag{5.34}$$

$$t = t_0 + \ldots \tag{5.35}$$

where each of p_0, ρ_0 and s_0 are given by the value of t at the origin. By starting the integration sufficiently close to the origin we can ensure that only the constant term in each case need be considered. Hence we see that b_0 and t_0 are the only parameters that we can choose freely at the origin. However, b_0 is not free, since ultimately B should be rescaled so as to tend to one at infinity for asymptotic flatness (the equations are such that A always tends asymptotically to one). Fortunately, the linearity of B in the equations means that this can always be done after the solutions are generated by simulation out from the centre, and furthermore it guarantees that the value of b_0 does not affect the solutions. Hence the only parameter of importance is the central density, which is given via t_0.

One thing to notice is that ϕ' vanishes at the origin, and by examining equation (5.26) we see that if the source term vanishes then ϕ'' will be zero and so ϕ' will always remain zero, giving ϕ equals a constant as the unique solution; in this case the scalar terms drop out and we will just get the original Oppenheimer-Volkoff solution. This tells us that when we have no explicit source term the derivative of the scalar is *forced* by the boundary condition at the centre of the star to vanish everywhere, and so the scalar will have a constant value and have no effect on the

equations of motion. We shall use the S = 0 results to reproduce those of Oppenheimer and Volkoff. Otherwise, we shall concentrate our interest on the choices

$$S = \frac{8\pi}{3} p \qquad \text{or} \qquad S = \frac{8\pi}{3} (p - \rho) \tag{5.36}$$

which correspond to an intrinsically five dimensional fluid description. In these cases the source term for ϕ (the first term in equation (5.26)) will induce a non-trivial solution for ϕ, as can also be seen from the expansion of equation (5.34). Hence we can expect to see new effects arising from the extra dimension which will now have a spatial variation in size.

(iii) Solutions and the Question of Maximum Mass

Here we consider the method of solution of the above equations and the possible consequences. As in earlier chapters, numerical integration will be employed to solve the equations. We integrate from the centre of the star outwards, with due regard to the boundary conditions. We can use the expansions of equations (5.32) to (5.35) to choose our boundary conditions at the centre so as to ensure a non-singular solution. We cannot start the integration exactly on r equals zero because some of the terms in the equations are singular there (though the solutions remain regular), so we begin at a point very close to the origin. We can see from our expansions that by making r sufficiently small we can neglect all but the zeroth term in the series; that is, we choose A to be one at the origin, ϕ' to be zero and leave B and t free to be chosen as we like.

We must also ensure that asymptotic boundary conditions are satisfied, as we wish our solutions to be asymptotically flat. The equations themselves will automatically force A to go to one asymptotically, but B may finish at any value. We can then rescale the B solution because the equations are linear in B, which has the

effect of fixing the value of B at the origin. Hence, as stated above, the central density of the star, given via t at the origin, is the only quantity that we are free to choose. The same normalisation argument applies to ϕ, for the equations are also linear in it. Hence its overall scale is decided by its value chosen as a boundary condition at infinity, which can be predicted from observations of coupling constants in the usual Kaluza-Klein manner.

One thing that we have to take great care over is the exterior solution to the star. As in conventional neutron star studies, we shall find that the star has a finite radius; that is, at some distance from the origin the value of t will become zero. In addition, it will do this with a non-vanishing derivative. At this point, to complete our solution, we must attach smoothly an exterior vacuum solution. If this cannot be done, then our solution is not valid. When S is not zero, the edge of the star will have some value of ϕ' associated with it, and so the exterior solution must also feature a varying scalar field from continuity requirements.

This raises the question of what our external solution might be. In the standard case, Birkhoff's theorem [64] tells us that the exterior metric must be the Schwarzchild one (true even if the internal matter is not static), and it can be shown that this metric can indeed be joined on to that of the interior region. Note that this joining need not preserve the continuity of all the derivatives of the metric, only those required to keep the curvature invariants finite, as we seek regular solutions. The curvature invariants include terms with the second derivative of B but only up to the first derivative of A. Hence it is these which must be finite. The function t is matched onto a constant $t = 0$ exterior solution; we do not require continuity of the derivative of t in this case.

In our case with the scalar field, Birkhoff's theorem no longer holds. However, for the static case it can be generalised to the scalar field case merely by recognising that it is possible to find the most general asymptotically flat solution to Einstein's equations coupled to a scalar - this then must represent the exterior metric. This

solution was first found by Janis, Newman and Winicour [65], and can be written

$$ds^2 = \left[\frac{2R+r_0(\mu+1)}{2R-r_0(\mu-1)}\right]^{\frac{1}{\mu}} dR^2 + r^2(d\theta^2 + \sin^2\theta d\psi^2) - \left[\frac{2R-r_0(\mu-1)}{2R+r_0(\mu+1)}\right]^{\frac{1}{\mu}} dt^2 \quad (5.37)$$

$$\phi = \frac{\alpha}{\mu} \ln\left(\frac{2R-r_0(\mu-1)}{2R+r_0(\mu+1)}\right) \quad (5.38)$$

where

$$r^2 = \frac{1}{4}\left(2R+r_0(\mu+1)\right)^{1+\frac{1}{\mu}} \left(2R-r_0(\mu-1)\right)^{1-\frac{1}{\mu}} \quad (5.39)$$

$$\mu = (1 + 16\pi\alpha^2)^{\frac{1}{2}} \quad (5.40)$$

This solution has two free parameters, here denoted α and r_0. The unusual radial coordinate R is an implicit function of r, and equation (5.40), defining μ, corrects a well known error in [65] (see for example [14]), with κ in [65] equalling 8π in our notation. The parameter r_0 is equal to 2m where m is the mass as determined by an asymptotic observer. Hence once we have attached this solution to our interior solution we use this parameter to tell us what the mass is.

Normally in the studies of black holes we find that α must be set to zero, otherwise the event horizon becomes singular; hence the statement that scalar charge must vanish [56,66] (the addition of gauge fields can resurrect the scalar charge [56]) for black holes. Here we see that because the neutron star prevents singularities arising a scalar charge can exist in this case; we do not have to worry about the central singularity as it is inside the star. This raises interesting questions as to whether gravitational collapse of such an object can proceed unless some way of radiating all the scalar charge is found; it may be speculated that the presence of

the scalar charge can halt the process of collapse [67] . We shall not deal with such issues here though it is a topic which certainly merits further examination. Some remarks on this are made in the conclusions in section (iv).

Our procedure is now clear. We start integrating from the centre of the star using the expansions of the variables there, using the numerical methods as described in previous chapters and in appendix one. After some finite distance we will reach the star boundary. At this point the program will actually crash, because it looks for solutions with more continuity properties than we require; for instance it will try and continue t into negative values because of its non-zero derivative, and this is not possible. We then take the final set of values for A, B and ϕ' at the star boundary, noting the radius at which it occurs, and match them onto the exterior solution using our less restrictive continuity requirements, which will give us a value for the asymptotically observable mass. We then vary the central value of the density to examine the whole parameter space. For our purposes we do not need to carry out the normalisation of B.

The attachment of the external solution proceeds as follows, once we have these values. We first find the parameter α which gives us the magnitude of the scalar field. We note that for Janis et al's solution we have the relation

$$\frac{A'}{A} = -\frac{1}{\alpha}\phi' \tag{5.41}$$

Hence at the boundary we can use equation (5.23) with vanishing ρ to obtain

$$\frac{1}{\alpha} = -4\pi r\phi' - \frac{1}{r\phi'}(1-A) \tag{5.42}$$

from which we can immediately obtain α. We can then find the value of μ via equation (5.40). At the boundary, we also have

$$\frac{r_0}{R} = \phi' \frac{r}{\alpha} \tag{5.43}$$

which can be obtained by direct differentiation of Janis et al's expression for ϕ with some manipulation. Rearranging equation (5.39) by dividing through by R^2 leaves a right hand side depending only on things we know, in particular the ratio on the left hand side of equation (5.43), and allows us to determine r^2 / R^2 at the boundary. Hence because we have r from the simulations we can find the corresponding value of the radial coordinate R of Janis et al. Finally then, equation (5.43) can be used to determine the mass which just equals $r_0 / 2$. We also have a cross check that the matching has been carried out correctly because we can find the value of A at the boundary as predicted from these matching parameters and confirm that it matches the value of A provided by the simulation up to the boundary.

When determining the mass in the case of S = 0, the situation is the considerably more simple one of Oppenheimer and Volkoff where the exterior solution is just the Schwarzchild one (with a constant scalar field). In this case, the standard Schwarzchild expression

$$A(r) = \left(1 - \frac{2M}{r}\right)^{-1} \tag{5.44}$$

can be applied at the boundary to give the mass directly.

The last remaining question is one of units. Following Oppenheimer and Volkoff we note that having fixed G and c to be one, we still have one scale to be fixed. This can be done by fixing K in equations (5.28) and (5.29) to equal $1/4\pi$; this corresponds to giving $\hbar$ some numerical value, the overall scale depending on the mass of the fermions used. For neutrons, this fixes our unit of length to be $1.36 * 10^4$ m and the unit of mass to be $1.83 * 10^{31}$ kg. This allows us to convert our numerical values into lengths and masses.

Finally, we are in a position to gain results. As a first check, simulations were

carried out with the source term set to zero and found indeed to reproduce the results of Oppenheimer and Volkoff. This situation was also used to check the performance of the numerical routine. As pointed out earlier, we cannot start exactly on r = 0 because some terms in the equations are singular there. The integrations were started at $r = 10^{-6}$ where it was assumed that only the zeroth order terms in the expansions (5.32) to (5.35) had to be taken into account. It is confirmed by varying this starting position that the results are independent of this approximation. At the edge of the star, the program terminates when t approaches zero, and it is tested how small t must be to allow the mass to be determined accurately; that is, how close to the edge of the star we must integrate. When t drops to a few hundredths, it is seen that the mass does not depend on the exact position of this cut off - this is no surprise as the edge of the star is encountered suddenly and the value of A, which determines the mass, cannot change rapidly due to continuity alone over these very short distances. With this confirmation that the simulations are providing accurate results, we can proceed to the case of a non-zero source term.

The simulations were carried out over a range of values of t0 for the two choices of equation of state, using an initial integration point and a t cutoff as described above. The values of the functions A and ϕ' at the edge of the star are noted along with the radius at the edge, and the formulae above are used to match on an exterior solution and determine the mass.

A sample matching is given here for the case of t0 = 1 with a source term $S = 8\pi (p - \rho) / 3$. The star radius is found to be 0.6070, and the values of A and ϕ' at the edge are 1.007050 and $-3.807952 * 10^{-3}$. Equation (5.42) gives $\alpha = - 0.33101$, from which μ and r_0 / R are found. Using (5.39) we find that the R value corresponding to the edge of the star is 0.6028, which allows the mass to be found as 0.0021 in the units of the equations, which translates to 0.02 solar masses. Other matchings are carried out in the same way.

The results for the mass and radii are shown in figures (5.1) and (5.2), for each

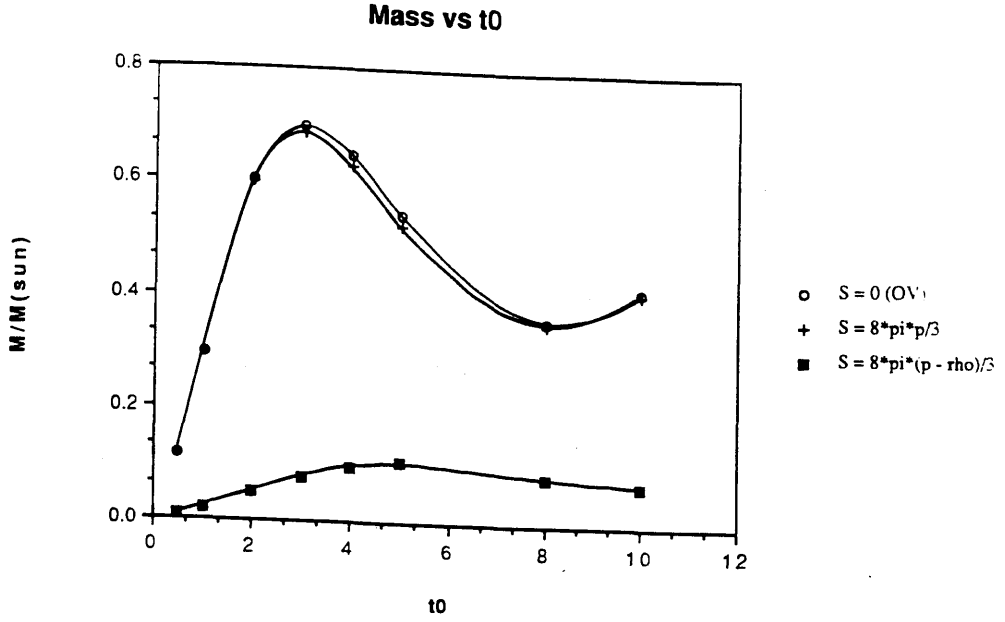

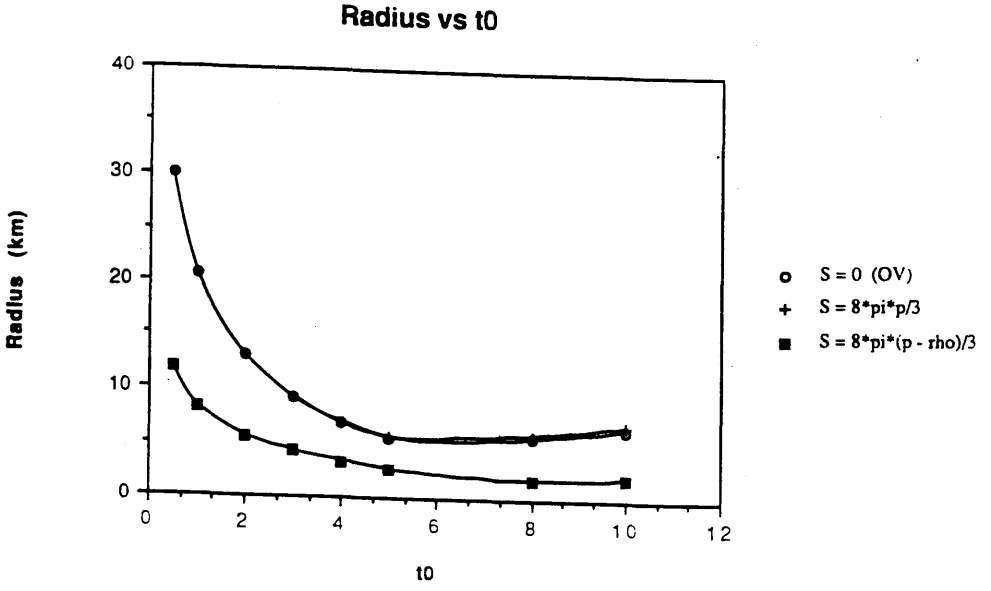

Figures 5.1 and 5.2 These graphs show the relations between mass against central density and radius against central density respectively, for each of the three choices of source term S. The masses are given as fractions of a solar mass and the radii are in kilometres. The results for S = 0 reproduce those of Oppenheimer and Volkoff. The results for $S = 8\pi p / 3$ closely mimic the Oppenheimer-Volkoff results, while those for $S = 8\pi (p - \rho) / 3$ are very different.

of the source terms. The $S = 0$ case is provided to give the Oppenheimer-Volkoff results for comparison. We see immediately from the mass curve for the source term $S = 8\pi (p - \rho) / 3$ that the inclusion of the extra dimension has had a drastic effect on the neutron star structures, with a vast lowering of the maximum mass. This feature alone is enough to rule out the possibility that the source term is allowed, as this trend can be expected to be carried through to more complicated equations of state, which can only just explain experimental observations as it is. Recalling that this choice of S corresponds to the natural generalisation of the fluid description of matter to five dimensions, we can see that this is going to pose some problems for the description of matter in Kaluza-Klein theories. It has already been noted [14] that this fluid description may cause difficulties even in our own solar system by being inconsistent with the precession of Mercury's perihelion, though there is a very small chance that electromagnetic effects may salvage this. It seems unlikely that they could do so in our case.

The mass curve for the source term $S = 8\pi p / 3$ is found to be very similar to that in the Oppenheimer-Volkoff case; there is a small reduction in the masses from the standard case, but of no more than a few percent and most prominent near the maximum mass. Thus we conclude from this that this choice of source term, again intrinsically five-dimensional, appears experimentally viable, though the trend of slightly decreasing the maximum mass is not promising. It seems from these studies however that the reduction is sufficiently small that if carried through to a more complicated equation of state it is unlikely to encounter difficulties with the maximum mass criterion.

The radii in this latter case also closely match those of the Oppenheimer-Volkoff case, though it should be emphasised that the exterior geometry of the star in this case is different to the Schwarzchild case due to the forced existence of the scalar charge. The radii with the other fluid description are generally much smaller leading to more compact objects. However, it should be remembered that neutron stars are

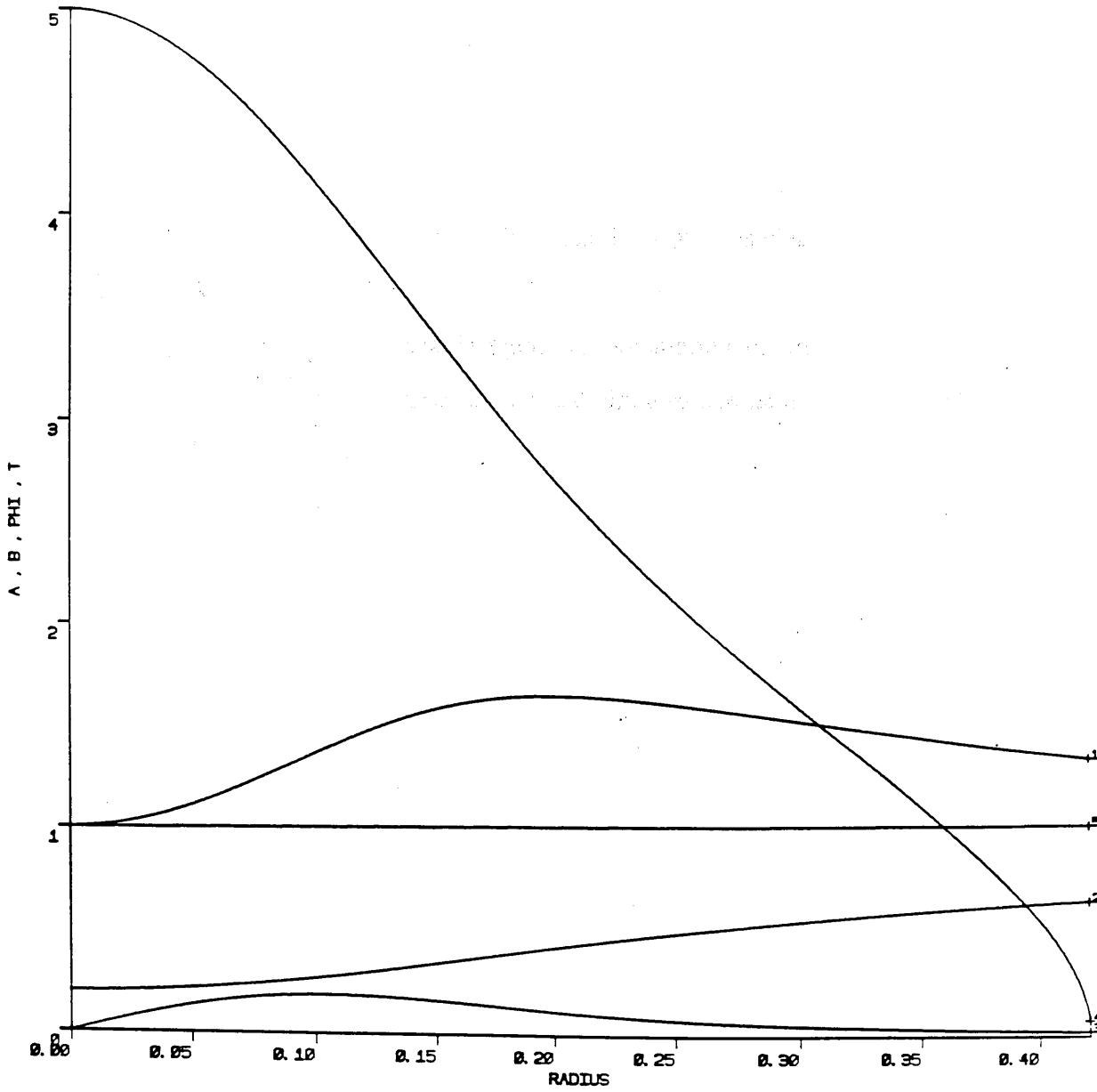

Figure 5.3 This graph shows a sample simulation where the source term is chosen as $S = 8\pi p / 3$ and a central density given by $t0 = 5$ is given. The lines marked 1 to 5 give A, B, ϕ', t and ϕ respectively. The integration takes us up to the star boundary where t becomes zero. At this point ϕ' is non-zero, demonstrating the need for an unusual exterior solution. ϕ does not vary much during this integration. This graph does not include a normalisation of B and ϕ which would scale them to match the asymptotic boundary conditions.

not stable below a mass of around a tenth of a solar mass since the gravitational energy no longer favours neutrons over electrons and protons, and instead white dwarfs will form. With this fluid description the masses are all so low that perhaps no neutron stars exist. In any event, this fluid description is clearly ruled out by these results.

Figure (5.3) shows a sample numerical simulation of one of the above situations. This illustration shows the results with a source term of $8\pi p / 3$ and a central density given by $t0 = 5$.

(iv) Conclusions I

What conclusions can be drawn from this work? The results of the study are for the most part negative - for instance one might have hoped that the extra dimension would lead to the possibility of higher maximum masses with some appropriate fluid description, but regrettably this is not so. What has been achieved is a demonstration of the pros and cons of the description of matter in a five dimensional theory, highlighted by the differing features obtained from the three sample equations of state. Each of the three choices leads to a rather different situation, and so we consider the status of each of the three below in turn.

1) $S = 0$

In this case we find that the scalar field is forced to vanish everywhere by the presence of the star, in order to preserve non-singularity at the origin. This is not a particularly deep result; it really amounts to no more than the lack of source for the scalar preventing it from having a spatial variation and the staticity assumption preventing wave motion. This certainly gives consistent results for neutron stars, as it exactly reproduces the results one obtains in conventional relativity. We use this limit to ensure the correct operation of the computer program. As a fluid description this is somewhat unsatisfactory from the five dimensional point of view, wherein we

would definitely expect the fifth dimension, in its role as a scalar, to play some part in the geometry.

2) $S = 8\pi (p - \rho) / 3$

This source term is that obtained when we make a straight generalisation of the normal description of a perfect fluid into the Kaluza-Klein context, i.e. by adopting a five dimensional version of equation (5.8). This is the obvious choice to make when considering fluids in a Kaluza-Klein theory, so it is somewhat alarming to find that the results which are obtained are in blatant contradiction with experiment, sufficiently so to rule out this equation of state. In this case we find that the effect of the source term is very large and results in a substantial drop in the neutron star masses associated with à particular central density. Given that even in conventional theories the maximum attainable mass is only barely high enough to explain the observation of masses of binary pulsars, such a drop makes the predictions of this version of the theory untenable.

3) $S = 8\pi p / 3$

This source term is also associated with an intrinsically five-dimensional description of the particle fluid. Here a slight modification is made to the description in five dimensions, but this still leads to a perfect fluid in the four dimensional reduced theory. It is the results with this source which are potentially the most interesting. They lead to a mass curve very similar to the Oppenheimer-Volkoff case, with at most a 4% drop in the mass for a given t0, indicating that the source term is in general small. This slight alteration is sufficiently small that it does not rule out this fluid description, so this appears to be an allowable five dimensional fluid description. It is fair to say however that these results for the mass curve are not of great interest, firstly because of their closeness to the conventional scenario and secondly because the mass change is downwards while most models are already

struggling to reach high enough mass ranges.

The interest in this equation of state is mostly centred on the geometry that it induces. As we have seen, the presence of the star in this case induces a spatial variation of the extra dimension, which corresponds to a scalar charge. This leads to the observation that the exterior metric outside the star will not be the standard Schwarzchild one, but instead will be its generalisation to the Einstein plus scalar equations - the Janis, Newman and Winicour solution. We have demonstrated that this solution can be matched onto the neutron star at the boundary. At large distances from the star this metric is indistinguishable from the Schwarzchild one, but very close to the star there may be observable effects connected to the variation in size of the extra dimension.

The importance of this solution also extends to consideration of the question of what the endpoint of gravitational collapse of these objects might be. Astrophysical folklore dictates that black holes may not have scalar charge [66], because of the problem of singular event horizons. One can postulate, for example, adding material onto one of our neutron stars until it exceeds the maximum mass; it is then unstable against collapse to a black hole. However, it then must find some way of radiating its scalar charge if it is to collapse completely, a process which appears difficult since the presence of the scalar charge is intimately connected to the star via the boundary condition at the centre required by the postulate of non-singularity. This situation should be contrasted with that covered by Price's theorem [68] which deals with the pure scalar case and tells us that the scalar charge will be radiated away during collapse. There such a process can occur as the scalar charge is a free parameter in the solution and there exist configurations without scalar charge. Here, however, the existence of the scalar charge is induced by the five dimensional matter coupling, and *there exist no static equilibrium solutions with vanishing scalar charge* . While there remains the possibility that this feature is absent in a dynamical solution, it appears that the prerequisite that matter is present forces a scalar charge and hence it cannot

be freely radiated away. There does however remain the possibility of other equilibrium configurations which we have not discovered, perhaps attributable to the strange nature of the exterior solution in which gravity can act repulsively at close distances [67]. To get a clearer idea of what might be occurring here we need a model of the collapse process itself. Some first steps towards this are given in the following section, though much further work would be required to get a complete picture of the collapse process even in the spherically symmetric case.

(v) The Metric of Dynamical Collapse

In this section we pursue a variant on the theme of studying the effect of extra dimensions in astrophysics, by examining a different astrophysical process - that of gravitational collapse. The history of studies of gravitational collapse goes all the way back to an original paper by Oppenheimer and Snyder [69], and indeed it is their treatment that we shall roughly follow. In their studies, they made several assumptions in order that the problem became analytically tractable. We imagine a spherically symmetric ball of pressureless dust, so that there are no forces to keep it from collapse. It is assumed to start from rest with a homogeneous density distribution, and the collapse proceeds, preserving spherical symmetry, from this initial configuration. This allows an analytic solution to be found in their case, and as we shall see the same approximations allow similar progress to be made in the Kaluza-Klein version. Modern treatments of this problem generally involve advanced numerical techniques, wherein the problem of non-symmetrical collapse can be considered [70], but the simple analytic model does provide some feeling for what occurs.

Here we will follow the exposition of Weinberg [63] on the Oppenheimer-Snyder model. Our treatment will this time be based on the Kaluza-Klein metric itself, i.e. an explicitly five-dimensional treatment, rather than using the scalar field analogy. We shall follow the same assumptions concerning the

nature of the collapsing materials as described in the preceding paragraph.

It is convenient to use what are known as comoving coordinates for this problem. What this entails is imagining the coordinate mesh to be fixed in the particle dust and falling in with it, so that a particular dust particle will retain the same spatial coordinates as it collapses along its geodesic. This will of course lead to a singularity when the dust particles meet at a central point, but it is easy to see that this is a real rather than a coordinate singularity by considering the behaviour of the density in the approach to this point. In such coordinates, with $\chi \in [0, 2\pi]$ as the coordinate of the circular extra dimension, the general time-varying spherically symmetric metric can be written as

$$ds^2 = - dt^2 + U(r,t)\, dr^2 + V(r,t)\, (d\theta^2 + \sin^2\theta\, d\psi^2) + S^2(r,t)\, d\chi^2 \qquad (5.45)$$

We wish to derive the Einstein equations from this using the energy-momentum tensor for a pressureless dust.

There are now five inequivalent non-trivial Einstein equations, coming from R_{rr}, R_{tt}, $R_{\theta\theta}$, $R_{\chi\chi}$ and R_{rt}. The energy momentum tensor for the dust is given by

$$T^{\mu}_{\nu} = \rho\, U^{\mu} U_{\nu} = \mathrm{diag}\,(- \rho\, , 0\, , 0\, , 0\, , 0\,) \qquad (5.46)$$

as, because of our choice of comoving coordinates, the fluid velocity with respect to these coordinates is entirely in the timelike direction. Standard calculations then lead to the following set of Einstein equations, where a dot signifies a time derivative and a dash a derivative with respect to r. The equations, in the same order as the components given above, are

$$\frac{\ddot{U}}{2} - \frac{V''}{V} + \frac{V'^2}{2V^2} + \frac{U'V'}{2UV} + \frac{\dot{U}\dot{V}}{2V} - \frac{\dot{U}^2}{4U} - \frac{S''}{S} + \frac{U'S'}{2US} + \frac{\dot{U}\dot{S}}{2S} = \frac{8}{3}\pi U \rho \qquad (5.47)$$

$$-\frac{\ddot{U}}{2U}+\frac{\dot{U}^2}{4U^2}-\frac{\ddot{V}}{V}+\frac{\dot{V}^2}{2V^2}-\frac{\ddot{S}}{S}=\frac{16}{3}\pi\rho \tag{5.48}$$

$$1-\frac{V''}{2U}+\frac{\ddot{V}}{2}+\frac{V'U'}{4U^2}+\frac{\dot{U}\dot{V}}{4U}-\frac{V'S'}{2US}+\frac{\dot{V}\dot{S}}{2S}=\frac{8}{3}\pi V\rho \tag{5.49}$$

$$-\frac{S''}{U}+\frac{S'U'}{2U^2}-\frac{S'V'}{UV}+\ddot{S}+\frac{\dot{S}\dot{U}}{2U}+\frac{\dot{S}\dot{V}}{V}=\frac{8}{3}\pi S\rho \tag{5.50}$$

$$-\frac{\dot{V}'}{V}+\frac{V'\dot{V}}{2V^2}+\frac{\dot{U}V'}{2UV}+\frac{\dot{U}S'}{2US}-\frac{\dot{S}'}{S}=0 \tag{5.51}$$

These constitute a complete set of equations to be solved.

Following Weinberg [63], we observe that if ρ is a function of time alone (our homogeneity assumption), then we can find separable solutions to these equations. Accordingly, we write U, V and S as

$$U(r,t)=\alpha^2(t)\,f(r)\,,\ V(r,t)=\beta^2(t)\,g(r)\,,\ S(r,t)=\gamma(t)\,h(r) \tag{5.52}$$

Substituting this into the R_{rt} equation, given by equation (5.51), we discover that α, β and γ must be multiples of each other, and by renormalising f, g and h we can arrange that $\alpha=\beta=\gamma$. We are then free to redefine the radial coordinate such that $g(r)=r^2$, which corresponds physically to letting the radius at a given time be determined by the surface area at that distance, exactly as in Schwarzchild coordinates. Hence we can write the metric as

$$ds^2=-dt^2+\alpha^2(t)\left(f(r)\,dr^2+r^2(d\theta^2+\sin^2\theta\ d\psi^2)+h^2(r)\,d\chi^2\right) \tag{5.53}$$

We now substitute equation (5.52) into the other Einstein equations. For the R_{rr}, $R_{\theta\theta}$ and $R_{\chi\chi}$ equations respectively we get the equations

$$\alpha\ddot{\alpha} + 3\dot{\alpha}^2 - \frac{8}{3}\pi\rho\alpha^2 = -\frac{f'}{rf^2} - \frac{1}{2}\frac{h'f'}{hf^2} + \frac{h''}{fh} \tag{5.54}$$

$$\alpha\ddot{\alpha} + 3\dot{\alpha}^2 - \frac{8}{3}\pi\rho\alpha^2 = -\frac{1}{r^2} + \frac{1}{fr^2} - \frac{f'}{2rf^2} + \frac{h'}{rfh} \tag{5.55}$$

$$\alpha\ddot{\alpha} + 3\dot{\alpha}^2 - \frac{8}{3}\pi\rho\alpha^2 = \frac{h''}{hf} - \frac{1}{2}\frac{h'f'}{hf^2} + 2\frac{h'}{hfr} \tag{5.56}$$

Here we see the benefits of the separable solution. Each left hand side is a function of time only, and each right hand side of space only. In addition, the time dependent parts of each equation are the same. Hence we conclude that the left hand side and each of the right hand sides must be equal to a fixed constant. For notational convenience later on, we denote this constant by -3k .

We concentrate first on solving the spatial part. From the first and third of these equations we obtain the simple relation

$$\frac{h'}{h} = -\frac{1}{2}\frac{f'}{f} \tag{5.57}$$

which on substitution into the middle relation gives a first order differential equation for f, namely

$$f' = \frac{f}{r} - \frac{f^2}{r} + 3krf^2 \tag{5.58}$$

This has the general solution

$$f = \left(\frac{D}{r} + (1 - kr^2)\right)^{-1} \tag{5.59}$$

giving, from equation (5.57)

$$h = C\left(\frac{D}{r} + (1 - k r^2)\right)^{\frac{1}{2}} \tag{5.60}$$

where C and D are arbitrary constants of integration. Note that if k is positive (we shall see later that it is) the spatial geometry is a closed 3-sphere in which case the range of r is restricted to [0, $1/\sqrt{k}$), with the singularity at $r = 1/\sqrt{k}$ a coordinate singularity only (exactly as if one used a radial coordinate on the Earth's surface with origin at the north pole; there would be an apparent singularity at the south pole where the radial lines meet) . In fact, the dust will only extend out to some value of r less than this, which gives the edge of the dust, and our solution is only valid within this radius. An exterior solution in the absence of dust should be smoothly joined at this point.

We now have the complete spatial metric, and can turn to considering the time components. Here we have two relationships. From the left hand sides of equations (5.54) to (5.56), we have the relationship

$$\alpha\,\ddot{\alpha} + 3\,\dot{\alpha}^2 - \frac{8}{3}\pi\,\rho\,\alpha^2 = -3\,k \tag{5.61}$$

which, through k, links us to the spatial part. We also still have the R_{tt} Einstein equation, which on substituting the separated ansatz gives

$$\ddot{\alpha} = -\frac{4}{3}\pi\,\rho\,\alpha \tag{5.62}$$

For convenience, it is easier to use the energy conservation equation given by

$$T^{\mu}_{t\,;\,\mu} = -\dot{\rho} - \rho\left(\frac{\dot{U}}{2U} + \frac{\dot{V}}{V} + \frac{\dot{S}}{S}\right) = 0 \tag{5.63}$$

which can be expressed as a total derivative

$$\frac{\partial}{\partial t}\left(\rho V S \sqrt{U}\right) = \frac{\partial}{\partial t}\left(\rho \alpha^4\right) = 0 \tag{5.64}$$

By normalising the radial term we can arrange that α_0 , the initial value of α, is equal to one. Then integration of this equation gives us

$$\rho = \rho_0 \alpha^{-4} \tag{5.65}$$

where ρ_0 is the initial value of the density.

We now solve for α by eliminating its second derivative from equations (5.61) and (5.62). This gives

$$\dot{\alpha}^2 = -k + \frac{4}{3}\pi \rho_0 \frac{1}{\alpha^2} \tag{5.66}$$

By imposing the initial condition that the fluid is at rest, i.e. the first derivative of α is zero when α is one, we find that k, as used in the spatial metric, is given by

$$k = \frac{4}{3}\pi \rho_0 \tag{5.67}$$

giving equation (5.66) the form

$$\dot{\alpha}^2 = \frac{k - k\alpha^2}{\alpha^2} \tag{5.68}$$

This equation is separable, and can immediately be integrated. Setting the initial time equal to zero when α equals one fixes the integration constant giving the expression for α as

$$\alpha = \sqrt{1 - kt^2} \tag{5.69}$$

This completes the derivation of the metric. It is the most general separable solution to the Einstein equations under the assumptions that we made initially, and written in full is

$$ds^2 = -dt^2 + (1-kt^2)\left\{\frac{dr^2}{\frac{D}{r}+(1-kr^2)} + r^2(d\theta^2 + \sin^2\theta\, d\psi^2) + C\left(\frac{D}{r}+(1-kr^2)\right)d\chi^2\right\}$$

$$\text{with } k = \frac{4}{3}\pi\rho_0 \ , \quad \rho(t) = \frac{\rho_0}{(1-kt^2)^2} \quad \text{and C, D and } \rho_0 \text{ constants} \qquad (5.70)$$

It may well be necessary to choose D = 0 to avoid a singularity at r = 0, but this is not clear as r = 0 should not be a special point; while it is the centre of the spatial 3-sphere, we have imposed that the dust be homogeneous. An evaluation of the curvature invariants may be needed to sort out its role. The other thing to notice is that the collapse ends after a finite coordinate time which is given by

$$t = \sqrt{\frac{1}{k}} = \sqrt{\frac{3}{4\pi\rho_0}} \qquad (5.71)$$

While this metric is strongly indicative of the behaviour seen in Kaluza-Klein gravitational collapse, a full treatment would require the attachment of an exterior solution to this metric at the edge of the collapsing sphere, in the same way as the Schwarzchild geometry is smoothly joined to the collapsing star in conventional general relativity.

(vi) Conclusions II

We have demonstrated an analytic solution of the simplest problem of collapse in a Kaluza-Klein theory - that of a homogeneous pressureless dust. On the face of it, the results found here closely mimic the standard general relativistic collapse which gives rise to a Friedmann collapse. Here we have an extra term of type D / r

appearing in the metric which may be of importance in the matching to an exterior solution, but more work is needed to elucidate its role.

There are several points which deserve pursuit in this model. Of primary importance is the discovery of an exterior solution. This procedure is however complicated by the lack of a Birkhoff's theorem in the scalar field case. As we saw in section (iii), in the static case we can find the most general solution to the field equations which must then represent the exterior to the static neutron star. In the dynamical case we have here the situation is different, because we are no longer in possession of such a general solution. We also have considerable extra difficulties over the standard case, because there Birkhoff's theorem dictates that the exterior metric will be static even though the interior is dynamic. This is understood as a manifestation of the fact that there are no monopole gravitational waves. Here we have no such theorem as we can have monopole scalar waves, and can expect that the exterior metric may be dynamical as well. Despite these reservations, the matching problem does not superficially seem impossibly difficult as the methods used here for the interior may well extend to the exterior region as well.

Another complication which exists is the question of how this solution might appear to the four dimensional observer. As stated at the beginning of the chapter in equation (5.5), we have to make a conformal transformation dependent on the extra dimensional metric in order to ensure the constancy of G in the effective theory. We can see from equation (5.70) that this transformation is time dependent, so in four dimensions the collapse probably does not appear to have the simple behaviour indicated by equation (5.71). This too merits further study.

As a final point, this model would have to be extended to include pressure terms and an examination of different fluid descriptions in five dimensions to uncover its full richness. Such a task would probably involve the use of advanced numerical techniques to handle the complicated set of partial differential equations which would describe such a system. A better understanding of this analytic model would be

useful in deciding whether such a study would offer any worthwhile rewards.

Chapter 6

Combined Bose-Fermi Stars

(i) Introduction : Bose-Fermi Stars?

The past decade or so has seen a huge influx of ideas from particle physics to cosmology, with the primary interest in the use of scalar fields for such purposes as inflation and cosmic string formation; in addition there is the light axion field introduced as a solution to the strong CP problem. Other theoretically suggested bosons may also have a role, such as the dilaton from superstring theory (presumably having acquired some mass), and we can expect many possibilities to be introduced in the future. Given this wide usage, there has been a revived interest in the possibility of stellar objects which may be made from these bosonic fields rather than the conventional fermions of neutron stars and white dwarfs. Such gravitational equilibrium configurations have been dubbed 'boson stars', and can be viewed as being held from collapse by a pressure arising from the uncertainty principle, while their fermionic counterparts exist due to a pressure arising from the exclusion principle.

The study of boson stars goes back to the work of Ruffini and Bonazzola [71] in nineteen sixty-nine, but it is only recently that this work has been followed up, presumably due to the increased interest in the physics of scalar fields. Ruffini and Bonazzola considered the simplest possibility - that of a non-interacting massive scalar field - and concluded that the masses of such boson stars would be extremely small relative to their fermionic counterparts. Later work [72] has introduced a self interaction of the scalar field (of $\lambda\phi^4$ type) which allows the existence of much larger masses. The stability of such objects has also been examined [73,74] with results similar to that of the neutron star case.

It is also possible to construct various other types of object from scalar fields, by the inclusion of gravity in non-topological solitons [75] and in Q-balls [76]. These constructs generally rely on at least two distinct boson fields, and their existence is in part owed to a trade-off between the interaction terms of these fields, which serves to localise the matter fields. In this chapter, however, we are very much following the original line of work where gravity is taken as the basic interaction.

In the literature mentioned above, only the case of purely bosonic stars has been examined in detail. Given that many of these objects are of primordial origin, being formed from an original gas of both bosons and fermions, we would expect that any stars that form could be made from a mixture of bosons and fermions, and certainly that if any bosonic stars form that they would later suffer some form of contamination by fermions. Such objects then are the topic of consideration in this chapter; we wish to investigate the possible structures that can be formed from the combination of a scalar field and a fermion one, which here shall be taken for the sake of a definite illustration to be a neutron field. We shall begin by outlining the basic structure of a boson star in section (ii), and then examine how to introduce a fermionic contamination into it in section (iii). Simple heuristic arguments due to Thirring [77] show that boson stars without self-interactions should have masses behaving as m_{planck}^2 / m_B while fermion stars have masses like m_{planck}^3 / m_F^2, but this situation for bosons is complicated by the introduction of a quartic self-coupling and the consideration of objects made from both bosons and fermions is naturally even more complicated.

The boson field, denoted ϕ, that we consider may be either a complex scalar field (which leads to a conserved current and hence a conserved charge Q) which in the equilibrium configuration has only one independent component, or it may be a real scalar field as in the formalism of Breit et al [78]. For simplicity we shall consider this latter case, for which we have a range of candidates such as axions, the

dilaton from superstring theories or the Higgs fields in some unified theories. This leads to interest in various different ranges of mass; the axion is generally expected to be very light while the Higgs boson would be expected to be considerably more massive. As we shall see, it is only for very light boson masses that the contributions from bosons and fermions are of similar magnitude.

Since there is still no candidate scalar field about which anything definite is known, the mass of the boson and the strength of its self-interaction must be considered free parameters for which we must explore the possible equilibrium configurations. For the fermions, in contrast, we are well aware of properties of the neutron such as its mass, so we do not have to worry about the possibility of a varying fermion mass. It should be remembered though that the use of the neutron is purely illustrative.

One other point that should be noted at this stage is that we do not consider any explicit coupling between the bosonic and fermionic fields, for example such as an $\omega\bar{\omega}\phi$ coupling term where ω is the Dirac field. We shall comment more on this later. There will however be an interaction induced through the coupling to the gravitational field. The neutrons will be treated as non-interacting as in the pioneering studies of Oppenheimer and Volkoff [60]; they will be described as a perfect fluid by making use of the Chandrasekhar equation of state as described extensively in chapter five. This is well known [71] to be a very good approximation because as all the states in the neutron star up to a certain energy are occupied the exclusion principle dictates that the neutrons cannot scatter and hence the mean free path is very large. Modern treatments of neutron stars require more complicated equations of state which take interactions into account, and these are needed to design models which can satisfy phenomenological observations. However, the Oppenheimer-Volkoff model gives a very good indication of the behaviour of neutron stars with regard to properties such as the maximum mass and stability criteria, and since our treatment of the scalar field is somewhat basic it would be

inconsistent to consider the fermions with great accuracy. Our results are therefore to be taken as an indicator of the structure of Bose-Fermi stars rather than an accurate description.

(ii) How to Make a Boson Star

In this section we outline the construction of a boson star, following roughly the methods used in [73,78]. Given that we have taken the scalar field to be massive and self-interacting, but with no other interactions other than gravity, our starting point is the Lagrangian

$$L = -\frac{1}{2} g^{\mu\nu} \partial_\mu \phi \partial^\nu \phi - \frac{1}{2} m^2 \phi^2 - \frac{1}{4} \lambda \phi^4 \qquad (6.1)$$

Here m is of course the boson mass and λ is the dimensionless self-coupling of the scalar. From the Lagrangian we can derive the energy-momentum tensor for the scalar field which is given by

$$T_{\mu\nu} = \partial_\mu \phi \partial_\nu \phi - \frac{1}{2} g_{\mu\nu} \left(g^{\rho\sigma} \partial_\rho \phi \partial_\sigma \phi + m^2 \phi^2 + \frac{1}{2} \lambda \phi^4 \right) \qquad (6.2)$$

The field ϕ can be expanded in terms of creation and annihilation operators in the usual manner, giving

$$\phi(r,t) = \sum_n \left(\frac{a_n}{\sqrt{2\omega_n}} \phi_n(r) e^{-i\omega_n t} + \frac{a_n^\dagger}{\sqrt{2\omega_n}} \phi_n^\dagger(r) e^{i\omega_n t} \right) \qquad (6.3)$$

Here $\phi = \phi^*$ as is appropriate for the real scalar field. We restrict ourselves to this case but a simple generalisation leads to the complex version appropriate to charged scalars with a conserved charge Q. The creation and annihilation operators obey the commutation relation

$$[\, a_m , a_n^{\dagger} \,] = \delta_{mn} \tag{6.4}$$

when the scalar is normalised as discussed below. Semi-classically, the components of $T_{\mu\nu}$ must be interpreted as expectation values between states of N_B bosons, given by $< N_B \mid :T_{\mu\nu}: \mid N_B >$ where the colons indicate normal ordering. This is equivalent to using a classical ϕ_c^2 field defined by

$$\phi_c^2 = < N_B \mid \phi^2 \mid N_B > \tag{6.5}$$

We are interested in the ground state of the boson stars, which will be obtained when ϕ is a nodeless function; this minimises the contribution of ϕ to the energy momentum tensor. We shall denote this ϕ_0, given by the lowest term in the expansion of equation (6.3). It has been demonstrated that higher node solutions are unstable [79]. We shall also restrict ourselves to the case of spherical symmetry, with the metric written in Schwarzchild form as

$$ds^2 = -B(r)\,dt^2 + A(r)\,dr^2 + r^2\,d\theta^2 + r^2 \sin^2\theta\, d\psi^2 \tag{6.6}$$

To ensure the canonical commutation relations of equation (6.4), we must normalise the scalar field as in Breit et al [78] according to

$$\int_0^{\infty} 4\pi r^2 \sqrt{\frac{A}{B}}\, |\phi_0|^2\, dr = 1 \tag{6.7}$$

Under our assumption that all the bosons are in the state ϕ_0 we can use equations (6.3) and (6.5) to write

$$\phi_c^2 = \frac{1}{\omega_0} \left(N_B + \frac{1}{2} \right) \phi_0^2 \tag{6.8}$$

giving our normalisation condition in terms of ϕ_c as

$$\int_0^\infty 4\pi r^2 \sqrt{\frac{A}{B}}\ \phi_c^2\, dr = \frac{1}{\omega_o}\left(N_B + \frac{1}{2}\right) \tag{6.9}$$

This scalar field will then provide the matter from which the boson star is constructed.

(iii) Adding Fermions

In this section we consider the addition of fermions into our scheme. The fermions shall be treated classically, as a degenerate relativistic Fermi gas. As described in the introduction, this was the technique adopted in the neutron star studies of Oppenheimer and Volkoff. A quantum mechanical justification has appeared in Ruffini and Bonazzola [71] where they demonstrate using a field theory method that the perfect fluid approximation is essentially exact for such large numbers of fermions as we shall encounter. The equation of state, first given by Chandrasekhar, is in parametric form with parameter t giving the pressure and energy density via

$$\rho = K\,(\sinh t - t) \tag{6.10}$$

$$p = \frac{K}{3}\left(\sinh t - 8\sinh\frac{t}{2} + 3t\right) \tag{6.11}$$

where

$$K = \frac{m_n^4\, c^5}{32\,\pi^2\,\hbar^3} \tag{6.12}$$

with m_n giving the fermion mass, here taken to be that of the neutron. For just now, we leave c and $\hbar$ in place pending a discussion on units in the next section. The

parameter t is defined by

$$t = 4 \log \left(\frac{p_0}{m_n c} + \left(1 + \left(\frac{p_0}{m_n c} \right)^2 \right)^{\frac{1}{2}} \right) \tag{6.13}$$

where p_0 is the maximum value of the linear momentum in the Fermi distribution. The particle density n in the distribution is equal to

$$n = \frac{1}{3 \pi^2 \hbar^3} p_0^2 \tag{6.14}$$

The equation of motion for the fermions will be obtained from the equation of hydrostatic equilibrium, a consequence of energy-conservation.

(iv) Equations of Structure, and the Question of Units

The Einstein equations are, as usual, given by

$$R_{\mu\nu} - \frac{1}{2} g_{\mu\nu} R = 8\pi G \left(T_{\mu\nu} (\phi_c) + T_{\mu\nu} (\rho , p) \right) \tag{6.15}$$

where we utilise the spherically symmetric metric given by equation (6.6). $T_{\mu\nu} (\phi_c)$ is defined by equations (6.2) and (6.5), and $T_{\mu\nu} (\rho, p)$ is given by the usual perfect fluid expression

$$T_{\mu\nu} (\rho , p) = (\rho + p) U_\mu U_\nu + g_{\mu\nu} p \tag{6.16}$$

with U_μ the fluid 4-velocity. The full set of equations are the Einstein equations coupled to the scalar equation of motion and to the equation of hydrostatic equilibrium. These can be obtained via energy conservation and are

$$\frac{dp}{dr} = - \frac{1}{2} (\rho + p) \frac{B'}{B} \tag{6.17}$$

and

$$\nabla\phi = m^2\phi + \lambda\phi^3 \tag{6.18}$$

where ∇ is the covariant D'Alembertian associated with the metric given by equation (6.6). (In fact, as in chapter five, these equations are a consequence of the Einstein equations, giving us a redundancy allowing us to drop two of the Einstein equations on the grounds that equations (6.17) and (6.18) are simpler to work with.)

It is convenient to make several rescalings of our variables before writing the equations. We now set $c = \hbar = 1$, but we will retain the gravitational constant G for the time being, pending our discussion on units. The most important redefinition is that of our radial variable; we make the change to

$$x = m\,r \tag{6.19}$$

where m is the mass of the boson. In combination with our other redefinitions, this will have the effect of removing m from an explicit appearance in the equations. The other redefinitions we wish to make are

$$\sigma=\sqrt{4\pi G}\,\phi_c \;;\; \Omega=\frac{\omega}{m} \;;\; \Lambda=\frac{\lambda}{4\pi G m^2} \;;\; \bar{\rho}=\frac{4\pi G\rho}{m^2} \;;\; \bar{p}=\frac{4\pi G p}{m^2} \tag{6.20}$$

Note that the redefined scalar field is now denoted σ. Using dashes to signify derivatives with respect to x as defined in equation (6.19), the complete set of equations for the system can be written as

$$A' = x A^2\left(2\bar{\rho} + \left(\frac{\Omega^2}{B}+1\right)\sigma^2 + \frac{\Lambda}{2}\sigma^4 + \frac{\sigma'^2}{A}\right) - \frac{A}{x}(A-1) \tag{6.21}$$

$$B' = x A B\left(2\bar{p} + \left(\frac{\Omega^2}{B}-1\right)\sigma^2 - \frac{\Lambda}{2}\sigma^4 + \frac{\sigma'^2}{A}\right) + \frac{B}{x}(A-1) \tag{6.22}$$

$$\sigma'' = -\left(\frac{2}{x} + \frac{B'}{2B} - \frac{A'}{2A}\right)\sigma' - A\left(\left(\frac{\Omega^2}{B} - 1\right)\sigma - \Lambda\sigma^3\right) \tag{6.23}$$

$$\bar{p}' = -\frac{1}{2}\frac{B'}{B}\left(\bar{\rho} + \bar{p}\right) \tag{6.24}$$

In the limit where there are no fermions these equations match those in [72], and in the limit where there are no bosons they match those of [60]. We shall employ the chain rule to rewrite this last equation as

$$t' = -\frac{1}{d\bar{p}/dt}\,\frac{1}{2}\,\frac{B'}{B}\left(\bar{\rho} + \bar{p}\right) \tag{6.25}$$

where now t is the variable of integration and throughout the redefined pressure and density are to be obtained via equations (6.10), (6.11) and (6.20).

The quantity of primary interest to us is that of the total mass of the Bose-Fermi configurations. Because in these solutions the scalar field disappears exponentially once we are sufficiently far out [78], this mass can be obtained in the usual way from the radial metric component; the mass as measured by an asymptotic observer is given via

$$A(x) = \left(1 - \frac{2M(x)}{x}\right) \tag{6.26}$$

with the total mass given by $M(\infty)$. The mass can be found by integrating out sufficiently far that the fermion and scalar terms are negligible and rearranging equation (6.26) as

$$M = \frac{x}{2}\left(1 - \frac{1}{A}\right) \tag{6.27}$$

This differs from the situation in chapter five, where we needed an exterior geometry which was not Schwarzchild, because the mass and coupling terms serve to localise

the scalar field.

The other quantities of interest are the total numbers of particles present. These are of interest because of the question of stability; if the total mass of the constituents in free assembly is less than the mass in the stellar configuration then the star will be unstable [80]. Hence we are interested in the free fermion and boson masses given by $(N_F m_n)$ and $(N_B m)$ respectively. By applying equation (6.9) (dropping the 1/2 as negligible compared to N_B) we find that

$$N_B = \omega \int_0^\infty 4\pi r^2 \sqrt{\frac{A}{B}}\, \phi_c^{\,2}\, dr \tag{6.28}$$

which can be rewritten in terms of σ as

$$N_B = \Omega \left(\frac{m_p}{m} \right)^2 \int_0^\infty \sqrt{\frac{A}{B}}\, \sigma^2 x^2\, dx \tag{6.29}$$

where $m_p = G^{-1/2}$ is the Planck mass. The total number of fermions can be found from equations (6.10) to (6.14), and is

$$N_F = \int_0^\infty 4\pi r^2 \sqrt{A}\, n\, dr = \frac{4}{3\pi} \left(\frac{m_n}{m} \right)^3 \int_0^\infty \sinh^3 \frac{t}{4}\, \sqrt{A}\, x^2\, dx \tag{6.30}$$

Notice that in the last expression the number of fermions depends on the boson mass m as well as the neutron mass; this is merely because the integration variable x depends on m.

We now digress on the question of what our units are. Having fixed $\hbar$ and c to be one, we still have one arbitrary scale to fix. We introduce a quantity α into the equation of state (6.10) so that it reads

$$\bar{\rho} = \alpha (\sinh t - t) \tag{6.31}$$

that is, we have from equations (6.13) and (6.20) that

$$\alpha = \frac{m_n^4}{8\pi m^2 m_p^2} \tag{6.32}$$

where we have rewritten G as m_p^{-2}. A particular choice of α fixes the overall scale as appropriate; we can see from equation (6.29) that giving a particular value to α is equivalent to selecting a value for m once we have chosen our fermion mass as that of the neutron. As an example, suppose that we choose α equal to one. Recalling that $m_n \sim 10^{-19}\, m_p$, this leads to a value for $m \sim 10^{-38}\, m_p$; that is, around 10^{-17} MeV (this value can of course be made precise.) We can examine different values of the boson mass by varying our choice of α in the above relations.

(v) Boundary Conditions and Numerical Tests

We now must consider the boundary conditions appropriate to our model and discuss their implementation. For most of the variables the situation is exactly that of chapter five, but, as we shall see, the problem posed for σ is an eigenvalue problem which complicates the scenario. Our requirement is that our solutions be non-singular (in particular at the centre), have finite mass, and are such that σ has no nodes. We examine the appropriate boundary conditions for each variable in turn.

A Non-singularity at the origin requires that A(0) should be one. Asymptotic flatness requires that $A(\infty)$ equals one, but this is automatically guaranteed by the equations.

B There is no restriction on B at the origin, but asymptotic flatness requires that $B(\infty)$ equals one. Fortunately, the equations are linear in B, so the solution can always be rescaled up or down as necessary. Ω^2 must be rescaled at the same time, so the normalisation of B is required to determine Ω.

σ' Non-singularity (or just spherical symmetry and continuity) requires that σ' be zero at the origin. Again, the equations guarantee that it falls to zero asymptotically when σ obeys its constraints as listed below.

t $t(0) = t_0$ gives the central fermion density via equation (6.11), and is a free parameter. The equations guarantee that at some *finite* radius t will become zero. We shall discuss later how we deal with this.

σ $\sigma(0) = \sigma_0$ gives the central boson density, and is a free parameter. The finite mass constraint requires that $\sigma(\infty)$ is zero, and we have stipulated that σ should be nodeless to gain the lowest energy configuration.

It is this last constraint that makes this an eigenvalue problem; we wish to determine the value of Ω which gives σ the desired form. We shall discuss how to do this.

The method used for the determination of the eigenvalue is what is known as a 'shooting method' [81]. What this involves is choosing a value for Ω^2 and integrating outwards from the origin with appropriate boundary conditions, paying attention to the behaviour of σ. The desired behaviour is that it tends asymptotically to zero with its derivative also tending asymptotically to zero. This is a separatrix between two generic types of behaviour; either σ becomes zero at some finite distance or σ' becomes positive before σ reaches zero. These behaviours are illustrated in figure (6.1). The first case tells us that Ω is too large, and the second case tells us that Ω is too small. Hence we can use an iterative procedure to determine the eigenvalue to arbitrary accuracy by sandwiching it between these two types of behaviour.

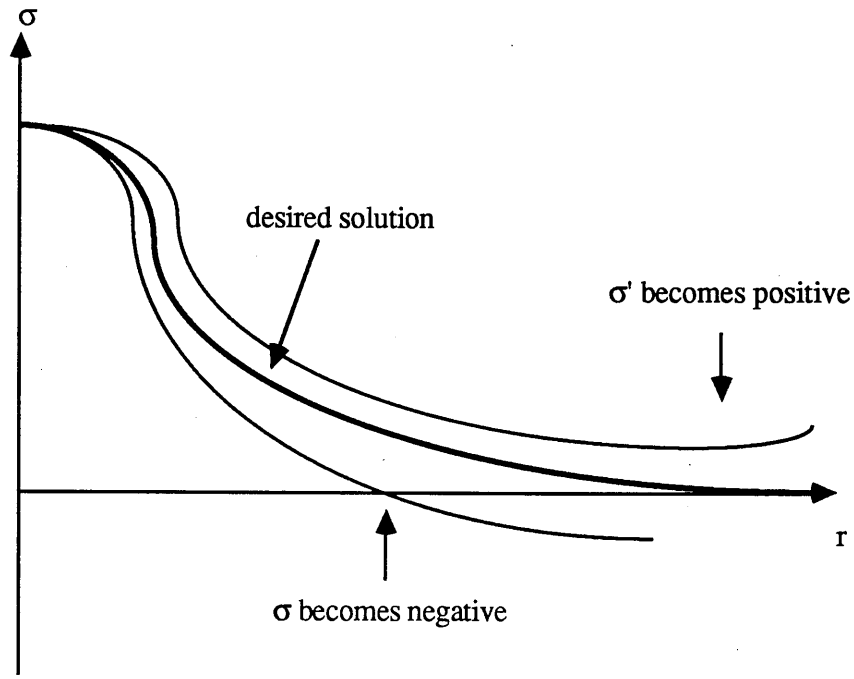

Figure 6.1 This demonstrates the eigenvalue search method. The bold line indicates the nodeless solution we require. If σ becomes negative as in the bottom line then Ω is too large, whereas if σ ' becomes positive while σ is still greater than zero then Ω is too small.

There is one further problem with this scenario for determining the eigenvalue, which is that this relies on our being able to integrate out to infinity, while in practice we can only go out to a finite distance. What we do to circumvent this is to arrange for the node of σ to be within a small range about some radius, and consider moving the position of the node outwards by shifting this range. Because at sufficiently large distances σ drops exponentially, once the node is far enough out we should get answers mimicking those for the node at infinity. It turns out that moving the node out corresponds to specifying the eigenvalue with greater and greater accuracy; once we are near the correct eigenvalue very small changes in Ω move the node about drastically and it becomes difficult to get the node into the correct range.

Numerical tests are performed to examine the accuracy which is required to determine the eigenvalue properly. For the sake of simplicity we examine the case

where there are only bosons present, by setting $t_0 = 0$. We choose $\Lambda = 10$ and $\sigma_0 = 0.07$ as sample values, and perform the integrations requiring that the node be at various different radii. The masses associated with these configurations are obtained by applying equation (6.27) *at the node* . This is equivalent to setting σ equal to zero at all radii outside the node, and this procedure will tend towards the correct answer as the node is moved outwards. Moving the node corresponds to altering the test value of Ω; increasing it brings the node in and decreasing it moves the node out.

Figures (6.2) and (6.3) demonstrate the results obtained. Figure (6.2) demonstrates how moving the node alters the mass. At small radii the answers obtained are completely incorrect, so our procedure has seriously affected the behaviour of σ as a function of r. As the node moves out to about $r = 25$, we see that our results stabilise with the same mass obtained for all node positions beyond this. These results tell us how far the node must be pushed out before the results become independent of the node position. Physically, this corresponds to having the node far enough out that replacing the small exponential tail of σ with zero makes a negligible change to the mass associated with σ.

While these results show us how to move the node for these particular parameters, the concept of radius is not very useful as the radius to which the node must be moved will be different for differing values of Λ, σ_0, and t_0. Moving the node out much further than the necessary amount is very wasteful of computer time and may require more accuracy in Ω than the computer can attain. A more useful concept, indicated in figure (6.3), is that of the number of significant figures to which Ω must be determined (to get the node in a small range about a certain radius) before the results become accurate. Here we make use of the feature that increasing the radius of the node requires greater accuracy for the eigenvalue. When Ω^2 is given to only two or three significant figures the results are inaccurate; we see that we need at least five or six significant figures to get an accurate evaluation of the mass. Such a figure remains the accuracy requirement regardless of the parameter values, so we

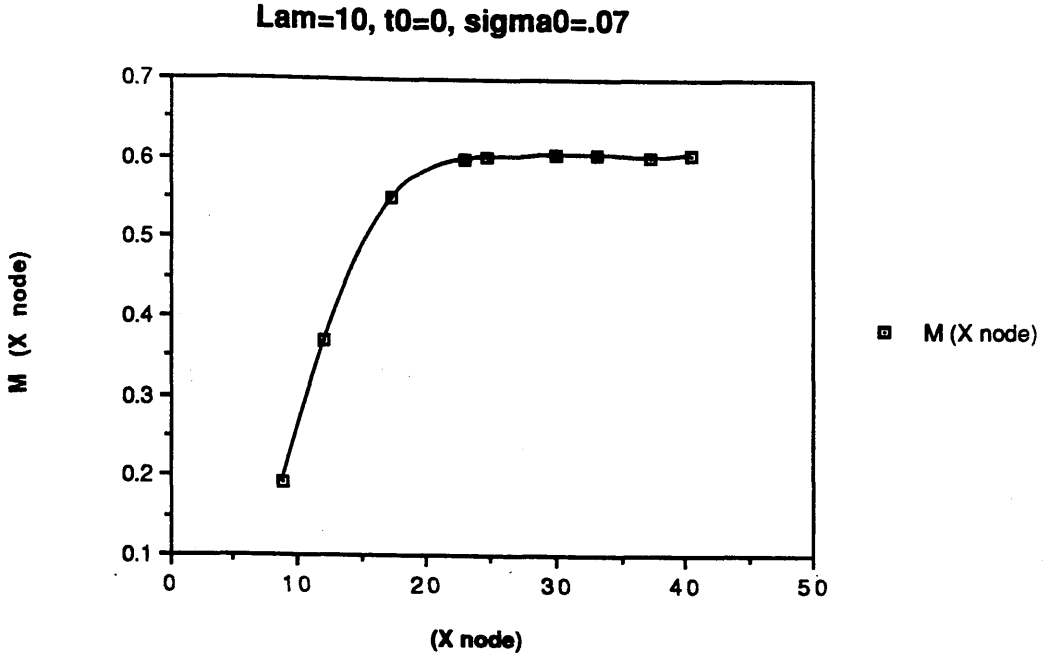

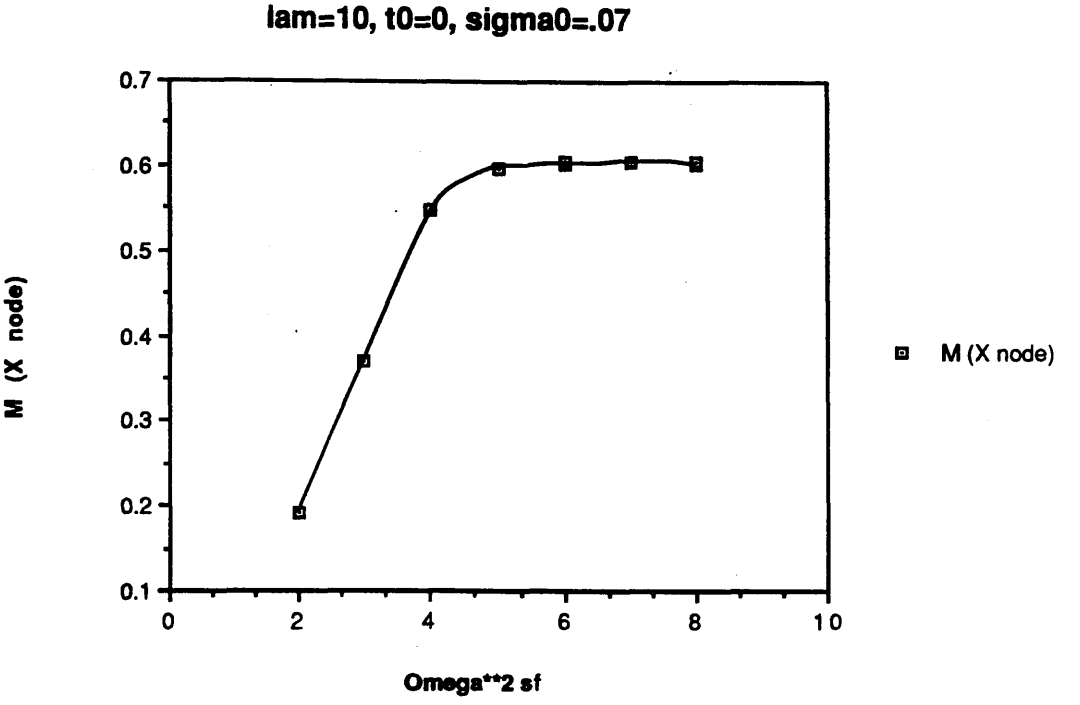

Figures 6.2 and 6.3 These graphs indicate how the mass obtained depends on the position of the node and on the accuracy to which Ω^2 must be determined. The figures clearly show the size that the radius and accuracy must be before we reach a region in which the results can be believed.

can use it as a criterion for whether or not we have attained a sufficient radius. For the figures in the following section on results, an accuracy of around eight significant figures for Ω^2 is the norm. This is well within the capability of a double precision numerical routine.

Another point which requires testing involves the behaviour of t. At some finite radius t reaches the value zero, which would be the radius of a pure neutron star. Because t' is not zero at this point, the computer program will crash (exactly the same as the situation described in more detail in chapter five); however we require a method of continuing the integration to determine the behaviour of σ and the eigenvalue. What we must do is attach a solution where t is exactly zero onto this interior solution; we do this by arranging for a cut-off for t below which the program will substitute the value zero whenever t occurs. It is tested that once this cut-off is sufficiently small the solutions become independent of the cut-off, demonstrating that the part of the t function we have removed is negligible. A cut-off of one thousandth is used for the numerical results, though actually a much larger value will still give completely satisfactory results. σ and σ' are continuous across the surface of the fermion core. Figure (6.4) demonstrates this change.

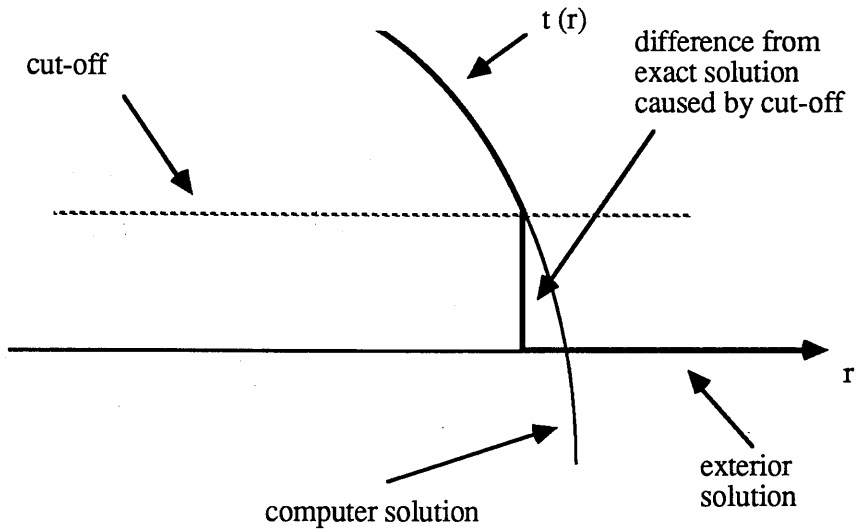

Figure 6.4 The fermion cut-off. The program tries to follow t(r) through t = 0 and will crash. The correct solution is obtained by attaching the exact computer solution to a t = 0 exterior solution. To facilitate this, a cut-off is introduced at which t is truncated to zero - the bold line. The difference from the exact solution, given by the small enclosed area, can be made arbitrarily small by lowering the cut-off.

(vi) Numerical Results

We now can discuss the range of equilibrium configurations. First of all, several limits were tested; the bosonless limit reproduces the results in [60] and without fermions the results reproduce those in [71] without scalar self-coupling and [72] when such a coupling is introduced. With this reassurance, we can go on to examine the richer situation where both bosons and fermions are present.

The starting point for our investigation is to examine a case where the relative strengths of the terms associated with the bosons and the fermions are about equal. We choose our value of α to be $1/4\pi$, which has the added advantage of allowing a direct numerical comparison with Oppenheimer and Volkoff who also made this choice, though in their case of pure neutrons this was only a choice of scale. It is sensible to first decide which boson mass this corresponds to. From the calculation

outlined at the end of section (iv), we find that the boson mass m = 5.11 * 10^{-17} MeV.

It is worth stressing just how light these bosons are. Previous studies of boson stars have capitalised on the fact that the boson mass drops completely out of the calculation and appears only as an overall scale, but this breaks down when fermions are introduced. We see from this that for the fermions and bosons to have a roughly equal influence the boson mass must be very light indeed - lighter than any currently conjectured field. We shall consider the case of more reasonable boson masses shortly, but it is worth finding the detailed results in this case first.

We choose Λ, as obtained from the self-coupling λ via equation (6.20), to be 10. This is taken as a sample value; the work of Colpi et al [72] indicates that the qualitative behaviour is unaltered by Λ though it does alter the magnitude of the masses obtained. We shall assume the results obtained from this Λ are representative of the whole parameter range of Λ.

We should briefly comment on what the values for the mass we obtain mean. By setting c and $\hbar$ equal to one, and by choosing G = 1 and hence $m_p = 1$, we are measuring things in natural units. However, we are using the new radial coordinate defined by equation (6.19), so when we use equation (6.27) to get the mass we must use

$$M(\text{star}) = m_p \frac{M}{(m/m_p)} = m_p^2 \frac{M}{m} \qquad (6.33)$$

where M(star), m and m_p are in grams and M is the dimensionless mass obtained from equation (6.27). In the purely bosonic case, all the boson mass terms disappear from the equations, so the results are independent of m. There the boson mass only gives the overall scale of the star. Here our situation is complicated by the presence of the fermions, so we must be careful about our scales. In our initial simulations, where $\alpha = 1 / 4\pi$ and hence m = 5.11 * 10^{-17} MeV, a value of 1 for the mass M

corresponds to 5.20 * 10^{33} grams, which is 2.62 solar masses. Hence one solar mass corresponds to M = 0.38. Changing α changes the overall mass scale.

As a sample result, figure (6.5) shows a simulation with $t_0 = 3$ and $\sigma_0 = 0.3$, plotting the five variables. It is arranged for the node of σ to be in the last fifth of the graph; we can see that this behaviour is very similar to if the node had been at infinity. The graph also shows how t falls to zero at a finite radius. The mass is determined to be 0.695, which is 1.8 solar masses, slightly higher than masses possible in advanced neutron star models. It should be emphasised though that this is an arbitrary choice of bosonic mass and self-coupling, so such a figure has no direct relevance to experiment.

Figure (6.6) shows a surface plot of the total mass as a function of t_0 and σ_0 as seen from two different perspectives (to aid visualisation). The ranges of the parameters are $0 \leq t_0 \leq 10$ and $0 \leq \sigma_0 \leq 1$, and the highest mass value is 0.915 (corresponding to around three solar masses) which is associated with a purely bosonic configuration with $\sigma_0 = 0.2$. In a similar manner to the pure neutron or boson case, the total mass tends to an asymptotic value as the central densities are increased. The $\sigma_0 = 0$ edge of the surface gives the Oppenheimer-Volkoff results and the $t_0 = 0$ edge gives the bosonic results of [72]. Arbitrarily small masses can be obtained in the corner where the central densities are each zero.

Equations (6.29) and (6.30) allow us to calculate the mass of a free assembly consisting of the same number of bosons and fermions as our star, and hence the binding energy of our configurations, which is just given by

$$BE = M(\infty) - (N_B m + N_F m_n) \qquad (6.34)$$

Positive values of the binding energy would correspond to configurations unstable against collective perturbations [80]. The boson and fermion numbers are computed by taking the differential versions of equations (6.29) and (6.30) and supplying N_B and N_F as additional integration variables. Because of the way that Ω and B appear

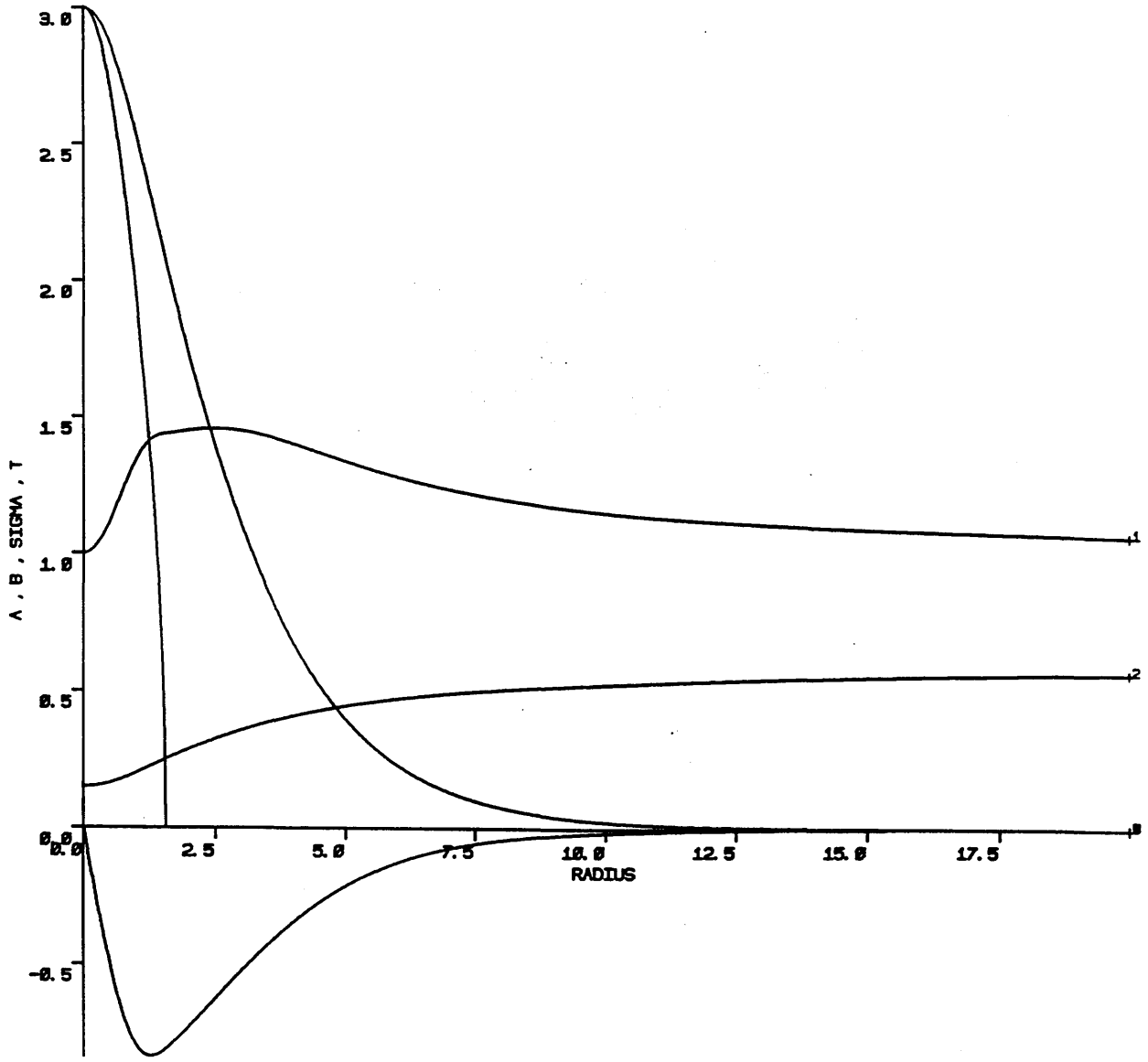

Figure 6.5 This is a sample simulation for $t_0 = 3$ and $\sigma_0 = 0.3$, with the eigenvalue search completed such that the node of σ falls in the last fifth of the graph, here at 17.4. The lines marked 1 and 2 are A and B, while the fermion component falls quickly to zero at a radius of 1.58, at which point a $t = 0$ exterior solution is attached. The other lines are σ (positive) and σ' (negative), both multiplied by ten for clarity. B has not been normalised so that $B(\infty) = 1$; this is not required for finding the mass.

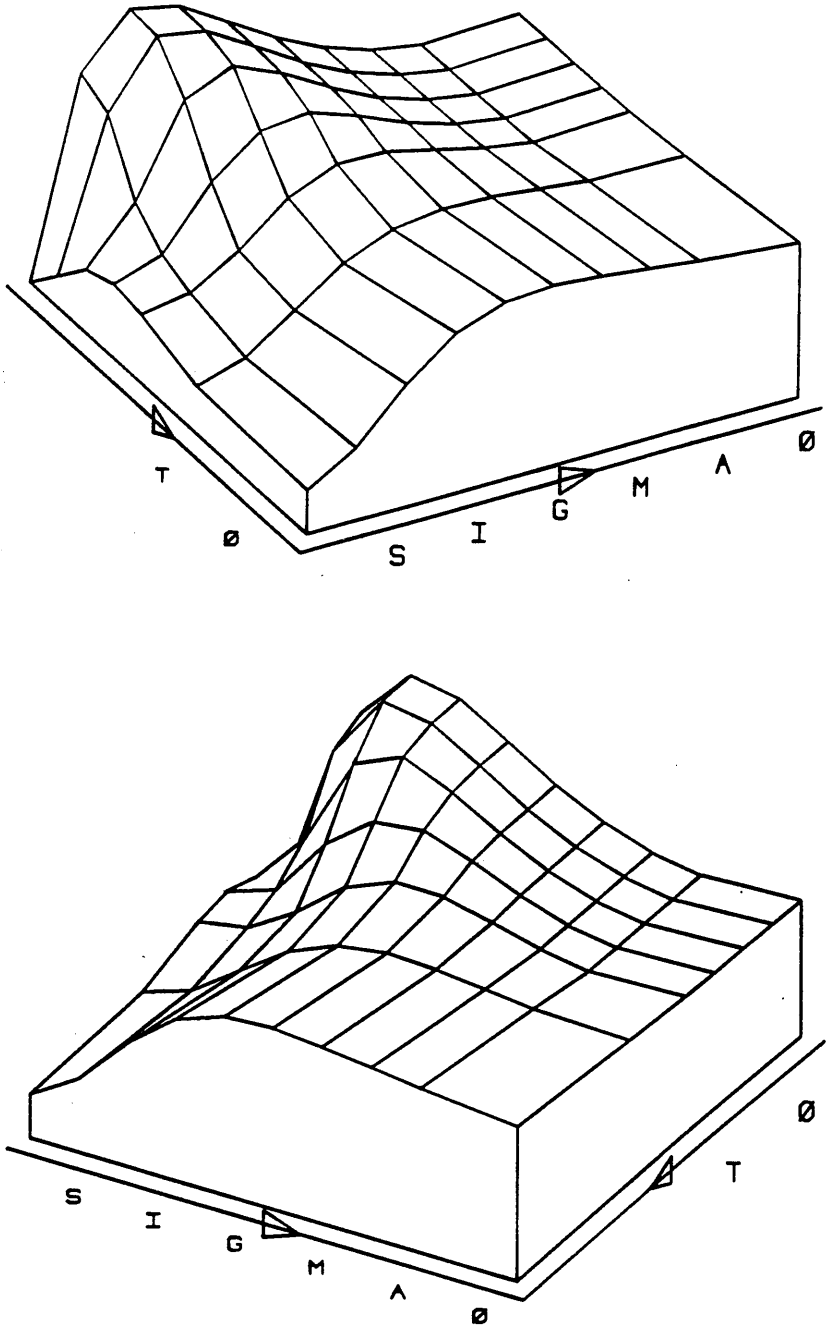

Figure 6.6 The mass surface as a function of t_0 and σ_0, as viewed from two different angles. The results without bosons and without fermions can be seen along the appropriate edges. We have $0 \leq t_0 \leq 10$ and $0 \leq \sigma_0 \leq 1$ as our parameter ranges, and the highest value of the mass is 0.915 in the units of our equations.

in equation (6.29), we do not need to perform the B normalisation here either, since such a normalisation is compensated by that of Ω.

Figures (6.7) and (6.8) demonstrate some results based on this. These graphs take the form of cross sections of $BE(t_0, \sigma_0)$ across a line of constant t_0 or constant σ_0. Figure (6.7) shows the variation of the binding energy with σ_0 at fixed values of t_0. For t_0 equal to one or three we see that the configurations have negative binding energy for low bosonic central densities and become unstable when σ_0 is higher. The arrows on the diagrams mark the points where the mass curve reaches its maximum for the corresponding value of t_0; for example, when t_0 equals one the maximum mass is given by σ_0 slightly greater than 0.2. When t_0 equals ten we see that the purely fermionic configuration is unstable; this result is well known from neutron star studies where instability is introduced at the maximum of the mass curve as a function of t_0. We see though that as σ_0 is increased there is a region where the binding energy is negative before we once more reach an unstable region. Notice that the transition to positive binding energies occurs well after the maximum mass in each case. This indicates that the binding energy test may not be particularly accurate as to where the instability occurs; it has been shown using a dynamical analysis [74] (which improves the results of [73]) that in the purely bosonic case it is at the maximum of the mass curve that the instability sets in, exactly mimicking the fermionic case. It is noted in [74] that for bosons the transition to positive binding energy occurs well after the onset of the dynamical instability. When interpreting these results, it is important to remember that while a configuration of positive binding energy is definitely unstable (at least to a collective dispersion to infinity, though not necessarily particle by particle [80]), one with negative binding energy is not necessarily stable as there may be other negative binding energy configurations which are favoured.

Figure (6.8) gives the corresponding picture for fixed σ_0. In each case here the maximum mass occurs at $t_0 = 0$; i.e. the purely bosonic case maximises the mass.

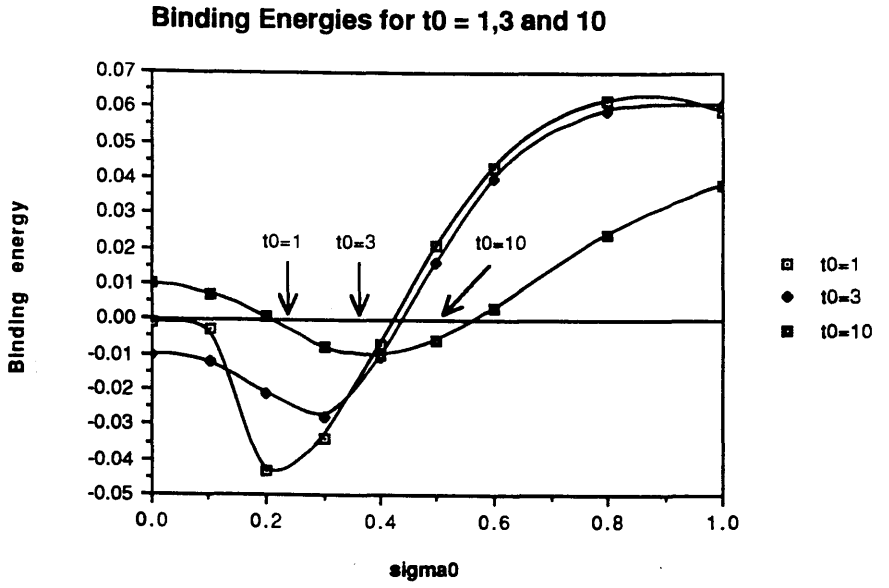

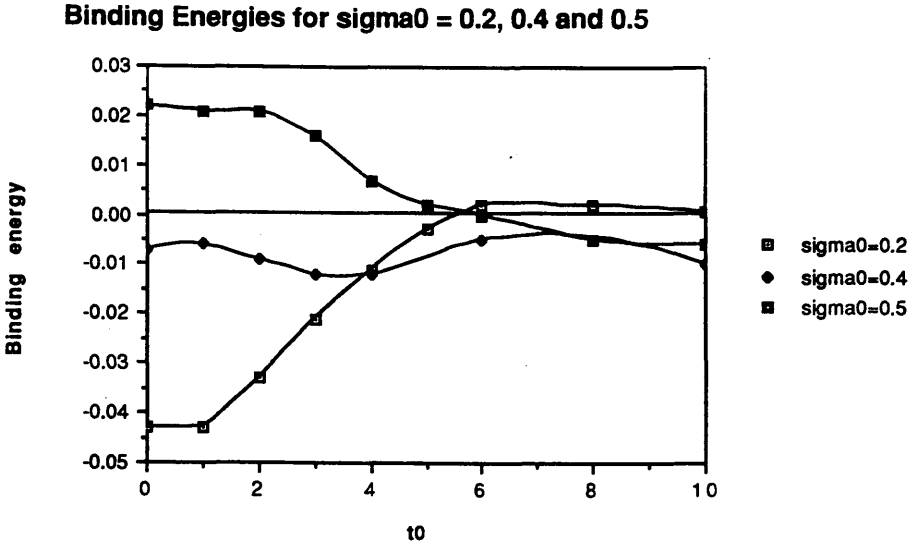

Figures 6.7 and 6.8 These graphs give the binding energies of configurations as the central densities vary. In each case $\Lambda = 10$ and $\alpha = 1/4\pi$. The top figure shows the binding energy for several fixed values of t_0 as σ_0 is varied; the horizontal line indicates where the binding energy is zero and the arrows indicate the value of σ_0 at which the maximum of the mass curve lies for a given t_0. The other graph shows the same for fixed σ_0 and varying t_0, where in each case the maximum mass is at $t_0 = 0$.

For σ_0 equalling 0.2 we get results essentially the same as in the fixed t_0 case. However, as we go to σ_0 equals 0.4 all the configurations have negative binding energy and when we reach 0.5 it is the configurations with low central density which are unstable and those with a higher central density which have a negative binding energy. At even higher σ_0 (e.g. σ_0 equals 0.8, omitted from figure (6.8) for clarity) none of the configurations we investigated were stable.

Figure (6.9) demonstrates the region of the t_0 - σ_0 plane where the binding energy is negative. Along the axes we get the results for the cases where we have only neutrons or only bosons. We can see here the results of the preceding figures; for example along $\sigma_0 = 5$ we see that the binding energy starts positive and becomes negative, and along the $t_0 = 10$ line we see that it starts positive, goes negative for a while and then becomes positive again.

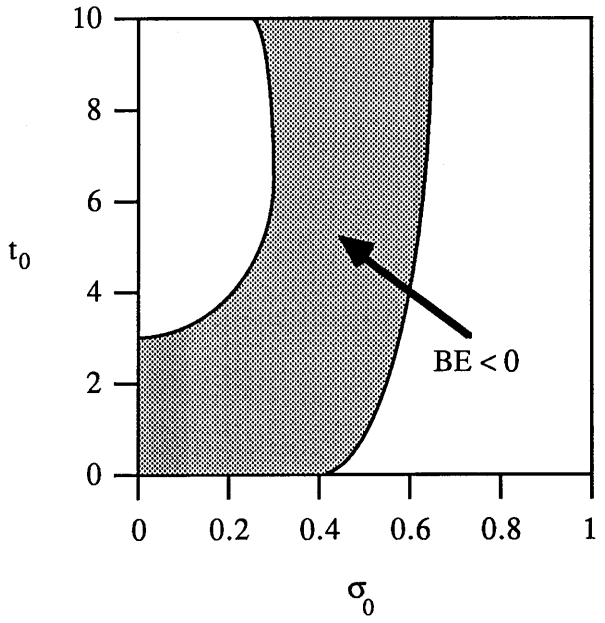

Figure 6.9 The region in the t_0 - σ_0 plane where the binding energy is negative is shaded in this figure, based on the results of figures (6.7) and (6.8) which can be seen along the appropriate vertical or horizontal line. It should be emphasised that this is only a rough drawing based on the results in figures (6.7) and (6.8).

The region of negative binding energy extends further upwards off the graph as far as we could test, e.g. the configuration with $t_0 = 20$ and $\sigma_0 = 0.4$ has negative binding energy. Once the central density gets this high, we can expect the fluid approximation to break down anyway, but it seems highly unlikely given the behaviour in the pure boson or fermion case that any of the configurations with high central densities are dynamically stable.

While the study of the binding energy gives some indication of the stability of these objects, it is far from being a complete guide to the details of the onset of an instability or its the characteristic frequency. As we noted above, it also can hide the full details; for instance a configuration of negative binding energy may still be unstable to collapse to a configuration with an even more negative binding energy, or one with positive energy may be stable against some types of small perturbations because of local minimum effects. The study of the onset of the dynamical instability of such configurations is of much interest for comparison with our results, though we shall not attempt this here. It would require an extension of the method developed by Chandrasekhar [82] beyond that made to purely bosonic stars by Jetzer [73], Gleiser [73] and Gleiser and Watkins [74].

We will now take some steps towards discovering the effects of varying the boson mass; from the formalism above we see is done by varying α. From equation (6.32), we see that the boson mass goes as $1 / \sqrt{\alpha}$, so by dividing α by some factor we increase the boson mass. The effect of this can be seen to simply reduce the size of the fermionic terms relative to the bosonic ones, because from equation (6.31) the pressure and density terms are proportional to α. From equation (6.20) we see that several of our parameters depend on the mass of the boson. As σ does not depend on m a given central density σ_0 is the same regardless of m, and we can see from equation (6.25) that the redefinitions cancel so that the central value of t gives the same pressure and energy density whatever value m takes. However, this is not true

for λ; if we change m then we must also alter Λ if we wish to be considering the same scalar coupling λ. From equation (6.33) we see that the overall scale will of course change.

First we examine how the total mass varies with α while keeping Λ constant and equal to ten. To enable easy comparison, we stick to the case where the central densities are given by $t_0 = 3$ and $\sigma_0 = 0.3$. We find that as α decreases (hence increasing the boson mass), the bosons become more and more predominant, and the mass becomes closer and closer to that which we would expect of a purely bosonic star. As α increases, we tend to a value for the dimensionless mass M of 0.881, which is exactly the value obtained in the purely bosonic case with this value of Λ. We can see however from equation (6.33) that the total mass in these cases is considerably lighter since M(star) ~ 1 / m.

With these results in place, we can consider altering m but keeping the scalar self-coupling λ fixed. This amounts to rescaling Λ in our equations as according to equation (6.20). We concentrate on the same values for the central densities. We can see that if we multiply the mass of the boson by some factor C, then we must divide Λ by C^2. Hence the value for Λ drops as we increase m. Having noted this, the results are exactly as one would expect from the analysis at constant Λ; once m is sufficiently large the star is again completely boson dominated and we tend towards the result for a pure boson star, this time with $\Lambda = 0$. Here m sufficiently large means only one hundred times larger than our original case, that is around $5*10^{-15}$ MeV, which is still tiny in comparison with the neutron mass.

These results appear in figures (6.10) and (6.11), as plots against m in units of 10^{-15} MeV. The first figure concentrates on the masses of the stars formed. One line gives the variation of the numerically determined mass m; this tends rapidly towards the value 0.631 which is that for a purely bosonic star with these central densities and $\Lambda = 0$. The other line gives the actual mass in units of the solar mass; from these logarithmic scales we see that the mass drops as 1/m, exactly as we expect of a

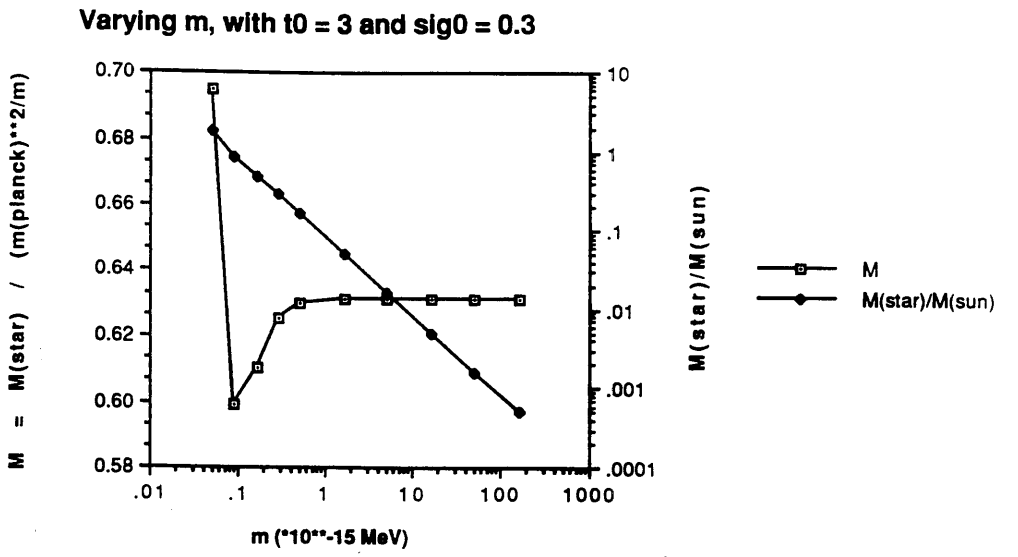

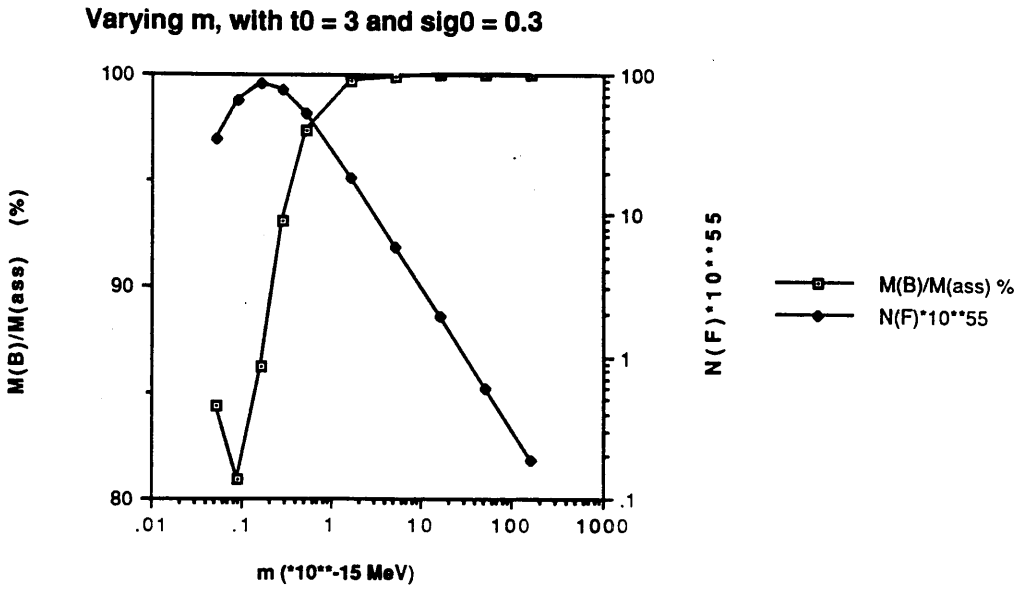

Figures 6.10 and 6.11 These figures demonstrate the behaviour of various features as we increase the boson mass at fixed central densities and self-coupling. Note that the plots have different axes for the two lines, and that several axes are logarithmic. m is in units of 10^{-15} MeV. The top figure shows the numerically determined mass M and the actual stellar mass in units of the solar mass. The lower figure shows the percentage of mass residing in the bosons when in free assembly (M(B) = mN_B and M(ass) is the total mass in free assembly), and the total number of fermions.

purely bosonic star. The second figure gives information on the types of particles present in these configurations; the first line shows that the percentage of mass present as bosons tends towards 100% while the second line shows that the absolute number of fermions drops as 1/m. Notice that the fraction of mass is determined from the free assembly; the concept of bosonic mass in the stellar configuration is not well defined. These results show that for these central densities increasing the constituent boson mass results in complete bosonic domination and results mimicking those for boson stars. This does not as yet however provide information of the nature of the range of configurations that exist when the boson mass in larger than in our previous investigations.

To this purpose, we now examine the whole mass surface for the case where the bosonic mass is greater than that considered in the results of figure (6.6). This situation differs from the first value of the boson mass that we considered because there are now two characteristic mass scales for the stars. The choice of $\alpha = 1/4\pi$ was made originally because then the purely bosonic stars and the purely fermionic stars had comparable masses, but with the choice of $\alpha = 1 / (4\pi * 10^6)$, corresponding via equation (6.32) to a boson mass one thousand times greater than before, this is no longer true. Because our scales have changed with the new choice of α, the dimensionless mass M for a neutron star is now of the order of a few hundred, though of course the actual mass is the same. However, the dimensionless mass of a boson star is still around one half, because the dimensionless mass of boson stars is independent of m [71], with the actual mass of boson stars going as 1/m. We shall shortly see the effects of the disparate characteristic masses.

We consider then the case of $\alpha = 1 / (4\pi * 10^6)$; we also choose $\Lambda = 0$. The reason for this latter choice is that for comparison with earlier results we wish to keep the self coupling λ constant, which requires from equation (6.20) that Λ is one million times smaller than its previous value of ten. The work in [72] shows that this will behave very much as in the $\Lambda = 0$ case, so for simplicity this is the one that we

shall consider. We again examine the variation of the mass with the central densities. It should be noted that a slight modification to the numerical technique is made here, because in many configurations the fermion radius is large and it is impossible to attain the accuracy required to position the scalar field node outside this. To counteract this, the node is positioned inside the fermions and near the node a cut-off is introduced where the scalar field and its derivative are set to zero, allowing the integration to continue out to the vacuum where the mass can be determined. This approximation is really exactly equivalent to determining the mass at the node as we did previously, and again tends to the correct result as the node is moved sufficiently far out and the cut-off lowered sufficiently far. Because the fermion terms are multiplied by α, which is very small, the scalar cut-off must be at very small values to ensure that these terms are negligible.

The results that we find are that there are two distinct types of configuration present as the central densities are varied - boson dominated configurations and fermion dominated configurations. The transition between these two extremes is very sudden, and the two types have the characteristic mass of a boson star and a neutron star respectively. The fermion radius is of a standard size (that is, comparable to that of a purely fermionic star) in a fermion dominated configuration but considerably smaller in a boson dominated configuration because there are very few fermions present in these cases. As with the mass variation, the transition to large radii is very sudden.

Some results are shown in figures (6.12) and (6.13). These are in the form of a variation of t_0 with σ_0 held constant at 0.3. Λ and α are as stated above. As background information, the maximum mass attained by purely fermionic configurations is about 272 at $t_0 = 3$, while the mass of a purely bosonic configuration at $\sigma_0 = 0.3$ and $\Lambda = 0$ is 0.631.

These figures show a very sharp transition, which occurs at $t_0 = 3.92$, between two generic behaviours. The first figure shows the mass on logarithmic scales while

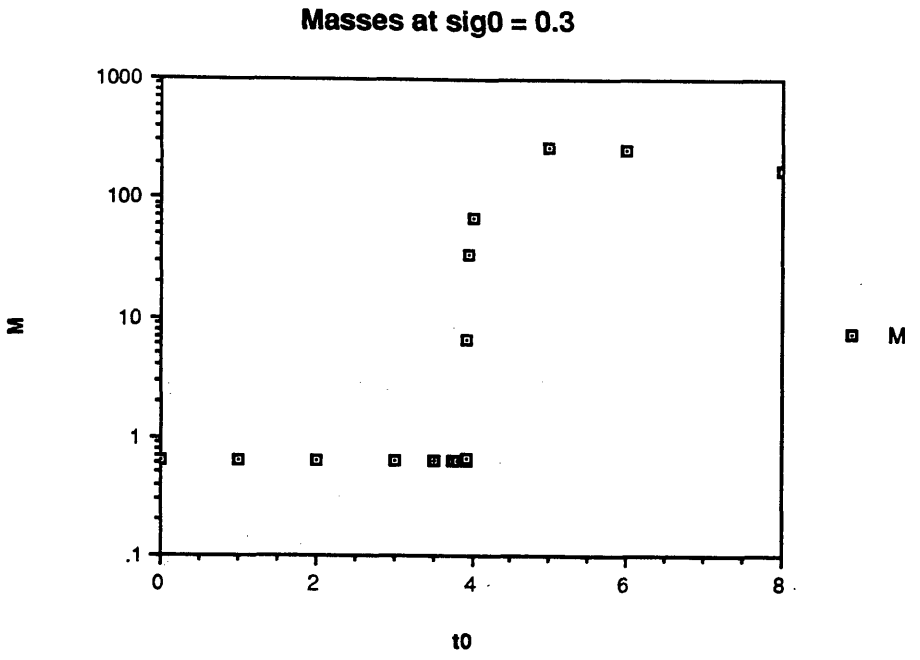

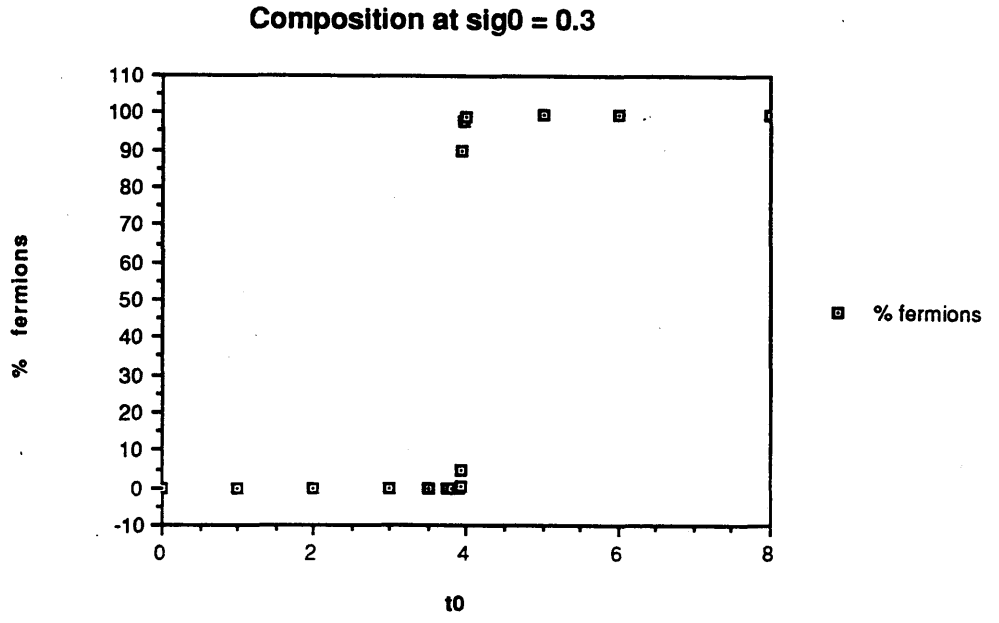

Figures 6.12 and 6.13 These show the possible equilibrium configurations with σ_0 equalling 0.3, in the case of a boson mass of $5 * 10^{-14}$ MeV with $\Lambda = 0$. The top figure shows the dimensionless mass M of the configurations while the lower one shows the percentage of the mass residing in the fermions in the free assembly. The transition from boson dominated to fermion dominated configurations is very sharp.

the second shows the percentage composition of these objects. As above, the percentage composition refers to the percentage of mass residing in the fermions when in free assembly. In fact the boson number is about the same for all these configurations; it is the fermion number which changes drastically. At low t_0, we see that the percentage of fermions is extremely near zero and the stellar mass is the 0.631 that we would expect of a purely bosonic star. After the transition the composition is almost completely fermions and the masses are of characteristic fermion magnitude. In fact, the maximum mass is very close to that of the pure neutron case; while none of the configurations examined actually exceeded the mass of the $t_0 = 3$ fermionic configuration, values very close to this were found. Results similar to this were obtained for other fixed values of σ_0. Figure (6.14) shows roughly the regions of boson and fermion domination discovered in our simulations (once more a rough drawing).

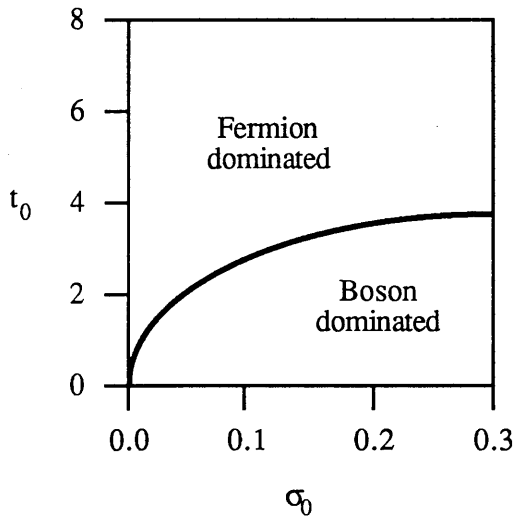

Figure 6.14 The regions of bosonic and fermionic domination of the configurations as t_0 and σ_o are varied.

Examination of the binding energies gives very similar results to before; for constant σ_0 the binding energy remains positive some way beyond the maximum of the mass curve. Again a dynamical analysis will give more stringent stability constraints.

(vii) Contrasts, Conclusions and Afterthoughts

Here we conclude the work of this chapter with some discussion of the results that we have obtained, their meaning and the relation to other work. We begin by contrasting our basic assumptions with those of other work which has been carried out recently in related fields. We then provide a summary of our results with some discussion of their meaning. Finally, we mention ways in which these investigations can be extended and also consider the corrections to our formalism that an explicit interaction term between the bosons and fermions would entail, including a demonstration that for the range of boson masses we have considered such an interaction should be negligible.

First we examine the relation between our work and that arising from the incorporation of gravity into non-topological solitons and Q-balls. In [75], Friedberg et al studied scalar soliton stars consisting of a complex scalar field ϕ and a real scalar field χ interacting gravitationally, and possibly having other interactions. The complex scalar field ϕ has a time dependence $e^{-i\omega t}$, resulting in ω playing the same role as the boson quantum frequency ω in our work. In the special example studied numerically ($\chi = 0$) the scalar soliton star has a huge mass of order m_P^4/m^3 where m is the mass of the ϕ boson. (The non-soliton based work of Colpi et al [72] with a different self-interaction of the complex scalar field ϕ gave a star mass of the order of m_P^2/m). Lee and Pang [83] studied fermion soliton stars with a fermion field ψ replacing the complex scalar field ϕ of the scalar soliton stars; the fermions interact with a neutral scalar field σ of Higgs type. No explicit time dependence appears in the problem, and there is no quantisation of the scalar field σ; thus there is no analogue of the quantum frequency ω which appears in our equations as an eigenvalue. In the fermion soliton stars again a huge mass of m_P^4/m^3 is found, where m is now the mass of the σ boson.

Recently Lynn [76] has initiated consideration of stars, dubbed Q-stars, where emphasis is placed on the non-gravitational interactions of the scalar field being of a

more usual particle physics magnitude (other work tending to require small couplings). His constructions correspond to incorporating gravity into Q-balls. With a complex scalar field having a quantum frequency ω and zero or one real scalar field he finds star masses of the order of m_P^3/m^2 where m is a mass scale appropriate to the scalar fields.

The main features of the above work are the existence of non-trivial couplings, usually with the aim of providing surface and volume terms to localise the fields. Our case differs from this in that gravity is the main interaction when it comes to localising the scalar field; though we do use a scalar self-coupling λ we also have configurations when λ equals zero. We have shown that in our model, once we have chosen a bosonic mass and self-coupling (having assumed the fermions to be neutrons, though this is not essential), the possible equilibrium configurations are parametrised by the central densities of the scalar and the fluid representing the fermions, and have examined a range of possibilities. We summarise these below.

Initially it was shown that for the bosonic and fermionic configurations to be of comparable size the boson mass has to be very light (we require the Compton wavelength of the bosons to be of similar size to the neutron star). The possible configurations were examined, and a surface plot of their masses was given in figure (6.6). It can be seen that for this boson mass there are some configurations, notably purely bosonic ones, which are heavier than the maximum mass obtainable using just fermions. While lately much interest has been generated in the masses and rotation speeds in pulsar models due to observations of the remnant of the 1987 supernova, it must be emphasised that this result is based on an arbitrary choice of boson mass and couplings, hence has no direct relevance to observation. A rudimentary stability test using the binding energy of these objects was invoked; a positive binding energy indicates that a configuration is unstable though unfortunately the converse is not true. Hence many of the configurations with negative binding energy may also be unstable. A proper dynamical analysis of the

instability would be required to examine this point adequately.

Having catalogued these configurations, progress was then made in the direction of examining the consequences of a larger boson mass. At fixed central densities, it was shown that as the boson mass increases the configurations become more and more boson dominated, and behave as boson stars. A choice was then made of a boson mass at which the boson and fermion contributions to the equations are of disparate size for a study of the complete mass surface. This leads to a situation where the characteristic mass for fermion stars is around one thousand times greater than that for bosonic stars. It was discovered that as the central densities are varied there are two generic behaviours for the configurations; they are either boson or fermion dominated. The transition between these, shown in figure (6.14), is very sudden. The boson and fermion dominated configurations have masses and radii appropriate to their type, so the fermion dominated configurations are generically around a thousand times heavier than their bosonic counterparts. Presumably a star made from roughly equal bosonic and fermionic contributions would have to find an equilibrium position with central densities on the transition line. In the case of higher boson mass, no configurations were found with a higher total mass than the most massive neutron star, though in general the difference can be very small.

To elucidate further what these results might mean, it would be well advised to have a particular boson mass (and, to some extent, self-coupling) in mind. The candidate particle that interests us most is undoubtedly the axion, because as we have seen it is the very light boson masses which give rise to the most interesting configurations. Until an observation of the axion is made, we obviously do not know its exact mass, but it is possible that it is within a few orders of magnitude of the two sample values of m we have examined here. It seems likely that the trend to having boson and fermion dominated configurations will continue to higher boson masses, so this may well be the relevant scenario for the possible equilibria. As we

shall see in our discussion on explicit interaction terms, our results are however unlikely to extrapolate up to masses such as those conjectured for the Higgs boson.

Our stability analysis certainly leaves much to be desired, though to confront the dynamical instability calculations would be to face up to an extremely complicated set of equations. To extend Chandrasekhar's variational principle to these configurations is a goal which may be well worth pursuing as in the purely bosonic case such an analysis certainly is required to give the full picture; clearly it will be needed here too. One can also ask what might happen if we took an equilibrium configuration containing near to the maximum allowed number of fermions (or, of course, bosons) and insisted on adding more and more fermions to it. It appears that there would be no equilibrium configuration available and hence collapse must proceed, even though the configuration may not be on the maximum of the mass surface (that is, it may have less mass than some purely bosonic configurations). Further thought is no doubt needed to determine what happens in such a situation - perhaps otherwise negligible interaction terms may become important and would mediate fermion to boson reactions to attain a stable equilibrium with different particle numbers. Our treatment is not sufficiently sophisticated to allow us to consider such possibilities.

Beyond these topics, future work would be much aided by having a specific case for examination. In the absence of this, a larger catalogue of results might discover other interesting phenomena. An example would be to consider boson masses smaller than those we first examined. Some exploration has indicated that in this case too that at fixed central densities the configurations become more and more bosonically dominated, with the fermion contribution tending to have a very small radius and hence little overall effect. We have not investigated this case in full, as there are no current candidates for scalar fields as light as this. One could also hope to extend the work to larger boson masses, though this would appear to necessarily entail taking an explicit boson-fermion interaction into account.

As a final rider, the number of free parameters available has meant that we have

had to pay little attention to varying λ. While the work of Colpi et al [72] indicates that no qualitative change occurs as Λ is altered, there does remain the possibility that this is no longer true for our case. Also Lynn [76] has emphasised that in all these studies the value of λ tends to be rather small. Extending this work to more sensible values of the self-coupling would also be very interesting.

To conclude, we now consider briefly the effects of an explicit coupling term between the bosons and the fermions, an analysis which will justify its neglect for the ranges of boson mass that we consider. We take the action for the scalar field as being

$$S = \int d^4x \sqrt{-g} \left(\frac{1}{2} m^2 \phi^2 + \frac{1}{2} \partial_\mu \phi \partial^\mu \phi + \frac{1}{4} \lambda \phi^4 + \frac{g}{2m_n} \bar{\psi} \gamma^\mu \gamma_5 \psi \partial_\mu \phi \right) \quad (6.35)$$

where the last term couples the fermion field ψ to the scalar with strength given by the coupling constant g. As far as the scalar field equation is concerned we can go over to an effective action formalism modifying the Lagrangian which will acquire extra terms, such as

$$L_I = \lambda_1 \phi^2 + \lambda_2 \phi^3 + \lambda_3 \phi^4 \quad (6.36)$$

where the λ_i depend on the type and magnitude of the interaction and on the fermion configuration. The first and last of these terms will correspond to a mass and coupling renormalisation, which will vary with the radius as the fermion condensate is spatially varying. Outside the fermion core these terms will vanish and the mass and charge will regain their vacuum values.

For the fermions we are considering an ideal cold star, so without the Yukawa interaction we have at each point in space a momentum distribution in which all states are filled up to the Fermi surface momentum $p_0(x)$ and all states outside the

Fermi surface are empty. In the presence of an interaction this picture will be modified with the Bose quanta inducing transitions such that the fermions can jump outside the surface leaving holes. Provided the interaction is small an equilibrium should be established in which the cold star Fermi distribution is modified by hole-particle pairs. For the frequency of Bose quanta considered here these pairs will occur near the Fermi surface, and will result in a modification of the equation of state for the fermions and hence a modification of the Chandrasekhar parametrisation of p and ρ.

We now estimate the size of the interaction term in relation to our other quantities. Following Ruffini and Bonazzola [71], we define a current

$$J^{\mu} = \bar{\psi} \gamma^{\mu} \psi \tag{6.37}$$

The first component, J^0, is just the number density of the fermion field, which we will denote χ, with a general relativistic correction provided by the metric [71]; that is

$$J^0 = \chi / \sqrt{g_{00}} \tag{6.38}$$

The interaction term appears in the equations as a scalar term multiplying an expectation value of the current with the γ_5 reinserted. We can therefore use J^0 to provide an estimate of the expectation term, as γ_5 will not affect the magnitude. From equation (6.38) we get the estimate that

$$J^0 \sim < \bar{\psi} \gamma^0 \gamma_5 \psi > \sim O\left(m_N^3 \sinh^3 \frac{t}{4} \right) \tag{6.39}$$

We must correct this result due to the fact that only fermions near the Fermi surface are able to interact, namely those in a shell of thickness $O(\omega)$ where ω is the Bose quanta, while the Fermi sphere has radius p_0 which we can find from equation

(6.13). Hence we must multiply equation (6.39) by a correction factor to account for the fraction of fermions able to interact. The extra term which appears in the equations of motion (for example equation (6.21)) is then of the form

$$\frac{1}{x\,A}\frac{dA}{dx} = \ldots\ldots\ldots + 4\pi g\,(\sinh^2\frac{t}{4})\,\Omega\,\frac{m}{m_N} \qquad (6.40)$$

The quantities in the last term are in general of order one except for the final m / m_N fraction, so it is this ratio which determines the importance of the interaction. In the case where the boson mass is small by many orders of magnitude relative to that of the fermion, as for instance when we consider the axion, it can be seen from equation (6.40) that the interaction term will have a negligible effect on the equations of motion. When the masses of the constituent particles become of similar magnitude, our approximation will break down and a full treatment requiring the interaction term to be given full consideration will be required. The physical picture is that only at large boson masses are the Bose quanta sufficiently large that a significant proportion of the Fermi sphere is able to interact. This then justifies our neglect of explicit interactions of this type in our studies.

Chapter 7

Conclusions and Future Work

"And this story, having no beginning, will have no end."

Weaveworld

Clive Barker

(i) Conclusions

Given that each chapter has its own conclusions, this section exists merely to provide a final overview of the work carried out in this thesis. More details are available in the appropriate conclusions section of chapters three to six.

Chapters two and three considered various cosmological solutions in ten dimensional supergravity within the context of a specific model. A variety of topics were considered, beginning with an investigation of the behaviour on the approach to the singularity backwards in time. It was found by means of an analytic argument involving bouncing between Kasner modes that the presence of a fundamental scalar field, known as the dilaton, moderated what would have been a chaotic approach to the singularity. This was confirmed by numerical means. Solutions forwards in time were found to be governed by an unusual type of attractor which precludes the possibility of a compactification scenario in the basic model. However, a modification to this model where the three form field **H** distinguishes three spatial dimensions from the rest does allow compactification solutions.

The basic models were enhanced by the introduction of a sample particle production mechanism, where the energy of scalar field oscillations is transformed into a relativistic fluid representing fermions. The behaviour of the system for several generic forms of the particle production term, which appears in the equations

as a viscous force, was investigated, though a substantial improvement on the basic scenarios was not obtained.

Chapter four considered the dynamics of inflation induced by scalar field potentials of an exponential type, leading to a class of inflation models known as power law inflation models. A more general solution than has previously appeared was found for the simplest case, and then it was demonstrated that when particle production effects are taken into account, again leading to viscous forces, the basic scenario is improved. These ideas were adapted for use in a more realistic model based on a supergravity theory, which has a scalar field potential well suited for the construction of an inflationary scenario. It was shown how the viscosity considerably eases the construction of a model within this context, and the outline is sufficiently general to demonstrate how such a model can be designed in other fundamental theories.

Chapter five examined the role that an extra dimension of Kaluza-Klein type may play in the physics of neutron stars and in the process of dynamical gravitational collapse. In the spherically symmetric case the extra dimension appears in the equations as a scalar field, and this feature was used to advantage in setting up the system of equations which describe a neutron star in Kaluza-Klein theories. Attention is centred on the description of the neutron fluid from which the star is formed; if we wish to describe this fluid in an intrinsically five-dimensional manner we gain a source term for the scalar field which results in a non-trivial solution of the scalar equation of motion, corresponding to the star carrying a scalar charge. It was shown that in this case we must consider an exterior geometry differing from the usual Schwarzchild one, using instead its generalisation to the coupled Einstein plus scalar solution as found by Janis et al. It was shown that such an exterior solution can be consistently attached at the boundary of the numerical solution for the interior of the star, and that we can use this to find the mass of the star. The effect of the extra dimension was shown to depend on the type of fluid description, but the

results clearly rule out the possibility that the fluid can be described by a straight generalisation of the four dimensional description.

The dynamical collapse problem in the context of Kaluza-Klein theories was also examined, under a set of simplifying assumptions. The most general separable solution to these equations was found in analytic form, and appears very similar to the corresponding solution in conventional general relativity, though enhanced with the addition of an extra term. The role of this term is concealed by the difficulties in attaching an exterior solution to the collapse metric, the situation being complicated by the breakdown of Birkhoff's theorem.

Finally, chapter six considered the possibility of stars made from a combination of bosonic and fermionic constituents. The basic equations for boson stars were reproduced and it was shown how to introduce fermions into the scheme. The solution of the system is an eigenvalue problem due to the existence of boundary conditions both at the centre of the star and at infinity. This was solved numerically by an iterative shooting method. The solutions for a given boson mass and self-coupling are parametrised by the central densities of the bosonic and fermionic parts, and the masses of the family of equilibrium solutions were found for a given (rather small) boson mass where the bosonic and fermionic terms were of roughly equal importance. A rudimentary stability test involving the binding energies of these objects was carried out as a preliminary guide to stability. The effect of an increase in the boson mass was then examined, and finally a brief analysis of the possible effects of an explicit interaction term in the Lagrangian was given.

(ii) Future Work

This final section suggests areas in which the work detailed in this thesis may be extended, and outlines some developments which may prove fruitful. Some of these topics are already under consideration at the time of writing. We consider each separate topic in turn.

The work in chapters two and three has no obvious continuation; the main drawback of the model is that in its current form it is too simplistic, but any attempt to extend the model would inevitably result in a system so complicated as to be intractable. A full treatment would entail including the fermionic contributions in a more fundamental manner than resorting to the fluid approximation, and the employment of accurate perturbation calculations to determine the coupling. Unfortunately, the treatment of the geometric sector of the theory is far too basic for the pursuit of the above goals to be fruitful, and in any case given the difficulties in obtaining a satisfactory low energy theory such as the standard model from the superstring it seems prudent to await further developments in the theory before attempting detailed cosmological modelling based upon it.

In contrast, the power law inflation scenario of chapter four offers many avenues along which investigation can be pursued. The implementation of these ideas in other theories featuring exponential potentials is well worth study; for instance, in higher dimensional Yang-Mills theories exponential potentials commonly arise and this may be the only way of implementing inflation in the cosmology of these theories. Within a particular theory, further investigations can be made of how, for instance, the departures from exact exponential potentials affect density perturbations. The transition to the conventional Friedmann universe can be studied in more depth with more emphasis placed on the final matter distribution and the dynamics of reheating. By enhancing the treatment to a full semi-classical analysis the effect of quantum fluctuations can also be investigated; for example, it may be possible to implement a reproducing inflationary model such as has been suggested

by Linde. Because the geometry of the power law inflation is not the de Sitter one, it is a non-trivial point of investigation. In principle, the exact form of the viscosity term within a given theory can be calculated, though in practice this may involve very complicated perturbation calculations.

In chapter five, we saw how the fluid description effects the structure of a neutron star, which gives constraints on the types of fluid description that we may use. Interest here centres on the consequences for gravitational collapse, as a five-dimensional fluid description seems to lead inevitably to a scalar charge which cannot be radiated freely as its existence is intrinsically tied up with the presence of the neutron fluid. For this purpose, a continuation of the study of the dynamical collapse solution would be very useful. An exterior solution must be found onto which the interior metric can be smoothly joined; this should elucidate the possible effects of the extra D/r term present in the metric above those that we find in conventional relativistic studies.

It is also important to consider how the collapse might look to the observer in four dimensions; this involves a conformal transformation of the metric involving the extra dimensional metric term. Because in this case g_{55} is both time and space dependent, this leads to a very complicated looking solution of the Einstein equations. Perhaps the use of subtle coordinate transformations can clarify the structure of this metric; its global structure is also of interest.

Another aim is to enhance the collapse model to include pressure terms and consider different fluid descriptions. This should help clarify the role of the scalar charge, but is likely to lead to a very complicated set of partial differential equations which are unlikely to be separable. Hence very sophisticated numerical techniques may be required to enable one to tackle this problem.

Chapter six also leaves many channels open for future investigation, partly because the work is still in progress at the time of writing. It is possible to tabulate more results concerning the equilibrium configurations, but this would be very time

consuming because there are so many free parameters to be chosen, namely the central densities of both bosons and fermions and the boson mass and self-coupling. Computing the eigenvalues to the required accuracy needs a substantial amount of computer time and also needs good initial estimates. Because of the large number of parameters chapter six has mostly assumed that altering the self-coupling will have no qualitative effect; this is borne out in the studies of purely bosonic stars. It may be best to stick to the qualitative picture until a specific scalar field is envisaged. The most promising candidate would be an axion. If a good estimate of its mass, and perhaps even its self-coupling, could be obtained then the cataloguing of the possible equilibrium configurations would be much simpler.

The stability of the configurations is definitely worthy of future study, as the simplistic binding energy test provided in chapter six tells us nothing of the onset of dynamical instability. Generalising the methods already used in the study of bosonic stars will lead to complicated perturbation equations, but the intuition provided by the purely bosonic or purely fermionic cases should prove useful.

Finally, it is also possible to enhance the study by taking into account an explicit boson-fermion coupling. The rough estimate provided in chapter six shows that this is probably not important until we consider boson masses comparable to the fermion mass, so for example if we were considering a Higgs particle interactions could be very important and in this mass range our results are presumably not valid. If the axion has a reasonably substantial mass then interactions will also be important in that case. To deal with such a situation it will probably be necessary to abandon the use of the perfect fluid approximation and return to a fundamental quantum mechanical treatment of the fermions, as carried out by Ruffini and Bonazzola. This again may lead to a very difficult numerical problem.

Appendix 1 On Numerical Integration

(i) Numerical Integration : Why and How

This appendix outlines the techniques of numerical simulation which were used to provide results detailed in chapters three, four and five of this thesis. The numerical work there was to provide solutions of coupled non-linear ordinary differential equations given particular initial conditions; that is, we wish to solve an initial value problem. Numerical simulation is required because it is only in the very simplest of these cases that an analytic solution can be found, though sometimes other techniques such as phase plane analysis (see references given in chapter four, section (ii)) can be used provided the system is plane autonomous. Solutions to non-linear equations are of course very different to the linear case in that the solutions cannot be scaled to satisfy the initial conditions given, so the solutions obtained can have a completely different form as the initial conditions are varied. It is therefore important to examine what happens for a wide range of initial conditions.

For numerical simulation, the system is first written as a first order system; in all our cases this is trivially done by defining first derivatives as new variables, though this is not possible in some pathological cases. If all the coefficients are sufficiently differentiable, as they always are in the cases that we consider, then general theorems guarantee that if we provide initial conditions for each of the variables then solutions do exist. There is however no guarantee that the solutions will exist throughout an interval of arbitrary size; in general there is the possibility that the solutions will go singular at some point. Here normally the computer simulation will terminate. It is important to distinguish actual physical singularities of this type which may arise, e.g. in general relativity, from artifacts of the numerical method. Such a situation arises in chapter three.

The actual simulations are done using library routines on an IBM 4361 mainframe computer housed in the physics department. The main routine, which

actually performs the integration, is provided by NAG (Numerical Algorithms Group) and is denoted by the name D02CBF. The algorithm which this routine uses is the variable-order, variable-step Adams method [81], which is a more accurate method than the standard Runge-Kutta Merson algorithm. It provides internal accuracy checks and works to a user-supplied accuracy level. Should the specified accuracy be unobtainable, the routine terminates with an appropriate error message. The routine can be intercepted to provide intermediate values of the quantities during the integration; this information is used to produce graphs of the solution by use of a library plotting routine (SIMPLEPLOT).

The rest of this appendix illustrates how a particular problem is set up for numerical integration via these routines. The problem chosen here is from chapter 4 - the simplest case of power law inflation induced by an exponential potential without viscosity. It is shown how the problem is set up for integration and then the appropriate program is given with details of its structure. This is the simplest such problem to appear in this thesis, but other cases such as in chapter 3 are simple rewritings of the method with extra variables and more complicated differential equations.

(ii) Setting Up the Problem

We consider here how to set up a numerical integration of a system of equations taken from chapter 4; that given by equations (4.4) and (4.5) which describe the behaviour of the universe's scale factor, a, and a scalar field, ϕ, when the scalar field has a potential of exponential form. The equations, as written in chapter 4, have the form

$$\left(\frac{\dot{a}}{a}\right)^2 = \frac{1}{6}\dot{\phi}^2 + \frac{1}{3}V_0 \exp(-\lambda\phi) \qquad \text{(A1.1)}$$

$$\ddot{\phi} + 3\left(\frac{\dot{a}}{a}\right)\dot{\phi} - \lambda V_0 \exp(-\lambda\phi) = 0 \qquad \text{(A1.2)}$$

For numerical simulation, these equations have to be written as a first order system. This is done by introducing a new variable ξ, equal to the derivative of ϕ. For convenience, we also change the scale factor variable to $\alpha = \ln(a)$. This gives

$$\dot{\alpha}^2 = \frac{1}{6}\xi^2 + \frac{1}{3}V_0 \exp(-\lambda\phi) \tag{A1.3}$$

$$\dot{\phi} = \xi \tag{A1.4}$$

$$\dot{\xi} + 3\dot{\alpha}\xi - \lambda V_0 \exp(-\lambda\phi) = 0 \tag{A1.5}$$

Two things remain to bring this into the appropriate form. Firstly, the square root of equation (A1.3) must be taken, to give an equation for α itself. Clearly there are two options, positive and negative, for the sign of the square root. We choose the positive one, as we are interested only in solutions with α increasing. Since the right hand side of equation (A1.3) never vanishes, we do not have to worry about the derivative of α changing sign; the universe remains expanding. Secondly, we must get rid of the derivative of α in the second term in equation (A1.5). This is simply done by substituting in equation (A1.3). Hence the final system, which is completely equivalent to the original equations, is

$$\dot{\alpha} = \sqrt{\frac{1}{6}\xi^2 + \frac{1}{3}V_0 \exp(-\lambda\phi)} \tag{A1.6}$$

$$\dot{\phi} = \xi \tag{A1.7}$$

$$\dot{\xi} = \lambda V_0 \exp(-\lambda\phi) - 3\xi\sqrt{\frac{1}{6}\xi^2 + \frac{1}{3}V_0 \exp(-\lambda\phi)} \tag{A1.8}$$

This gives the derivatives of α, ϕ and ξ in terms of α, ϕ and ξ alone, which is exactly the form required to carry out a numerical simulation.

(iii) The Program Itself

At the end of this appendix is a printout of the actual program, called PLINFL (for Power Law INFLation), which does the integration, complete with job control parameters and comments. The rest of this appendix is a description of the program, which follows the flow chart shown below.

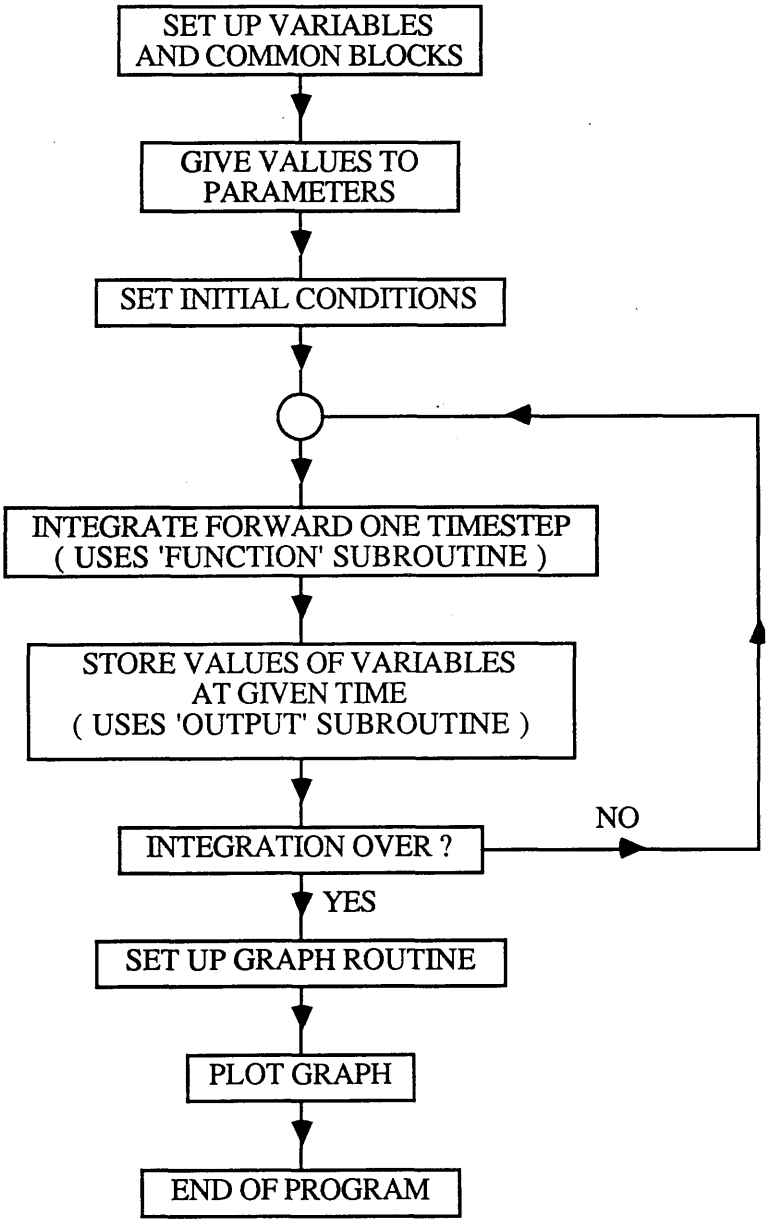

Figure A1.1 Flowchart for the program PLINFL

For the most part, the program PLINFL is a setting up of the various variables required for the call to the NAG routine which actually carries out all the work. At the start all variable types are declared and a common block set up for transfer of variables to subroutines. All variables are set to be double precision to ensure high accuracy; the NAG routine called is also a double precision routine. Then the various parameters in the equations are set, here λ and V_0. The endpoints of the integration are specified; it is to be from time X, where the initial conditions are supplied, up to time XEND.

The values of the three variables to be integrated are stored in the array Y(N), with α, ϕ and ξ written as Y(1), Y(2) and Y(3) respectively. Their initial values are set (here all zero), the fail registers and accuracy requirements for the NAG routine are set and the NAG routine D02CBF is called with all the relevant variables. The routine finds the values of the derivatives, as given by equations (A1.6) to (A1.8), from the user-supplied routine FUNCTION. The formulae for F(1), F(2) and F(3) specify the derivative for Y(1), Y(2) and Y(3) respectively. Every so often, the user-supplied subroutine OUTPUT intercepts the NAG routine and stores the values that α, ϕ and ξ have attained. When the simulation has reached its endpoint as given by XEND, the NAG routine finishes and warns if any errors have resulted (drastic errors such as loss of accuracy will terminate the program in mid run). Finally, the intermediate values which have been stored by OUTPUT during the simulation are converted to single precision numbers and are sent to a library plotting routine (SIMPLEPLOT) to produce a graphical solution, which can be sent either to screen or one of a variety of printers. The graphs used as figures throughout this thesis are produced by the QMS Laserwriter.

```
//TH35PLIN JOB TH35,LIDDLE,CLASS=R,TIME=(0,59),MSGCLASS=T                PLI00010
// EXEC FVCLG,LINES=10000,                                               PLI00020
// REGION.G=1000K                                                        PLI00030
//C.SYSIN DD *                                                          PLI00040
C                                                                        PLI00050
C     Program to generate numerical solutions to the equations           PLI00060
C     resulting from coupling a scalar field with an exponential         PLI00070
C     potential to Einstein gravity using NAG routines.                  PLI00080
C     The program takes specified initial conditions and uses the        PLI00090
C     differential equations to produce a numerical solution.            PLI00100
C     The initial conditions should be specified within the program.     PLI00110
C                                                                        PLI00120
C     Set the common block for variables used in the subroutines.        PLI00130
C                                                                        PLI00140
      IMPLICIT DOUBLE PRECISION (A-H,O-Z)                                PLI00150
      COMMON/PARAM/LAMBDA,V0,TMSTEP,ANS,CO                               PLI00160
C                                                                        PLI00170
C     Initialise variables needed for the NAG routines.                  PLI00180
C                                                                        PLI00190
      DOUBLE PRECISION LAMBDA,V0,TMSTEP                                  PLI00200
      INTEGER N,IFAIL,IRELAB,CO,SEED,LOOP                                PLI00210
      DOUBLE PRECISION X,XEND,TOL,Y(3),W(3,18),S1,S2,S3                  PLI00220
      EXTERNAL FCN,OUTPUT                                                PLI00230
      DOUBLE PRECISION T,F(3),XSOL,ANS(0:3,1500)                         PLI00240
      INTEGER NX,NY                                                      PLI00250
      REAL AX(1500),AY(4500)                                             PLI00260
      CHARACTER BANNER*73                                                PLI00270
      CHARACTER FLAG*57                                                  PLI00280
      CO=0                                                               PLI00290
C                                                                        PLI00300
C     Any free parameters should be set here (remember to define the     PLI00310
C     variable type in each subprogram if more are added).               PLI00320
C                                                                        PLI00330
      LAMBDA=DSQRT(2.D0)                                                 PLI00340
      V0=1.D0                                                            PLI00350
C                                                                        PLI00360
C     The initial and final times should be set here.The initial time    PLI00370
C     should be set in the variable X (=tau) , and the final time in     PLI00380
C     XEND.                                                              PLI00390
C     The timestep variable TMSTEP should also be set for the output.    PLI00400
C                                                                        PLI00410
      X=1.D0                                                             PLI00420
      XEND=1.D6                                                          PLI00430
      TMSTEP=(XEND-X)/1000.D0                                            PLI00440
      LOOP=INT((XEND-X)/TMSTEP+1.D0)                                     PLI00450
C                                                                        PLI00460
C     Set the initial condition variables here :-                        PLI00470
C          Y(1)=alpha  ;  Y(2)=phi  ;  Y(3)=xi                           PLI00480
C                                                                        PLI00490
      Y(1)=0.D0                                                          PLI00500
      Y(2)=0.D0                                                          PLI00510
      Y(3)=0.D0                                                          PLI00520
      S1=Y(1)                                                            PLI00530
      S2=Y(2)                                                            PLI00540
      S3=Y(3)                                                            PLI00550
C                                                                        PLI00560
C     Call to the NAG routine D02CBE                                     PLI00570
C     The tolerances and fail registers must be set here.                PLI00580
C                                                                        PLI00590
      TOL=.00000001D0                                                    PLI00600
      IFAIL=0                                                            PLI00610
      IRELAB=1                                                           PLI00620
      CALL D02CBF (X,XEND,3,Y,TOL,IRELAB,FCN,OUTPUT,W,IFAIL)             PLI00630
C                                                                        PLI00640
C     The output routine to call the Simpleplot program should be        PLI00650
C     inserted here ; it plots the values of the ANS array               PLI00660
C                                                                        PLI00670
C     Set up the simpleplot axes using call to JBAXES                    PLI00680
C                                                                        PLI00690
      DO 4100 J=1,LOOP                                                   PLI00700
         AX(J)=SNGL(ANS(0,J))                                            PLI00710
 4100    CONTINUE                                                        PLI00720
      DO 4300 I=1,3                                                      PLI00730
         DO 4200 J=1,LOOP                                                PLI00740
              AY((I-1)*LOOP+J)=SNGL(ANS(I,J))                            PLI00750
```

```
 4200         CONTINUE                                                  PLI00760
 4300    CONTINUE                                                       PLI00770
      NX=-LOOP                                                          PLI00780
C                                                                       PLI00790
C     Make this value and the one below to 3 to also plot xi (=phi dot).PLI00800
C                                                                       PLI00810
      NY=2*LOOP                                                         PLI00820
      CALL JBAXES(AX,NX,20.,'TIME',4,AY,NY,20.,'ALPHA(T),PHI(T)',15)    PLI00830
C                                                                       PLI00840
C     Call join point routine.                                          PLI00850
C                                                                       PLI00860
C     This is the other value to make three (see above).                PLI00870
C                                                                       PLI00880
      DO 4500 I=1,2                                                     PLI00890
         CALL BREAK                                                     PLI00900
         DO 4400 J=1,LOOP                                               PLI00910
              CALL JOIN PT(AX(J),AY((I-1)*LOOP+J))                      PLI00920
 4400         CONTINUE                                                  PLI00930
         CALL NUMB PT(AX(LOOP),AY(I*LOOP),3,I)                          PLI00940
 4500    CONTINUE                                                       PLI00950
      BANNER (1:23) = 'PLINFL 1  JUNE 1988    '                       PLI00960
      WRITE (BANNER(24:33),5300) S1                                     PLI00970
      BANNER (34:35) = ' '                                              PLI00980
      WRITE (BANNER(36:45),5300) S2                                     PLI00990
      BANNER (46:47) = ' '                                              PLI01000
      WRITE (BANNER(48:57),5300) S3                                     PLI01010
      BANNER (58:73) = '                '                             PLI01020
 5100 FORMAT ( I5)                                                      PLI01030
 5200 FORMAT ( D9.3)                                                    PLI01040
 5300 FORMAT ( D10.4)                                                   PLI01050
      FLAG(1:9)='Lam**2 = '                                             PLI01060
      WRITE(FLAG(9:18),5300) LAMBDA**2                                  PLI01070
      FLAG(19:31)='   V SUB 0 = '                                       PLI01080
      WRITE(FLAG(32:41),5300) V0                                        PLI01090
      FLAG(42:57)='                '                                    PLI01100
      CALL TITLE (1,2,BANNER,73)                                        PLI01110
      CALL TITLE(2,2,FLAG,57)                                           PLI01120
      CALL END PLT                                                      PLI01130
C                                                                       PLI01140
 5000 STOP                                                              PLI01150
      END                                                               PLI01160
C                                                                       PLI01170
C                FUNCTION SUBROUTINE                                    PLI01180
C     This subroutine specifies the functions to be used when the       PLI01190
C     first order system is numerically integrated.                     PLI01200
C     The array F(I) should contain the I th derivative function .      PLI01210
C                                                                       PLI01220
      SUBROUTINE FCN (T,Y,F)                                            PLI01230
      IMPLICIT DOUBLE PRECISION (A-H,O-Z)                               PLI01240
      COMMON/PARAM/LAMBDA,V0,TMSTEP,ANS,CO                              PLI01250
      DOUBLE PRECISION T,F(3),Y(3),LAMBDA,VO,TMSTEP,ANS(0:3,1500)       PLI01260
      INTEGER CO                                                        PLI01270
      F(1)=DSQRT((Y(3)**2)/6.D0+(1.D0/3.D0)*V0*EXP(-LAMBDA*Y(2)))       PLI01280
      F(2)=Y(3)                                                         PLI01290
      F(3)=LAMBDA*V0*EXP(-LAMBDA*Y(2))-3*Y(3)*                          PLI01300
     &   DSQRT((Y(3)**2)/6.D0+(1.D0/3.D0)*V0*EXP(-LAMBDA*Y(2)))         PLI01310
      RETURN                                                            PLI01320
      END                                                               PLI01330
C                                                                       PLI01340
C                    OUTPUT SUBROUTINE                                  PLI01350
C     This subroutine collects the output values of the variables at    PLI01360
C     time T=XSOL . On exit , XSOL should be set at the value for the   PLI01370
C     next required output values.                                      PLI01380
C                                                                       PLI01390
      SUBROUTINE OUTPUT (XSOL,Y)                                        PLI01400
      IMPLICIT DOUBLE PRECISION (A-H,O-Z)                               PLI01410
      COMMON/PARAM/LAMBDA,V0,TMSTEP,ANS,CO                              PLI01420
      DOUBLE PRECISION TMSTEP,ANS(0:3,1500),Y(3),LAMBDA,V0,XSOL         PLI01430
      INTEGER CO                                                        PLI01440
      CO=CO+1                                                           PLI01450
      ANS(0,CO)=XSOL                                                    PLI01460
      DO 1000 I=1,3                                                     PLI01470
         ANS(I,CO)=Y(I)                                                 PLI01480
 1000    CONTINUE                                                       PLI01490
      XSOL=XSOL+TMSTEP                                                  PLI01500
```

```
      RETURN                                                            PLI01510
      END                                                               PLI01520
/*                                                                      PLI01530
//L.SYSLIB DD DSN=SYS1.NAGLIB,DISP=SHR                                  PLI01540
//L.SYSIN DD *                                                          PLI01550
      INCLUDE SYSLIB(SIMPTNX)                                           PLI01560
//G.FT06F001 DD SYSOUT=T                                                PLI01570
//G.FT08F001 DD SYSOUT=P,DCB=(RECFM=FBA,LRECL=133,BLKSIZE=1330)         PLI01580
//G.SYSIN DD *                                                          PLI01590
```

References

"What I tell you three times is true."

The Hunting of the Snark

Lewis Carroll

[1] M. S. Turner , "Inflation in the Universe, circa 1986" , Fermilab preprint

[2] L. Shapiro and S. A. Teukolsky, "Black holes, White Dwarfs and Neutron Stars" , Wiley-Interscience (1983)

[3] C. W. Misner, K. S. Thorne and J. A. Wheeler, "Gravitation" , W H Freeman (1973)

[4] A. C. Hearn, "Reduce 3.2 Users Manual" , The Rand Corporation, Santa Monica (1985)

[5] M. B. Green, J. H. Schwarz and E. Witten, "Superstring Theory" , Vols I and II, Cambridge (1987)

[6] T. P. Cheng and L. F. Li, "Gauge Theory of Elementary Particles" , Oxford (1984)

[7] M. B. Green and J. H. Schwarz, Phys Lett B149 (1984) 117

[8] J. H. Schwarz, Int J Mod Phys A4 (1989) 2653

[9] P. Candelas, G.T. Horowitz, A. Strominger and E. Witten, Nucl Phys B258 (1985) 46

[10] J. H. Schwarz in "Superstrings and Supergravity" eds A.T. Davies and D.G. Sutherland, SUSSP (1985)

[11] G. F. Chapline and N. S. Manton, Phys Lett B120 (1983) 105

[12] A. B. Henriques and R. G. Moorhouse, Phys Lett B194 (1987) 353

[13] P. G. O. Freund, Nucl Phys B209 (1982) 146

[14] R. Coquereaux and G. Esposito-Farese, "General Relativity with a U(1) Scalar Field" , Centre de Physique Theorique preprint CPT 87/P 2065

[15] E. Kasner, Amer J Math 43 (1921) 217

[16] C.W. Misner, Phys Rev Lett 22 (1969) 1071

C.W. Misner, Phys Rev 186 (1989) 1319,1328

V. A. Belinsky and I. M. Khalatnikov, Zh Eksp Teoret Fiz 56 (1969) 1700

V. A. Belinsky and I. M. Khalatnikov, Zh Eksp Teoret Fiz 57 (1969) 2163

[17] J. D. Barrow, Phys Rep 85 (1982) 1

[18] A. H. Guth, Phys Rev D23 (1981) 347

[19] V. A. Belinsky, E. M. Lifshitz and I. M. Khalatnikov, Uspekhi Fiz Nauk 102 (1970) 463 (Soviet Physics Uspekhi 13 (1971) 745)

A. G. Doroshkevich, V. N. Lukash and I. D. Novikov, Zh Teor Fiz 60 (1971) 1201

[20] P. Halpern, Gen Rel and Grav 19 (1987) 73

[21] M. A. H. M^{ac}Callum in "General Relativity, an Einstein Centenary Survey" , eds S. W. Hawking and W. Israel, Cambridge (1979)

V. A. Belinsky, I.M. Khalatnikov and E. M. Lifshitz, Adv in Phys 31 (1982) 639

[22] A. J. Lichtenberg and M. A. Leiberman, "Regular and Stochatic Motion" , Springer, Berlin (1983)

[23] V. A. Belinsky and I. M. Khalatnikov, Zh Teor Fiz 63 (1972) 1121 (Soviet Physics JETP 36 (1973) 591)

[24] A. Hosoya, L. G. Jensen and J. A. Stein-Schabes, Nucl Phys B283 (1987) 657

[25] Y. Elskens and M. Henneaux, Nucl Phys B290 (1987) 111

Y. Elskens and M. Henneaux, Class Quant Grav 4 (1987) L161

Y. Elskens, Journ Stat Phys 48 (1987) 1269

[26] J. D. Barrow and J. A. Stein-Schabes, Phys Rev D32 (1985) 1595

[27] M. Gleiser, S. Rajpoot and J. G. Taylor, Ann Phys (N.Y.) 160 (1985) 299

J. A. Stein-Schabes and M. Gleiser, Phys Rev D34 (1986) 3242

[28] A. Albrecht, P. Steinhardt, M. Turner and F. Wilczek, Phys Rev Lett 48 (1982) 1437

[29] E. Alvarez and M. Belen-Gavela, Phys Rev Lett 51 (1983) 931

E. W. Kolb, D. Lindley and D. Seckel, Phys Rev D30 (1984) 1205

R. D. Abbott, S. Barr and S. Ellis, Phys Rev D30 (1984) 720

R. G. Moorhouse and J. A. Nixon, Nucl Phys B261 (1985) 172

A. B. Henriques, Nucl Phys B277 (1986) 621

[30] M. D. Pollock and D. Sahdev, Phys Lett B222 (1989) 12

[31] A. Albrecht and P.Steinhardt, Phys Rev Lett 48 (1982) 1220

[32] A. D. Linde, Phys Lett B108 (1982) 389

[33] L. F. Abbott and S.-Y. Pi, "Inflationary Cosmology" , World Scientific (1986)

[34] J. Preskill, Phys Rev Lett 43 (1979) 1365

[35] S. Coleman and E. Weinberg, Phys Rev D7 (1973) 1888

[36] K. Maeda and M. D. Pollock, Phys Lett B173 (1986) 251

P. Binetruy and M. K. Gaillard, Phys Rev D34 (1986) 3069

[37] L. F. Abbott and M. B. Wise, Nucl Phys B244 (1984) 541

[38] J. J. Halliwell, Phys Lett B185 (1987) 341

[39] J. D. Barrow, Phys Lett B187 (1987) 12

[40] E. Cremmer, S. Ferrara, C. Kounnas and D. V. Nanopoulos, Phys Lett B133 (1983) 61

J. Ellis, A. B. Lanahas, D. V. Nanopoulos and K. Tamvakis, Phys Lett B134 (1984) 429

M. Dine, R. Rohm, N. Seiberg and E. Witten, Phys Lett B156 (1985) 55

J. P. Derendinger, L. E. Ibanez and H. P. Nilles, Nucl Phys B267 (1986) 365

[41] K. Maeda and M. Nishino, Phys Lett B154 (1985) 358

K. Maeda and M. Nishino, Phys Lett B158 (1985) 381

[42] A. B. Burd and J. D. Barrow, Nucl Phys B308 (1988) 929

[43] J. Yokoyama and K. Maeda, Phys Lett B207 (1988) 31

[44] L. F. Abbott, E. Fahri and M. B. Wise, Phys Lett B117 (1982) 29

[45] A. Salam and E.Sezgin, Phys Lett B147 (1984) 47

H. Nishino and E. Sezgin, Phys Lett B144 (1984) 187

[46] G.W. Gibbons and P.K. Townsend, Nucl Phys B282 (1987) 610

[47] J. J. Halliwell, Nucl Phys B286 (1987) 729

[48] F. Lucchin and S. Matarrese, Phys Rev D32 (1985) 1316

[49] A. D. Linde in "300 Years of Gravitation" , eds S. W. Hawking and W. Israel, Cambridge (1987)

[50] M. D. Pollock, Phys Lett B185 (1987) 34

E. T. Vishniac, K. A. Olive and D. Seckel, Nucl Phys B289 (1987) 717

[51] J. Yokoyama, Phys Lett B212 (1988) 273

J. Yokoyama, Phys Rev Lett 63 (1989) 712

[52] V. A. Kuzmin, V. A. Rubakov and M. E. Shapostnikov, Phys Lett B155 (1985) 36

S. Yu. Khlebnikov and M. E. Shapostnikov, Nucl Phys B308 (1988) 885

[53] Th. Kaluza, Sitzungsber Preuss Akad Wiss Phys Math Kl (1921) 966

O. Klein, Z Phys 37 (1926) 895

[54] A. Chodos and S. Detweiler, Gen Rel and Grav 14 (1982) 879

[55] G. W. Gibbons and D. L. Wiltshire, Annals of Physics 167 (1986) 201

[56] P. Breitenlohner, D. Maison and G. W. Gibbons, Comm Math Phys 120 (1988) 295

[57] V. Belinsky and R. Ruffini, Phys Lett B89 (1980) 195

[58] R. D. Sorkin, Phys Rev Lett 51 (1983) 87

[59] D. J. Gross and M. J. Perry, Nucl Phys B226 (1983) 29

[60] J. R. Oppenheimer and G. M. Volkoff, Phys Rev 55 (1939) 374

[61] S. Chandrasekhar, Monthly Notices of RAS 95 (1935) 222

[62] C. E. Rhoades and R. Ruffini, Phys Rev Lett 32 (1974) 324

[63] S. Weinberg, "Gravitation and Cosmology" , Wiley (1972)

[64] G. D. Birkhoff, "Relativity and Modern Physics" , Harvard (1923)

[65] A. I. Janis, E. T. Newman and J. Winicour, Phys Rev Lett 20 (1968) 878

[66] J. Bekenstein, Phys Rev D5 (1972) 1239

[67] A. B. Henriques, Int J Mod Phys A4 (1989) 1125

[68] R. H. Price, Phys Rev D5 (1972) 2419

[69] J. R. Oppenheimer and H. Snyder, Phys Rev 56 (1939) 455

[70] M. M. May and R. H. White, Phys Rev 141 (1966) 1232

V. de la Cruz, J. E. Chase and W. Israel, Phys Rev Lett 24 (1970) 423

[71] R. Ruffini and S. Bonazzola, Phys Rev 187 (1969) 1767

[72] M. Colpi, S. L. Shapiro and I Wasserman, Phys Rev Lett 57 (1986) 2485

[73] M. Gleiser, Phys Rev D38 (1988) 2376; (E) D39 (1989) 1257

P. Jetzer, Nucl Phys B316 (1989) 411

[74] M. Gleiser and R. Watkins, Nucl Phys B319 (1989) 411

[75] T. D. Lee, Phys Rev D35 (1987) 3637

R. Friedberg, T. D. Lee and Y. Pang, Phys Rev D35 (1987) 3640,3658

[76] B. W. Lynn, Nucl Phys B321 (1989) 465

S. B. Selipsky, D. C. Kennedy and B. W. Lynn, Nucl Phys B321 (1989) 430

[77] W. Thirring, Phys Lett B127 (1983) 27

[78] J. D. Breit, S. Gupta and A. Zaks, Phys Lett B140 (1984) 329

[79] T. D. Lee and Y. Pang, Nucl Phys B315 (1989) 477

[80] B. K. Harrison, K. S. Thorne, M. Wakano and J. A. Wheeler, "Gravitation Theory and Gravitational Collapse" , University of Chicago (1965)

[81] G. Hall and J. M. Watt (eds), " Modern Numerical Methods for Ordinary Differential Equations" , Oxford (1976)

[82] S. Chandrasekhar, Phys Rev Lett 12 (1964) 437

S. Chandrasekhar, Ap J 140 (1964) 417

[83] T. D. Lee and Y. Pang, Phys Rev D35 (1987) 3678